TURUN YLIOPISTON JULKAISUJA
ANNALES UNIVERSITATIS TURKUENSIS

SARJA - SER. D OSA - TOM. 1108

MEDICA - ODONTOLOGICA

CHARACTERISATION OF FUNCTIONAL BROWN ADIPOSE TISSUE IN ADULT HUMANS

by

Janne Orava

TURUN YLIOPISTO
UNIVERSITY OF TURKU
Turku 2014

From the Department of Clinical Physiology and Nuclear Medicine, and the Department of Medicine, Institute of Clinical Medicine, Doctoral Programme of Clinical Investigation – CLIDP, University of Turku, Turku, Finland;

The National Graduate School of Clinical Investigation;

Turku PET Centre

Supervised by

Docent Kirsi A. Virtanen, M.D., Ph.D.

Turku PET Centre

University of Turku, Turku, Finland

and

Professor Pirjo Nuutila, M.D., Ph.D.

Turku PET Centre and the Department of Endocrinology

University of Turku and Turku University Hospital, Turku, Finland

Reviewed by

Assistant Professor Aaron M. Cypess, M.D., Ph.D.

Section of Integrative Physiology and Metabolism, Research Division

Joslin Diabetes Center, Harvard Medical School, Boston, USA

and

Professor Atso Raasmaja, Ph.D.

Division of Pharmacology and Pharmacotherapy, Faculty of Pharmacy

University of Helsinki, Helsinki, Finland

Dissertation opponent

Docent Heikki A. Koistinen, M.D., Ph.D.

Department of Medicine, Division of Endocrinology

Helsinki University Central Hospital;

Minerva Foundation Institute for Medical Research,

Biomedicum 2U, Helsinki, Finland

The originality of this dissertation has been checked in accordance with the University of Turku quality assurance system using the Turnitin OriginalityCheck service.

ISBN 978-951-29-5703-3 (PRINT)
ISBN 978-951-29-5704-0 (PDF)
ISSN 0355-9483

Painosalama Oy – Turku, Finland 2014

To those who have believed in me along the way

ABSTRACT

Janne Orava

CHARACTERISATION OF FUNCTIONAL BROWN ADIPOSE TISSUE IN ADULT HUMANS

The Department of Clinical Physiology and Nuclear Medicine, and the Department of Medicine, and Turku PET Centre, University of Turku, Turku, Finland

Annales Universitatis Turkuensis
Painosalama Oy, Turku, Finland 2014

The white adipose tissue mainly serves the purpose of energy storage, while brown adipose tissue (BAT) has the capacity to generate heat under cold conditions in mammals and in human infants. BAT is controlled by the central nervous system, and BAT function is accompanied by increased energy expenditure. However, it was not previously certain whether adult humans also have functional BAT.

The aim of this doctoral work was to identify functional BAT in adult humans and to characterise its glucose uptake and blood flow under cold and insulin stimulation conditions in lean and in obese humans, by using positron emission tomography. Further, the impact of weight loss on BAT glucose uptake was assessed. Cerebral glucose uptake was also studied in relation to BAT function and cold exposure.

The results showed that healthy adult humans have functional BAT, as assessed by the intense cold-induced glucose uptake and by biopsies. BAT was also found to be a highly insulin-sensitive tissue in lean humans, but the effects of insulin and cold exposure were attenuated in obese humans, although the glucose uptake capacity of cold-activated BAT might be increased by weight loss. Blood flow in the BAT of lean humans was associated with whole-body energy expenditure. The presence of cold-activated BAT was related to lower body mass index and higher insulin sensitivity. Finally, BAT activation was linked to the activity of the cerebellum, the thalamus and certain neocortical regions. The cold-induced cerebral glucose uptake was also lower in obese than in lean adult humans.

Keywords: brown adipose tissue, glucose uptake, blood flow, positron emission tomography, cold exposure, insulin, weight loss, obesity, brain.

TIIVISTELMÄ

Janne Orava

AIKUISTEN IHMISTEN TOIMINNALLISEN RUSKEAN RASVAKUDOKSEN KARAKTERISOINTI

Kliinisen fysiologian ja isotooppilääketieteen oppiaine, sisätautioppi sekä Valtakunnallinen PET-keskus, Turun yliopisto, Turku
Annales Universitatis Turkuensis
Painosalama Oy, Turku 2014

Nisäkkäiden ja vastasyntyneiden ihmisten valkoiset rasvasolut toimivat ensisijaisesti energiavarastona toisin kuin ruskeat rasvasolut, joilla on kyky tuottaa lämpöä ja kuluttaa siten samalla energiaa elimistön kohdatessa kylmän ympäristön. Ruskean rasvakudoksen toimintaa säätelee keskushermosto. Aiemmin ei kuitenkaan ollut varmaa, onko aikuisilla ihmisillä toiminnallista ruskeaa rasvakudosta.

Väitöskirjan tavoitteena oli osoittaa, että aikuisilla ihmisillä on toiminnallista ruskeaa rasvaa ja lisäksi karakterisoida kylmäaltistuksen ja insuliinin vaikutuksia ruskean rasvakudoksen glukoosin käyttöön ja verenvirtaukseen hyödyntämällä positroniemissiotomografiaa. Lisäksi tutkittiin lihavuuden vaikutusta ruskean rasvakudoksen aineenvaihduntaan ja sitä, muuttaako laihduttaminen ruskean rasvan glukoosin käyttöä. Myös aivojen glukoosin käyttöä mitattiin suhteessa ruskean rasvakudoksen toimintaan ja kylmäaltistukseen.

Tulokset osoittivat, että terveillä aikuisilla ihmisillä on toiminnallista ruskeaa rasvaa, sillä tutkitun rasvakudoksen glukoosin käyttö lisääntyi voimakkaasti kylmäaltistuksen aikana, ja kyseiseltä alueelta otetuissa kudosnäytteissä oli ruskeaa rasvakudosta. Normaalipainoisten aikuisten ruskea rasva osoittautui myös erittäin insuliiniherkäksi kudokseksi. Lihavien ihmisten ruskea rasvakudos ei ollut yhtä herkkä kylmäaltistuksen ja insuliinin vaikutuksille, mutta laihduttaminen saattaa lisätä kylmäaltistukseen liittyvää glukoosin kulutusta ruskeassa rasvassa. Ruskean rasvakudoksen verenvirtauksen todettiin myös olevan yhteydessä suurentuneeseen kokokehon energiankulutukseen. Lisäksi koehenkilöillä, joilla oli aktiivista ruskeaa rasvaa, oli myös alempi painoindeksi ja suurempi kokokehon insuliiniherkkyys kuin niillä, joilla aktiivista ruskeaa rasvaa ei todettu. Ruskean rasvakudoksen aktivaation todettiin liittyvän pikkuaivojen, talamuksen ja isoaivojen kuorikerroksen tiettyjen osien toimintaan. Lisäksi havaittiin, että kylmäaltistuksen aikana lihavilla ihmisillä aivojen glukoosin käyttö oli alentunut verrattuna normaalipainoisiin henkilöihin.

Avainsanat: ruskea rasvakudos, glukoosin käyttö, verenvirtaus, positroniemissiotomografia, kylmäaltistus, insuliini, laihduttaminen, lihavuus, aivot.

TABLE OF CONTENTS

ABBREVIATIONS

[^{11}C]Acetate	carbon-11-labelled acetate
[^{11}C]MET	carbon-11-labelled methionine
^{123}I	iodine-123
[^{15}O]CO	oxygen-15-labelled carbon monoxide
[^{15}O]H_2O	oxygen-15-labelled water
[^{15}O]O_2	oxygen-15-labelled oxygen
[^{18}F]FDG	2-deoxy-2-[^{18}F]fluoro-D-glucose
[^{18}F]FTHA	[^{18}F]fluoro-6-thia-heptadecanoic acid
^{201}Tl	thallium-201
^{67}Ga	gallium-67
^{99m}Tc	technetium-99m
AC	adenylyl cyclase
AFOV	axial field-of-view
AR	adrenergic receptor
ATGL	adipose triglyceride lipase
ATP	adenosine-5'-triphosphate
AUC	area under the curve
BAT	brown adipose tissue
BMI	body mass index
BMP	bone morphogenetic protein
BP	blood pressure
cAMP	3'-5'-cyclic adenosine monophosphate
CNS	central nervous system
CREB	cAMP-response-element-binding protein
CT	computed tomography
D2	type 2 5′-deiodinase
DMH	dorsomedial hypothalamus
EE	energy expenditure
eNOS	endothelial nitric oxide synthase
$FADH_2$	flavin adenine dinucleotide
FFA	free fatty acid
FFM	fat-free mass
FGF21	fibroblast growth factor 21
fMRI	functional magnetic resonance imaging
FUR	fractional uptake rate
GABA	γ-aminobutyric acid
GLUT1	glucose transporter type 1
GLUT4	glucose transporter type 4
G_s protein	stimulatory G protein
HbA_{1c}	glycosylated haemoglobin A_{1c}
HDL	high-density lipoprotein
HIV	human immunodeficiency virus
HR	heart rate
HSL	hormone-sensitive lipase
IDIF	image-derived-input-function

IML	intermediolateral nucleus
iNOS	inducible nitric oxide synthase
IR	insulin receptor
IRS1	insulin receptor substrate protein 1
IRS2	insulin receptor substrate protein 2
K_i	influx rate constant
LC	lumped constant
LDL	low-density lipoprotein
LPB	lateral parabrachial nucleus
MIBG	metaiodobenzylguanidine
MIBI	methoxyisobutylisonitrile
MnPO	median preoptic subnucleus
MPO	medial preoptic subnucleus
MR	magnetic resonance
MRI	magnetic resonance imaging
mRNA	messenger ribonucleic acid
Myf5	myogenic factor 5
NA	noradrenaline
NADH	nicotinamide adenine dinucleotide
OGTT	oral glucose tolerance test
p38 MAPK	p38 mitogen-activated protein kinase
PCR	polymerase chain reaction
PET	positron emission tomography
PGC-1α	peroxisome proliferator-activated receptor γ coactivator 1α
PKA	protein kinase A
POA	preoptic area
PPARγ	peroxisome proliferator-activated receptor gamma
PRDM16	PR domain containing 16
ROI	region-of-interest
RQ	respiratory quotient
SCWAT	subcutaneous white adipose tissue
SNS	sympathetic nervous system
SPECT	single photon emission computed tomography
SPM	statistical parametric mapping
SUV	standardised uptake value
T3	triiodothyronine
T4	thyroxine
TAC	time-activity curve
TCA	tricarboxylic acid
TR	thyroid hormone receptor
TRH	TSH-releasing hormone
TSH	thyroid stimulating hormone
TSH-R	TSH receptor
UCP1	uncoupling protein-1
VAT	visceral adipose tissue
$\dot{V}CO_2$	carbon dioxide production
$\dot{V}O_2$	oxygen consumption
WAT	white adipose tissue

LIST OF ORIGINAL PUBLICATIONS

I Virtanen KA, Lidell ME, Orava J, Heglind M, Westergren R, Niemi T, Taittonen M, Laine J, Savisto NJ, Enerbäck S, Nuutila P. Functional brown adipose tissue in healthy adults. The New England Journal of Medicine. 2009;360(15):1518-25.

II Orava J, Nuutila P, Lidell ME, Oikonen V, Noponen T, Viljanen T, Scheinin M, Taittonen M, Niemi T, Enerbäck S, Virtanen KA. Different metabolic responses of human brown adipose tissue to activation by cold and insulin. Cell Metabolism. 2011;14(2):272-9.

III Orava J, Nuutila P, Noponen T, Parkkola R, Viljanen T, Enerbäck S, Rissanen A, Pietiläinen KH, Virtanen KA. Blunted metabolic responses to cold and insulin stimulation in brown adipose tissue of obese humans. Obesity (Silver Spring). 2013;21(11):2279-87.

IV Orava J, Nummenmaa L, Noponen T, Viljanen T, Parkkola R, Nuutila P, Virtanen KA. Brown adipose tissue function is accompanied by cerebral activation in lean but not in obese humans. Journal of Cerebral Blood Flow & Metabolism. In press.

1 INTRODUCTION

The principal components of adipose tissue are white and brown adipocytes in mammals, and they form two tissues, white adipose tissue (WAT) and brown adipose tissue (BAT), respectively (1). The white adipocytes are the predominant cell type in humans (2).

WAT and BAT have different functions. WAT mainly serves as energy storage, while BAT is capable of thermogenesis, i.e., generation of heat (3). Brown adipocytes uniquely express a protein called uncoupling protein-1 (UCP1), which uncouples the respiratory chain from adenosine-5'-triphosphate (ATP) synthesis in mitochondria (4). This process is accompanied by an increase in energy expenditure (EE) (5). BAT is innervated by the sympathetic nervous system (SNS), which stimulates BAT by releasing noradrenaline (NA) from its nerve endings under cold conditions (6). Thermoregulation in homeothermic mammals involves complex neural mechanisms in the central nervous system (CNS) (7).

The profound effects of BAT on body temperature, especially in rodents, but also in human infants, have been acknowledged, whereas BAT in adult humans has previously been regarded as a vestigial tissue with no or only minimal function (8). Furthermore, the central BAT-controlling mechanisms have been undetermined in humans. Moreover, in spite of the numerous studies on rodents showing intense metabolic activity of BAT that can counteract obesity (9), the role of human BAT in obesity has not yet been resolved, and in fact current strategies of weight management have not been successful. The proportion of overweight and obese humans has increased to the extent that 35% of adults worldwide currently have a body mass index (BMI) ≥ 25.0 kg • m^{-2} (10).

As the use of imaging devices that combined positron emission tomography (PET) with computed tomography (PET/CT) became more common in nuclear imaging, it was gradually realised that the cervical adipose tissue of some patients demonstrates highly active metabolism that can mimic pathological conditions (11). Subsequently, it was postulated that this incidental metabolic activity represents activated BAT (12), but conclusive evidence for the hypothesis was for many years lacking (**I**). However, it is now known that most healthy adult humans have functional BAT that is activated at least by cold exposure (**I**, 13), and that BAT metabolic activity is responsible for the confounding effect sometimes observed in clinical PET imaging (14). Further, evidence suggests that there are two kinds of BAT in adult humans. The classical BAT is similar to that found in the interscapular region of rodents (15). In addition, distinct cells, called brite or beige adipocytes, are also found (16); they have many characteristics of classical brown adipocytes, but are thought to be inducible in a predominantly white adipose depot (17–18).

The aims of this doctoral work included the identification of functional BAT in healthy adults, and subsequently, the characterisation of its glucose uptake rate and tissue blood flow responses to cold exposure and insulin stimulation *in vivo*, by using PET imaging. Because rodent studies show that poorly functioning BAT predisposes to obesity, the metabolic responses of BAT to cold and insulin stimulation were also investigated in obese humans. Furthermore, the impact of weight loss on cold-induced glucose uptake by BAT was assessed in order to study whether BAT capacity can be increased. Finally, cerebral glucose uptake was investigated in relation to the BAT function and cold exposure, in order to elucidate the central thermoregulatory mechanisms in man.

2 REVIEW OF THE LITERATURE

2.1 Adipose tissue

2.1.1 White adipose tissue

It has been suggested that the progenitors of white adipocytes reside in the mural cell compartment of the blood vessels of WAT (19). The mature white adipocytes have a unilocular morphology, as triacylglycerols, i.e., lipids, are packed in one large droplet inside the cells (20).

Depots of WAT are found throughout the body in humans; however, subcutaneous and intra-abdominal depots are the main compartments (21). The main subcutaneous WAT (SCWAT) depots are the abdominal and the gluteal depots, while intra-abdominal WAT is distributed between omental, visceral and retroperitoneal adipose tissue depots. Smaller amounts of WAT are found, for instance, in periarticular (22), epicardial (23), mediastinal (24) and perivascular regions (25) in humans. White adipocytes are also found in bone marrow (26) and in retro-orbital space (27) in humans.

Obesity is accompanied by increased lipid deposits within and around organs outside common adipose depots, and this phenomenon is called ectopic fat storage (28). Ectopic fat is typically found around the heart and blood vessels (29), and lipid stores within non-adipocyte cells exist especially in skeletal muscle (30), myocardium (31) and hepatocytes (32) in humans.

2.1.2 Brown adipose tissue

The brown adipocytes are smaller than white adipocytes, and the lipids are located in multiple small droplets, giving the brown adipocyte a multilocular histological appearance (20). BAT is also abundant with large mitochondria (33) and more densely vascularised than WAT (34), both of which contribute to its brownish macroscopic colour (1).

It is currently considered that BAT is only found in mammals (9). The first description of BAT was presented in 1551 by Konrad von Gesner (35–36), but the thermogenic capacity of BAT was not recognised until the 1960s (37). BAT is of special importance in young mammals, because smaller animals are exposed to a greater degree of heat loss due to their larger surface area relative to their basal metabolism than are bigger animals (9). BAT is also a significant organ in hibernating mammals, in which increased BAT activity is detected in conjunction with arousal from hibernation (38). Indeed, BAT in rodents is also called the hibernating gland. The first undisputed documentation of human BAT was provided in 1902 by Shinkishi Hatai, who described a tissue in the cervical region of human embryos as resembling BAT in rodents (39).

It is now known that active BAT is mostly found above the collar bones bilaterally in the cervical region in adult humans – within an anatomical region that is called the supraclavicular adipose tissue (**I**, 12). From the supraclavicular depot, active BAT extends to the axillae and runs parallel to the thoracic spine, and further to the posterior intercostal spaces (40) (Fig. 1). Active BAT is also found to some extent within the mediastinal (41), perirenal (41) and periadrenal regions (42), and possibly within mesenteric (43) and pelvic adipose tissue (44).

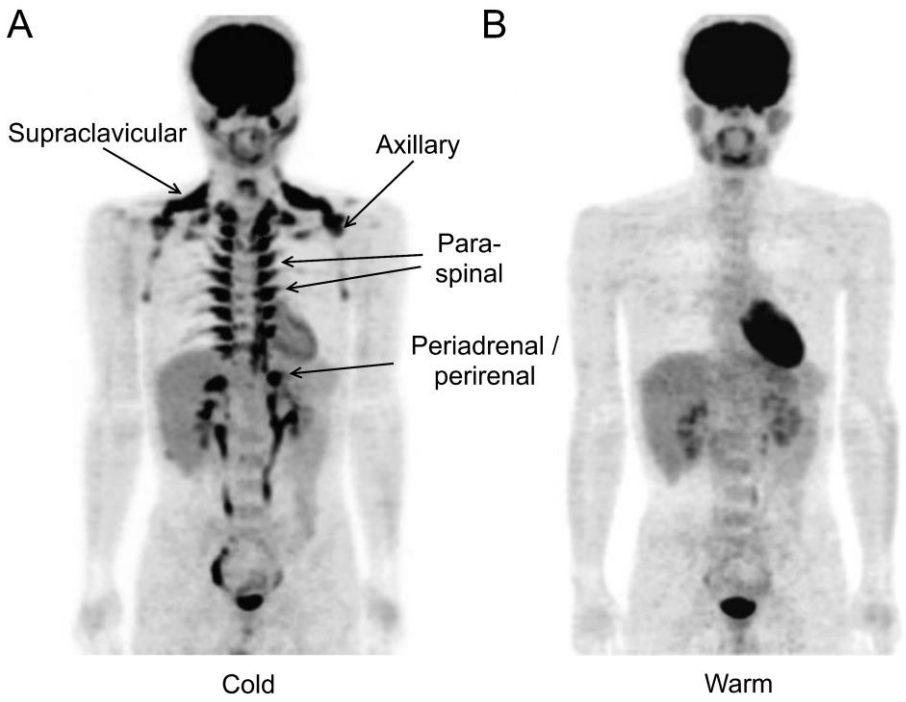

Figure 1. Main depots of active BAT in adult humans
The primary regions, where functional BAT can be found in adult humans, are shown in a PET image. BAT is activated by cold exposure (**A**), whereas minimal uptake of glucose is seen under warm conditions (**B**). Modified from Saito et al., 2009 (40).

2.1.3 Embryonic origin of classical brown adipocytes

In recent years, research with cell models has significantly broadened the overall conception of the embryonic origin of BAT. Presently, it appears that there are two different origins for human BAT. The origin of classical BAT is related to that of skeletal muscle (45), while the brite or beige adipocytes are thought to be inducible within WAT (18).

It is now known that classical BAT has a common origin with skeletal muscle, since specific cells of the dermomyotome give rise to both skeletal muscle and brown adipocytes (46). This conclusion is supported by a finding according to which the regulator of skeletal muscle differentiation, myogenic factor 5 (Myf5), is only expressed in brown adipocytes and myocytes or their precursors (47). The transcriptional regulator, PR domain containing 16 (PRDM16), which forms a transcriptional complex with the active form of the CCAAT/enhancer-binding protein beta (48), specifies brown adipocyte lineage from a common progenitor that expresses Myf5 (47, 49). The effect of the retinoblastoma protein on BAT is also regarded as an important regulatory event in the formation of BAT (50). The bone morphogenetic proteins (BMPs) have also been shown to have an important role in promoting brown adipocyte differentiation in the mesenchymal precursor cells (51–52).

However, the assessment that skeletal muscle cells and classical brown adipocytes are exclusively derived from the Myf5-lineage is partly contradictory, since Myf5-positive mesenchymal precursors have also been shown to generate some white adipocytes (53).

Further, Myf5 positivity of the cells in SCWAT has been found to be negatively associated with the expression of genes specific to brown adipocytes (54).

2.1.4 Brite or beige adipocytes

In addition to the classical brown adipocytes, brown adipocyte-like cells arising from a Myf5-negative lineage exist in rodents and in humans (16), and they are called 'brite' or 'beige' adipocytes, but also either 'recruitable brown' or 'inducible brown' adipocytes. The brite, i.e., brown-in-white, cells are found within WAT, and they share many features with the classical brown adipocytes (17), but have a distinct gene expression profile (55). It has been postulated that the brown adipocytes, interspersed in a predominantly white adipose depot, actually result from reversible white-to-brown transdifferentiation (3). In concert with this notion, the white adipocytes, which are derived from human adipose stem cells, have been shown to be able to differentiate into brite adipocytes (56–57). Further, a recent study suggests that the genetic ablation of classical BAT in mice leads to the promotion of beige cells within white adipose regions (52).

In humans, recent studies suggest that BAT in adults consists mainly of brite adipocytes (16, 58–59). This might also explain an observation suggesting that differences in gene expression exist between the BAT of adult humans and the interscapular BAT of mice (60). However, studies also suggest that classical brown fat, i.e., fat similar to the constitutive BAT in the interscapular region of rodents, overlaps with the brite adipocytes in adult humans (15, 61), or can at least be found in human infants (62).

White-to-brown conversion can result from physiological and pharmacological stimuli. It has been shown that after cold acclimation, some white adipocytes turn into brown adipocytes (63–64), and that this process is largely mediated by the β_3-adrenoreceptor in mice (65). There is evidence that repeated cold exposure increases the amount and activity of BAT in humans as well (66–69). Furthermore, the abundance of BAT in the retroperitoneal adipose tissue has been found to be higher during the winter months, as shown in patients operated on for benign adrenal tumours (70). Further, at least in humans with a pheochromocytoma, which is a catecholamine-secreting tumour, the excess adrenergic stimulation leads to browning of adipose tissue (18).

Formation of BAT is induced by the pharmaceuticals that are ligands of the nuclear receptor peroxisome proliferator-activated receptor gamma (PPARγ) (71–73). Recent findings also suggest that treatment with fibroblast growth factor 21 (FGF21) (74), melatonin (75), bone morphogenetic protein 7 (76), or growth differentiation factor-5 (77), promotes a brown phenotype of adipose tissue in rodents. The BAT-promoting effect of FGF21 has also been demonstrated in human cervical adipose tissue samples (78). Intriguingly, the cardiac natriuretic peptides also have a capacity to induce a brown phenotype within adipose tissue (79).

Interestingly, BAT may also be promoted by physical exercise, at least in rodents (e.g. 80–81). It has been shown that a skeletal muscle-derived hormone, named irisin and induced by physical exercise, promotes a brown phenotype within WAT in mice (82), and possibly in humans as well (83). However, the effect of irisin in humans has also been questioned, since the gene encoding the precursor of irisin is mutated and may not produce functional protein in humans (84). Further, a recent study does not support the idea of irisin-induced browning of SCWAT after a 12-week period of endurance and strength training in humans (85).

2.2 Effects of cold on metabolism in humans

2.2.1 Definition of thermogenesis

The production of heat, i.e., thermogenesis, takes place in all tissues to some extent, since heat is generated as a by-product of all metabolic activity (obligatory thermogenesis). Obligatory thermogenesis is therefore closely related to the basal metabolism (86). However, some tissues are actively utilised to defend body temperature in a cold environment or to fight pathogens during fever.

The term facultative or thermoregulatory thermogenesis denotes a rapid change in the thermogenic function of a tissue, for example under cold environmental conditions. On the other hand, adaptive thermogenesis is related to a gradual change in the thermogenic capacity of a tissue, which occurs, for instance, after repeated cold exposure (87).

Further, thermogenesis may also be either shivering or non-shivering, depending on whether or not involuntary action of skeletal muscles is involved in the heat production (88). Shivering thermogenesis involves increased involuntary contractile activity of skeletal muscles, which is accomplished by contractions of agonistic and antagonistic muscles, while non-shivering thermogenesis involves enhanced heat-producing metabolic processes other than involuntary skeletal muscle activity, for instance, the metabolic activation of BAT.

2.2.2 Measurement of whole-body energy expenditure

Whole-body EE can be measured directly by determining the heat produced by the body, or indirectly, by measuring carbon dioxide production ($\dot{V}CO_2$) and oxygen consumption ($\dot{V}O_2$) (89). Whole-body EE is usually measured with an indirect calorimeter, which is connected either to a respiratory chamber or to a ventilated hood (90). It is noteworthy that whole-body EE can also be estimated; however, despite the numerous equations developed for this purpose, a significant discrepancy, 10% or more, between the estimated and the measured EE values still exists (91). Whole-body EE values are affected by many subject characteristics, of which fat-free mass (FFM) is the most significant (92). Therefore, EE values are often adjusted for FFM. Besides FFM, other factors apparently have an impact on whole-body EE, since interindividual variation in the measured basal EE between subjects of similar age, weight, height and gender is close to 10% (93).

2.2.3 Cold-induced thermogenesis

When exposed to acute cold, two kinds of physiological responses occur in humans to defend core body temperature (88). The insulative response leads to a decrease in surface temperature due to peripheral vasoconstriction, and the metabolic response causes an increase in whole-body EE (facultative thermogenesis). Evidence suggests that there is significant interindividual variation in the relative contributions of the insulative and metabolic responses during mild cold exposure in humans (94).

It has been shown in numerous studies that acute cold exposure increases whole-body EE in humans (e.g. 94–96). Further, obesity is accompanied by a lower increase in whole-body EE as response to mild cold exposure (97). In the early stages of cold exposure, shivering thermogenesis is not usually encountered, but later on, shivering begins, at least if the intensity of the cold exposure is sufficiently robust (98). Indeed, shivering provides more heat than does non-shivering thermogenesis (99), and both shivering and non-shivering thermogenesis may coincide under extreme cold conditions (88). It has also been shown that, as cold exposure is

prolonged during shivering, the proportion of carbohydrates and lipids as fuel sources of heat production increases and decreases, respectively (100). In general, when wearing light clothing in an ambient temperature of 16 ºC, only non-shivering thermogenesis is observed in adult humans (101–102), and therefore, many studies on non-shivering thermogenesis have been performed using this cooling protocol. Individual thresholds for cold-induced shivering, as defined by the time needed to elicit shivering, exist, but it has not been fully clarified which characteristics of the subject affect these differences (99). Interestingly, an inverse relationship between BAT activity and shivering might exist in adult humans (103).

In rodents, BAT is considered to be the principal site of non-shivering thermogenesis (104), and the capacity can be increased by chronic cold exposure (105). However, in humans, the physiological mechanisms behind increased thermogenesis under mild cold conditions are still to some extent disputed.

It has been shown that exposure to cold weather improves the ability to defend core body temperature in a cold environment without affecting shivering, which suggests enhanced insulative response or increased non-shivering thermogenesis, or both (106). Already fifty years ago a study showed that repeated cold exposure improves cold-induced non-shivering thermogenesis in humans (107). It was shown that cold acclimation decreases the cold-induced shivering response, while non-shivering thermogenesis is increased as a compensatory measure (107). Further evidence on improved non-shivering thermogenesis was provided when it was shown that, after being cold-acclimatised, infusion of NA produced a significant increase in $\dot{V}O_2$ in healthy men (108). Interestingly, the increments in whole-body EE induced by mild cold exposure and overfeeding are highly correlated within subjects, suggesting a common regulatory mechanism for these two different conditions (109).

A possible mechanism for cold-induced non-shivering thermogenesis in adult humans is mitochondrial uncoupling in skeletal muscle (102, 110). However, there is an increasing amount of evidence that BAT also plays a role in cold-induced non-shivering thermogenesis in adult humans (e.g. **II**, 68, 111), an issue which is discussed in detail in section 2.7.9 of this review of the literature.

2.2.4 Changes in circulation under cold conditions

Acute cold exposure elicits significant alterations in the function of the cardiovascular system in humans. Importantly, systolic and diastolic blood pressures (BPs) are elevated (112), and early tachycardia is followed by a decline in the heart rate (HR) (113–114). In addition, changes in the blood concentrations of various hormones can be observed. For instance, NA, which spills into the circulation from the peripheral sympathetic nerve endings (115), is significantly increased, whereas adrenaline concentration remains unchanged by cold exposure (e.g. 116–117). The thyroid stimulating hormone (TSH) may be slightly decreased (118), while the thyroid hormones are not usually affected by acute cold exposure (114, 116). Although plasma cortisol is regarded as an indicator of stress, it is suggested that its blood concentration decreases as a response to cold exposure (116, 119). Some studies suggest a cold-induced decline in insulin levels (120), while others have not found such a connection during acute cold exposure (96, 121). On the other hand, cold exposure seems to elevate the blood glucagon level (121). Further, changes are also observed in the blood quantities of energy-containing compounds. Blood glucose is usually unchanged (96), but the circulating levels of lactate and free fatty acids (FFAs) are slightly (96) and robustly (122) increased, respectively, under cold conditions.

2.3 Central regulation of facultative thermogenesis

Facultative thermogenesis is initiated by the CNS as a response to cold sensation, a fall in core body temperature and the action of various pyrogens, especially prostaglandin E2 (123), during fever. The main target tissues of facultative thermogenesis in mammals are skeletal muscle, heart and BAT (7). It is of note that voluntary physical activity is also increased as a facultative response to exposure to a cold environment (88). Knowledge of the central control of thermogenesis is mainly based on rodent studies, and direct evidence on the central regulation of thermogenesis in humans is extremely scarce.

2.3.1 Principal neural networks of thermoregulation in mammals

Thermoreceptors are located in the body surface (skin) and inner body parts, for example in the abdominal cavity (124). Various cutaneous regions in the body have different thresholds for cold sensation. For instance, the hands are more sensitive to cold stimuli than the feet (125). The neural pathways from the skin thermoreceptors to the brain and the subsequent BAT-activating route have been quite well characterised (126) (Fig. 2).

Environmental temperature obviously has a more rapid impact on the skin temperature than on the receptors inside the body (127). Therefore, thermal afferents from the skin receptors provide a signal for the initiation of the thermogenic response. The role of thermoreception inside the body is presumably to adjust the intensity of the thermogenic responses according to the changes in core body temperature (7).

The lamina I neurons in the spinal dorsal horns receive cutaneous thermal signals (128). The lateral parabrachial nucleus (LPB) in the pons has projections from the dorsal horn (129), and these pathways most likely convey afferent thermal signals. The lamina I neurons also provide the thalamus with axons (130), which relay thermal signals to the primary somatosensory cortex. Thus, the thermal perception and localisation is mediated by the spinothalamocortical pathway. From the LPB the afferents also project to the preoptic area (POA), and they constitute the end part of the spinoparabrachiopreoptic pathway (131). The thermosensory signals are mainly transmitted to the median preoptic subnucleus (MnPO) of POA (132). The POA is the key regulator of core body temperature and is located in the hypothalamus (133).

It has been postulated that the neurons in the MnPO, which mediate cold thermal signals, provide inhibitory γ-aminobutyric acid (GABA) input to the warm-sensitive neurons in the medial preoptic subnucleus (MPO) of the POA, and that these warm-sensitive neurons subsequently decrease their tonic inhibition of the dorsomedial hypothalamus (DMH) (126). Thus the sympathoexcitatory neurons of the DMH can excite the premotor neurons, which are mainly located in the rostral raphe pallidus of the medulla (134).

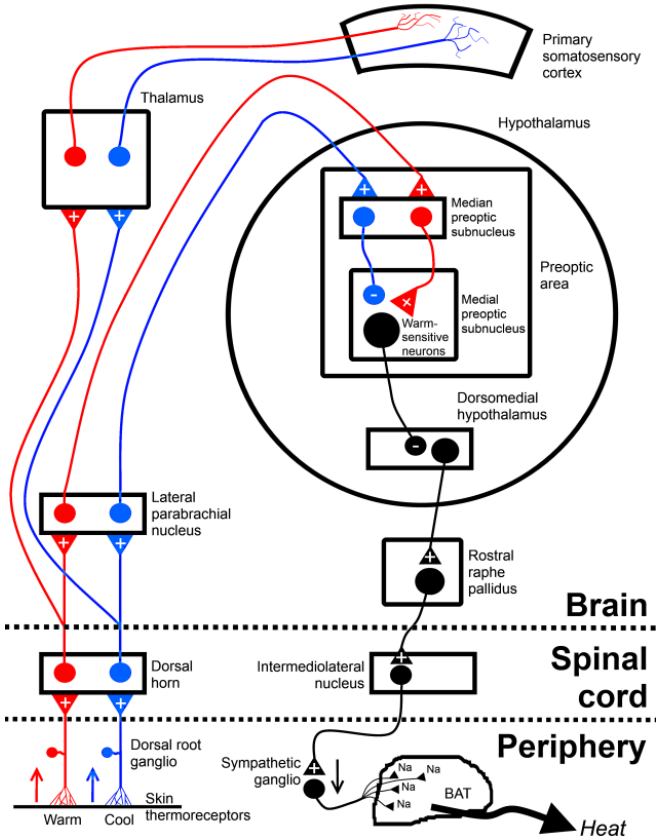

Figure 2. Principal neuroanatomical pathways regulating BAT thermogenesis
Thermal signals are mediated via the lateral parabrachial nucleus in the pons to the preoptic area (POA) located in the hypothalamus. Thermal signals also reach the thalamus and somatosensory cortex. In the median preoptic subnucleus (MnPO) of POA, interneurons are excited by either cold or warm signals. Cold signals inhibit the warm-sensitive neurons in the medial preoptic subnucleus (MPO) of POA, while warm signals have the opposite effect. These warm-sensitive neurons in turn have an inhibitory influence on the dorsomedial hypothalamus (DMH), whose neurons excite the BAT premotor neurons in the rostral raphe pallidus of the medulla. Further, the BAT sympathetic preganglionic neurons in the intermediolateral nucleus are connected to the rostral raphe pallidus via excitatory nerves. Finally, BAT-activating signals are mediated by the peripheral SNS. Modified from Morrison et al., 2012 (126).

The premotor neurons project to the BAT sympathetic preganglionic neurons in the spinal intermediolateral nucleus (IML). The neurons in the sympathetic ganglia innervate BAT (126). The initial increase in HR in response to cold exposure is also sympathetically mediated (135).

It is of note that the function of neuropeptide Y in the DMH seems to have an essential role in modulating the SNS signals to BAT (136). It is also suggested that the orexinergic neurons modulate BAT thermogenesis via the rostral raphe pallidus (137). Further, the peripheral vagal afferent nerves may also have a role in regulating BAT function. For example, at least the suppressive effect of ghrelin on BAT activity is eliminated by vagotomy (138). Interestingly, it has also been demonstrated in adult humans that vagal nerve stimulation for refractory epilepsy increases EE, which is associated with an increase in BAT activity (139).

It has also been proposed that, instead of cold thermal signals, cutaneous warm signals act via the excitatory glutaminergic interneurons of MnPO on the warm-sensitive neurons in MPO. Subsequently, the warm-sensitive neurons could increase their inhibition of the sympathoexcitatory neurons in DMH (126).

The CNS network controlling skeletal muscle activity during cold-induced shivering is not as well understood, but it presumably includes the transmission of cutaneous cold signals through the LPB, integration of thermoregulatory signals in the POA and activation of the motor neurons, which is dependent on the rostral raphe pallidus (140).

2.3.2 Effects of cold exposure on cerebral metabolism in humans

Despite the frequency in everyday life and potential medical implications of cold exposure, remarkably few studies related to cold-induced cerebral metabolic responses have been carried out. Further, the results of these studies are somewhat varied, possibly because different imaging modalities and cold exposures have been applied.

By using ultrasound imaging, it has been suggested that blood flow velocity increases in the posterior cerebral artery in healthy humans during the cold pressor test (141). Further, by measuring regional blood flow with PET, it has been shown that a painful cold stimulus to the left hand activates large areas in the brain: the sensorimotor, premotor and anterior cingulate cortices, anterior insula and lenticular nucleus on right side, and ipsilaterally the lateral prefrontal and anterior cingulate cortices, insula, parts of precentral cortex and the thalamus (142). The cerebellar vermis may also be activated by the cold pain stimulus (142). In a functional magnetic resonance imaging (fMRI) study, the cold-induced activation of the thalamus, insula, cingulate, somatosensory, precentral, premotor and motor cortices has also been described (143). An fMRI study also suggests that a pain-causing cold stimulus activates the secondary somatosensory cortex, while mild cold exposure only activates the thalamus and insula (144). A PET study also suggests that the perceived intensity of cold is associated with activation in the ipsilateral insular and orbitofrontal cortices (145).

Whole-body cooling has also been applied, and subsequently, regional blood flow, as measured with PET, has been shown to increase bilaterally in the somatosensory, anterior cingulate cortices and insula (146). Further, whole-body cooling-related discomfort has been linked to the activation of both amygdalas (147), and mild whole-body cooling to the activation of the rostral raphe pallidus (148), as assessed with fMRI. Slight, although not statistically significant, cold-induced increase in glucose metabolism in the brain has also been suggested in patients with vagal nerve stimulation for refractory epilepsy (139). However, only one study on the effect of cold exposure on cerebral glucose metabolism in healthy humans has previously been carried out, and the study suggests that the cortex has an inhibitory influence on the brain autonomic centres, which control general sympathetic responses (149). Thus, a decrease in cortical activity was found in conjunction with whole-body cold exposure (149). It should be pointed out that this study did not account for the differences in the plasma clearance of the glucose analogue PET tracer between thermoneutral and cold conditions, although cold exposure most likely induced changes in the glucose uptake of various tissues in the body.

Very little is also known about the role of CNS in activating human BAT. There are only two studies that address the relationship between human BAT activity and cerebral function. In one study it was demonstrated in patients who underwent diagnostic PET scans, that incidentally detected BAT activity is associated with increased metabolism in the right inferior parietal lobule and hypometabolism in the left insula and right cerebellum (150). The other study

suggested that, compared to the BAT-negative participants, the BAT-positive participants have lower activity in the inferior parietal lobule, limbic system and frontal lobe, and higher activity in the precuneus, as estimated by 2-deoxy-2-[^{18}F]fluoro-D-glucose-([^{18}F]FDG)-PET (151). However, no prospective studies with cold exposure, which is essential for activating BAT, and quantitative modelling of cerebral metabolism, have previously been carried out to elucidate the BAT-controlling mechanisms in the human brain.

2.4 Metabolism in brown adipose tissue

This chapter emphasises the important basic findings related to the metabolism of BAT. Current understanding of the metabolic processes in BAT is mostly derived from preclinical studies on rodents or cell cultures.

2.4.1 Regulation of thermogenesis in brown adipocyte

The SNS has widespread connections to various tissues in the body, including adipose tissue (Table 1). Differences exist between species in the distribution of the adrenergic receptors and their contribution to the regulation of metabolism in the white and brown adipocytes.

Cold exposure elicits an elevation in the tone of the peripheral SNS (152). BAT is provided with a dense network of sympathetic nerve endings that release NA onto adrenergic receptors (ARs) on the brown adipocyte surface (3) (Fig. 3). All three main types of adrenergic receptors (α_1, α_2 and β) are present on brown adipocytes (9).

Table 1. Receptors of the sympathetic nervous system in some tissues

Tissue	Main receptor(s) in the tissue	Main effect(s) of stimulation
Radial muscle of iris	α_1	Mydriasis
Ciliary muscle	β_2	Relaxation for far vision
Heart	β_1, β_2	Heart rate ↑ Force of contraction ↑ Rate of conduction ↑
Arterioles		
Skin	α_1	Vasoconstriction
Abdominal viscera	α_1	Vasoconstriction
Kidney	α_1	Vasoconstriction
Most skeletal muscles	α_1, β_2	Weak vasoconstriction
Lungs		
Airways	β_2	Bronchodilatation
Glands	α_1, β_2	Secretion ↓
Liver	α_1, β_2	Glycogenolysis and gluconeogenesis
WAT	α_2, β_1, β_2	Lipolysis
BAT	α_1, β_1, β_3; α_2	Lipolysis and thermogenesis ↑; Lipolysis and thermogenesis ↓
Sweat glands	Muscarinic; α_1	Generalised sweating; localised sweating
Piloerector muscles	α_1	Contraction
Adrenal medulla	Nicotinic	Secretion of adrenaline and noradrenaline
Salivary glands	α_1, β_2	Secretion of saliva
Intestine		
Motility	α_1, β_2	Decreased
Sphincters	α_1	Contraction
Exocrine pancreas	α	Enzyme secretion ↓
Pancreatic β cells	α	Insulin secretion ↓
Detrusor muscle	β_2, β_3	Relaxation
Kidney	β_1	Renin secretion ↑

The principal actions of the sympathetic stimulation in the body are described. Modified from McCorry, 2007 (153).

Of the three subtypes of β-adrenoceptors (β_1, β_2 and β_3), the β_3-adrenoreceptor is presumably the most important in mature brown adipocytes (154), mediating most significantly thermogenesis (155–156). However, in the brown preadipocytes, the stimulation of the β_1-adrenoceptor, but not the β_3-adrenoceptor, mediates cell proliferation (157). It is likely that the β_2-adrenoceptors are not significantly expressed in brown adipocytes (158).

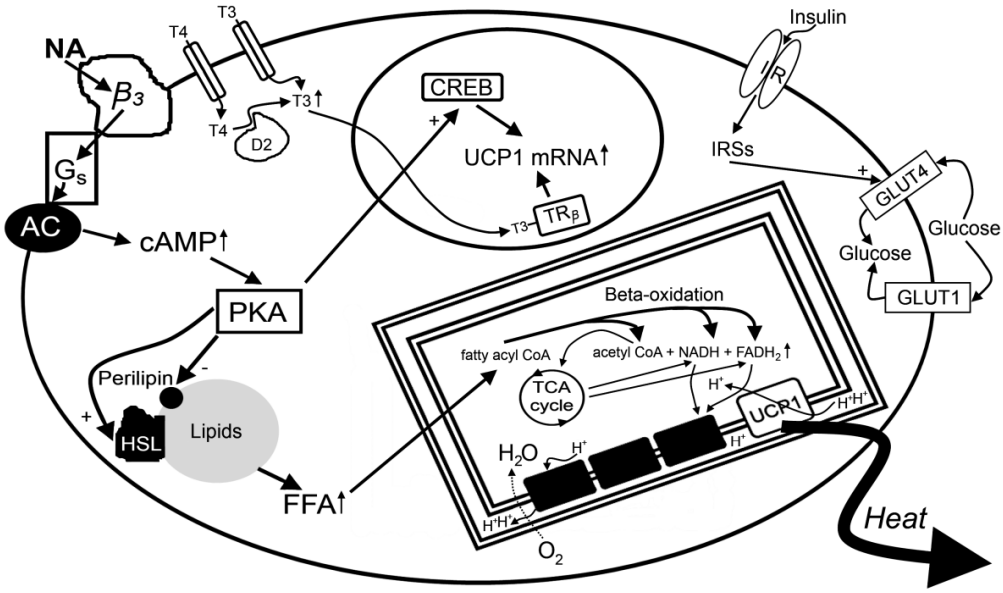

Figure 3. Schematic illustration of key regulatory pathways in brown adipocyte
NA acts through G_s protein-coupled β_3-adrenoreceptors to activate AC, which produces cAMP. The intracellular cAMP activates PKA, which phosphorylates CREB, uniquely inducing UCP1 messenger ribonucleic acid (mRNA) expression in brown adipocytes. The enzyme that converts thyroxine (T4) to triiodothyronine (T3), type 2 5′-deiodinase (D2), is also activated by PKA. Subsequently, the thyroid hormone receptor β (TRβ) with its ligand, T3, induces UCP1 gene expression in the nucleus. PKA phosphorylates HSL and perilipin, and thus, fatty acids are released. Fatty acids are the main fuel of thermogenesis, but glucose is also consumed. Unlike NA, insulin does not induce thermogenesis, although GLUT4 is the most important glucose transporter in the brown adipocyte. During thermogenesis, glucose probably enters glycolysis, or it may be utilised in the TCA cycle. Fatty acids move to mitochondria where they are beta-oxidised. The beta-oxidation and the TCA cycle provide reduced coenzymes, acetyl CoA, nicotinamide adenine dinucleotide (NADH) and flavin adenine dinucleotide (FADH), to the electron transport chain generating a proton gradient. The electron transport chain is uncoupled from the ATP synthase by the UCP1 allowing protons to move through the inner mitochondrial membrane. Thus, heat is generated. Modified from Cannon et Nedergaard, 2004 (9).

NA acts through the stimulatory G protein (G_s)-coupled β_3-adrenoreceptor to activate adenylyl cyclase (AC) (159), an enzyme that converts ATP to 3'-5'-cyclic adenosine monophosphate (cAMP) in cytoplasm (160). The cAMP works as a second messenger of the adrenergic signalling pathway by binding to the regulatory subunits of protein kinase A (PKA), and thus, activating the enzyme (161). Subsequently, the PKA phosphorylates a number of proteins (9), for instance, the cAMP-response-element-binding protein (CREB) (162), the peroxisome proliferator-activated receptor γ coactivator 1α (PGC-1α) (163) and the p38 mitogen-activated protein kinase (p38 MAPK) (164), which regulate the expression of the thermogenic genes, most importantly the UCP1. Stimulation by the NA also inhibits apoptosis of the brown adipocytes (165).

The activation of the α_1-adrenoceptors in brown adipocytes by the NA also leads to increased thermogenic activity. Thus, the phosphorylation of CREB is induced not only by the β_3-adrenoreceptor route but also by the α_1-adrenoceptor-mediated pathway (162). The stimulation of the α_1-adrenoceptors also results in increased intracellular calcium ion concentration, which is thought to be important for the thermogenic function of the brown adipocyte (166).

Interestingly, the α_2-adrenoceptors are also present in brown adipocytes, and they are coupled to the inhibitory G proteins that decrease the activity of AC (159). It is, however, not fully clear how the stimulatory and the inhibitory adrenergic pathways act in concert to maintain functional balance in the thermogenic activity and capacity of BAT (9).

Finally, it should be pointed out that the cascades described above represent a simplified perception of the regulation of the brown adipocyte, since many of the molecular mechanisms that control BAT thermogenesis are probably as yet undetermined (167). In fact, it was recently discovered that, without any involvement of the SNS and stimulation by NA, the brite adipocytes can directly respond to low temperatures by thermogenesis, whereas the classical brown adipocytes seem to lack this characteristic (168).

2.4.2 Utilisation of substrates by brown adipose tissue

The main energy substrates of BAT thermogenesis are fatty acids, either released from lipid droplets within the cell or cleared from the circulation, although glucose is also consumed.

Lipolysis, i.e., the hydrolysis of triacylglycerols from lipid droplets within the cell into glycerol and fatty acids, induces thermogenesis in brown adipocytes per se, and in fact, no thermogenesis can be elicited without simultaneously initiating lipolysis. It has been postulated that fatty acids influence the activity of UCP1 or its transport to the mitochondria (9). In mature brown adipocytes, lipolysis is physiologically stimulated by NA, presumably mainly via β_3- and α_1-adrenoceptors (155, 162). Subsequently, cytosolic cAMP is increased, resulting in activation of the PKA (169) (Fig. 3). PKA phosphorylates perilipin, which dissociates from the lipid droplet (170), exposing it to the action of hormone-sensitive lipase (HSL), which is also thought to be activated by the PKA (171). Adipose triglyceride lipase (ATGL) also has an important role in the first step of lipolysis in adipocytes (172). In the cytoplasm, fatty acids are presumably bound to fatty acid binding proteins (173–175) and subsequently, moved across the inner mitochondrial membrane by diffusion, or in the case of long carbon chains, by the carnitine shuttle (176). Inside the mitochondria, fatty acids are beta-oxidised – a process in which fatty acids are degraded, generating the acetyl coenzyme A, which enters the tricarboxylic acid (TCA) cycle. In general, this catabolic pathway of fatty acids is thought to work similarly in brown adipocytes as in other eukaryotes (9).

FFAs are also cleared from the circulation by BAT. Cold exposure and NA stimulate lipoprotein lipase synthesis (177), which leads to the clearance of triacylglycerols from the circulating chylomicrons and lipoproteins. In fact, at least in short-term cold-acclimatised mice, BAT is shown to have a key role in triacylglycerol clearance in the body (178). Imported FFAs also seem to play a vital role for the function and maintenance of BAT, since a lack of the fatty acid transport protein results in decreased lipid droplets and defective thermogenesis (179).

Glucose is also cleared from the blood stream via transporters by brown adipocytes (180), and cold exposure markedly increases the rate of glucose uptake in BAT (181–182). The insulin-sensitive glucose transporter type 4 (GLUT4) is regarded as the main glucose transporter in brown adipocytes (183–184), and indeed, glucose uptake is significantly stimulated by insulin (185). However, the mechanism of insulin-stimulated glucose uptake is likely to be distinct

from the cold-activated NA-driven process (186), since cold exposure significantly increases glucose uptake despite low circulating insulin levels (181). It is as yet undetermined by which precise mechanism the NA-cAMP pathway influences glucose transport (9), but increased activity of the glucose transporter type 1 (GLUT1) has been proposed (187–188).

It has been estimated that only a small fraction (2–16%, depending on the degree of activation) of energy is derived from glucose (189–190), and that fatty acids are the main fuel during adrenergic-mediated thermogenesis in the BAT of rats (189). Further, a study on β_3-agonist-treated rats suggests that fatty acids inside the brown adipocyte are the initial fuel for thermogenesis, while the role of the FFAs cleared from the bloodstream becomes more important as thermogenesis continues (191). The fate of glucose inside the brown adipocyte is somewhat disputed; glucose is either channelled solely to glycolysis (189), or it may be utilised to replenish the TCA cycle during thermogenesis (192).

2.4.3 Uncoupling of oxidative phosphorylation

The beta-oxidation and TCA cycle provide the electron transport chain with reduced coenzymes for oxidation. The transfer of electrons through the respiratory chain establishes a mitochondrial membrane potential, i.e., a proton gradient across the inner mitochondrial membrane (176).

The brown adipocytes uniquely express UCP1 (4), which uncouple the respiratory chain from ATP synthesis in the mitochondria (5). That is to say, UCP1 elicits a loss of the proton gradient between the mitochondrial matrix and the mitochondrial intramembranous space by allowing the protons leak through the inner mitochondrial membrane without the generation of ATP (9). This discharge of the proton gradient is accompanied by generation of heat, in other words, dissipation of energy. The key role of UCP1 in cold-induced thermogenesis has also been demonstrated indirectly in mice with a deletion of the UCP1 gene (193).

Interestingly, additional uncoupling proteins have also been identified, the uncoupling proteins-2–5 (Table 2), but these proteins are not related to non-shivering thermogenesis in BAT (194), and probably not in skeletal muscle either (104).

Table 2. Uncoupling proteins currently identified

UCP	Tissue distribution of gene expression	Physiological function
1	BAT	Facultative thermogenesis
2	BAT, WAT, skeletal muscle, heart, kidney, lungs, spleen, macrophages, thymus, bone marrow, brain, gastrointestinal tract and liver	Adjustment of whole-body metabolic efficiency? Regulation of reactive oxygen species? Control of hormone secretion (e.g. insulin)?
3	Skeletal muscle, heart and BAT	Facultative thermogenesis in skeletal muscle? Regulation of reactive oxygen species?
4	Brain, testis and liver	Protects against oxidative damage?
5	Brain, testis and liver	Protects against oxidative damage? Brain development in early life?

Presently, five different uncoupling proteins have been specified in vertebrates. The tissue distributions of the UCPs, as defined by gene expression, are shown. Only the function of the UCP1 is clearly characterised, but several roles have been proposed for the other UCPs in the physiology. After Erlanson-Albertsson, 2002 (195).

Detailed knowledge of how the uncoupling proteins actually function at the molecular level is currently lacking. It has been postulated that fatty acids act either as allosteric regulators of UCP1, as cofactors, or as proton shuttles during the uncoupling (9).

2.4.4 Insulin and brown adipose tissue

Insulin markedly affects glucose metabolism in most tissues. Insulin binds to insulin receptor (IR) on the cell surface, which causes autophosphorylation of the tyrosine residues of the receptor, and subsequently, phosphorylation of the insulin receptor substrate proteins (IRSs) inside the cell (196). The IRSs mediate the insulin's anabolic effects, for instance, glucose uptake and synthesis of triacylglycerols (197).

Insulin has been shown to stimulate glucose uptake in brown adipocytes (198–200). The increased glucose uptake is achieved by insulin-sensitive GLUT4 (201), whose translocation is thought to be mediated by IRS-2 (202). Insulin also enhances the gene expression of GLUT4 (203), whereas the stimulation by NA represses it during fasting (204). GLUT1 does not seem to contribute to the insulin-stimulated glucose uptake in brown adipocytes (205).

In general, insulin inhibits the action of HSL in adipose tissue (206), but it also enhances lipoprotein lipase activity in BAT (207), thus probably providing FFAs primarily for storage (208). In fact, no synthesis of lipids takes place without insulin (209). Indeed, insulin is required for the maintenance of BAT thermogenic capacity, since NA-induced expression of the UCP1 gene is dependent on insulin when the cells are cultured for long periods (210). Studies also suggest that chronic insulin deficiency decreases the thermogenic capacity of BAT (211–212). In concert, disrupted insulin signalling in adipose tissue leads to a significantly reduced thermogenic metabolism in BAT (213).

However, insulin does not seem to stimulate thermogenesis in brown adipocytes directly (190, 214), but it may promote BAT thermogenesis via central mechanisms, for instance, by inhibiting the warm-sensitive neurons in hypothalamus (215). Insulin also potentiates cold-induced glucose uptake in BAT (216).

Studies on rodents with increased quantities of BAT provide support for the concept that insulin-sensitive BAT is beneficial for whole-body glucose metabolism (217–218). Further, it has been shown in mice that BAT-derived hormonal factors also affect the insulin sensitivity of other organs, such as the WAT and the myocardium, thereby contributing to a more insulin-sensitive phenotype (219). Interestingly, even in type 1 diabetes, the amelioration of glucose homeostasis might be possible by increasing the amounts of BAT in the body (220).

2.4.5 Diet-induced thermogenesis

In general, weight gain is associated with increased whole-body resting EE in rodents (221) and humans (222). Interestingly, it has been shown in sedentary young men that overfeeding does not automatically result in equal increases in body mass and composition, but identical twins have rather similar responses to positive energy balance (223), implying individual responses to excess energy intake.

Intake of food, especially carbohydrates, increases the activity of SNS (224). The idea of diet-induced BAT thermogenesis is based on observations according to which increased SNS and BAT metabolic activities in diet-induced obesity are accompanied by lower weight gain than expected from caloric intake in rodents (225). Meals have an acute effect on BAT activity (226), but in genuine diet-induced BAT thermogenesis, the capacity of BAT to respond to a meal is enhanced in a chronic fashion (9). It has been shown that specific neurons in the locus coeruleus in the brain adapt their tone according to extracellular glucose concentration, leading to increased BAT-sympathetic activity (227). The concept of diet-induced BAT thermogenesis is widely acknowledged, although it has also been disputed by arguing that the function of

BAT is to defend body temperature under cold conditions, and not to dissipate energy in an environment with a wealth of calories (228). Indeed, from this evolutionary point of view, the doubtful conclusion is very rational. Further, the results of rodent studies relating to diet-induced thermogenesis seem to be rather equivocal.

Rats fed with a carbohydrate-rich diet showed increased BAT thermogenesis (229). Further, under NA stimulation, cafeteria-fed rats demonstrated larger BAT oxygen consumption than did the control animals (230), implying enhanced BAT capacity. Moreover, a 2–3-fold elevation of BAT UCP1 expression in response to dietary fat (231) and an increment of BAT blood flow after a single low-protein, high-carbohydrate meal (232) have also been observed in rodents. Further, a diet rich in essential fatty acids stimulates BAT thermogenesis (233), and moreover, the genetic ablation of BAT causes obesity even before hyperphagia develops in mice (234).

However, rodent studies also suggest that BAT oxygen consumption is not increased by diet-induced thermogenesis (221, 235), and that despite UCP1 deficiency, EE is increased in diet-induced obesity (236), suggesting that other tissues rather than BAT are actually mainly responsible for elevated EE. Further, UCP1-ablated mice are cold-sensitive but not necessarily obese (193), although at thermoneutrality, the lack of UCP1 clearly results in obesity and defective diet-induced thermogenesis (237). In addition, cold acclimation seems to enhance BAT capacity to a similar degree in rats fed with or without restriction of energy intake (238), suggesting that the cold recruitment of BAT is not significantly affected by food intake.

However, there are numerous rodent studies on leptin – a hormone that acts via the hypothalamus (239), and whose concentration in the blood is positively associated with the amount of WAT in the body (240) – demonstrating the stimulatory effect of leptin on BAT thermogenesis. Therefore, it can be postulated that diet-induced obesity activates BAT, which could provide a counteractive force to weight gain in the long-term. It has been shown that leptin treatment increases BAT UCP1 expression (241–242), which is mediated by the increased sympathetic outflow to BAT (243–244). On the other hand, mice genetically lacking leptin, show decreased activity in BAT mitochondria (245), which indirectly implies that leptin promotes BAT capacity. However, it should be pointed out that leptin also acts as a satiety factor (246), and therefore, the stimulatory effect of leptin on BAT is probably not the only anti-obesity aspect in its physiological function.

Taken together, it is probable that some dietary factors can induce BAT thermogenesis in the short-term, but it is not fully clarified, whether diet-induced thermogenesis is robust enough to counteract concurrent excess intake of energy in the long-term.

2.4.6 Thyroid function and brown adipose tissue

The hypothalamic TSH-releasing hormone (TRH) stimulates TSH secretion from the anterior pituitary, and this process is affected by feedback from circulating thyroid hormones (247). Subsequently, TSH acts on the TSH receptor (TSH-R) on the thyroid gland, leading to synthesis and secretion of the thyroid hormones, thyroxine (T4) and triiodothyronine (T3) (247).

TSH-Rs are also present in adipose tissue (248–249), and interestingly, TSH-R activation has been linked to increased UCP1 expression in human orbital preadipocytes (250). Further, a study in mice suggests that TSH-R in brown adipocytes and stimulation by TSH are involved in the expression of UCP1, and thus, in the generation of cold tolerance (251).

The role of T4 and T3 in the regulation of BAT thermogenesis has been studied using both animal and *in vitro* models (252). Brown adipocytes actively convert the prohormone T4 to T3, in order to sustain increased metabolism during thermogenesis (253) (Fig. 3). In fact, the enzyme responsible for converting T4 to T3, type 2 5′-deiodinase (D2), is actually vital for the development of BAT (254), and for the cold-activated (255) and diet-induced (256) functions of BAT. The activity of D2 is increased by adrenergic stimulation (257). The thyroid hormone receptor (TR) gene has two major isoforms, TRβ and TRα (258). Studies in mice indicate that TRβ is required for UCP1 induction, and thus, it is essential for BAT function as well (259) (Fig. 3). The TRβs with no T3-ligand act as repressors of UCP1 mRNA expression. The function of T3 is to decrease this repression by binding to the TRβ. The TRα in turn seems to be involved in the thyroid hormone-dependent augmentation of adrenergic signalling in BAT (260).

Interestingly, activated BAT might also have a role in controlling the circulating levels of thyroid hormones since, at least in rodents, BAT is able to generate T3 for the circulation (261). Thyroid hormones have also been shown to affect the hypothalamus with subsequent activation of BAT in rats, leading to increased EE (262). It has in fact been found that systemic hyperthyroidism as well as central administration of T3 leads to activation of the SNS, and subsequently to BAT thermogenesis (262). Finally, an intriguing finding suggests that bile acids increase EE in brown adipocytes by elevating the activity of D2 (263). However, in experimental thyrotoxicosis in rats, increases in lipid metabolism were found in many tissues with the exception of BAT, where FFA uptake was actually found to be decreased (264). It is hypothesised that intense thermogenesis during thyrotoxicosis evokes a compensatory decrease in the sympathetic stimulation to BAT (264).

Very little is known about the effects of hypothyroidism on BAT. It has been suggested that induced hypothyroidism does not have any significant influence on BAT lipid metabolism (264), but also that it prevents the mobilisation of lipids (265). A study implies reduced thermogenic activity in hypothyroidism (266). Further, hypothyroidism might decrease the capacity of BAT to respond to adrenergic stimulation by causing a functional alteration in the AC in the plasma membrane of brown adipocytes (267).

Increased thyroid function has been detected in humans chronically exposed to a cold environment (268), but the role of the thyroid gland in the regulation of human BAT is largely undetermined. However, it has been shown that hyperthyroidism increases glucose uptake in human BAT (269). In addition, a case report, regarding a patient on TSH-suppressive levothyroxine therapy (200–250 μg • d^{-1}) for papillary thyroid cancer, has been published, and this study also suggests that the thyroid hormones induce BAT metabolism (270). Further, it has been shown that T3 treatment increases the expression of UCP1 in differentiated human multipotent adipose-derived stem cells, suggesting that T3 can induce a brown phenotype within WAT (271).

2.4.7 Blood flow in brown adipose tissue

BAT has abundant capillary vessels, which provide nutrients for BAT but also transfer heat elsewhere in the body during thermogenesis. Interestingly, the vessel structures in BAT also have certain unique characteristics, which at least enable the use of specific ligands to distinguish BAT from WAT (272).

Early and indirect measurements with rubidium-86 suggested that blood flow in the BAT of squirrels is markedly enhanced when BAT is metabolically active during arousal from

hibernation (273), and that stimulation by NA increases BAT blood flow in rats (274). It was also shown by direct invasive measurements that NA significantly increases blood flow in the BAT of rabbit (275), and that this effect can be reduced by an antisympathomimetic drug (276). Later, the utilisation of radioactive microsphere techniques (277) clearly showed that BAT blood flow in rodents robustly increases when the animals are exposed to a cold environment (278–280). BAT blood flow in mice has also been evaluated recently by a nuclear imaging based method (281).

Current evidence suggests that brown adipocytes express both endothelial and inducible nitric oxide synthases (eNOS and iNOS, respectively) in response to sympathetic stimulation (282–284), which presumably induces vasodilation in BAT (285). In general, the blood flow of a tissue is increased together with elevated oxygen consumption (286), and there is no reason to think otherwise in the case of BAT. Indeed, vasodilation in the rodent BAT seems to be closely related to the oxygen-consuming thermogenic response (287–288). The connection between thermogenic metabolism and blood flow has also been shown indirectly in UCP1-ablated mice, since they fail to increase BAT blood flow in response to β_3-adrenoreceptor activation, while BAT blood flow in wild-type mice is increased (289).

2.4.8 Energy expenditure by brown adipose tissue

The wide medical interest in BAT ultimately arises from the fact that BAT has an enormous capacity to consume energy when it is activated, as shown in rodents. Activated BAT produces heat and thus dissipates energy in an effortless manner. Physiologically, BAT is primarily activated by cold exposure, but pharmaceuticals – clearly shown with β_3-adrenoceptor agonists – can also increase EE by BAT. BAT metabolism may also be promoted by dietary factors (diet-induced thermogenesis) and perhaps even by physical exercise (80).

The capacity of BAT in rodents to produce heat is greatly enhanced by chronic cold exposure (adaptive thermogenesis) (290). Calculations, based on changes in tissue blood flow, suggest that cold-induced BAT thermogenesis could account over 40% of total oxygen consumption, i.e., over 40% of whole-body EE, after cold acclimation (279). Interestingly, BAT thermogenesis has also been linked to cancer cachexia – a phenomenon characterised by increased EE and decreased appetite – since the thermogenic capacity of BAT is elevated in mice implanted with neoplasms (291–292). Whether BAT also plays a role in increased EE in human cancer patients is still unclear, albeit evidence suggests such an involvement (293–294).

2.4.9 β_3-adrenoceptor agonists and brown adipose tissue

An “atypical β-adrenoceptor”, subsequently named the β_3-adrenoceptor, was identified in 1984, when it was realised that the commonly used β_1- and β_2-antagonists could not block lipolysis and thermogenesis in BAT, which were elicited by novel β-agonists (155). Subsequently, the gene of the β_3-adrenoceptor has been cloned in humans (295), mice (296) and rats (297). The β_3-adrenoceptor is considered to be the main adrenoceptor of brown adipocytes (154), and the gene expression and function of the β_3-adrenoceptor have been demonstrated in humans (298–299). The β_3-adrenoceptors are also expressed in human white adipocytes (300).

The β_3-adrenoceptor-mediated pathway is important for the function of BAT. It has been demonstrated that a reduced amount of β_3-adrenoceptors in the adipose tissue of rodents is related to obesity (301–302). Further, the capacity of β_3-agonists to stimulate BAT thermogenesis *in vivo* has been shown in multiple rodent studies (e.g. 303–305). Further, treatment of rodents with β_3-agonists has a weight-reducing effect that is accompanied by

increased BAT activity (e.g. 306–309). Thus even after a single dose of a β_3-agonist, BAT shows depletion of lipid droplets and increased mitochondrial activity, while chronic treatment causes BAT hypertrophy and improves cold tolerance (306). Stimulation of rodent BAT by β_3-agonists is also beneficial for glucose homeostasis, since these drugs increase glucose uptake in BAT *in vitro* (310), and most importantly, the treatment results in enhanced glucose tolerance at whole-body level (e.g. 311–314). The increased glucose disposal might also partly be due to the increased insulin sensitivity of WAT (315).

It should be noted that, so far, it has not been shown whether selective β_3-agonists can stimulate human BAT as well.

2.5 Physical basis of positron emission tomography

PET imaging is based on simultaneous detection (within ~10 ns) of two photons that are travelling in opposite directions (~180 º angle) and have a specific energy (511 keV each) (316). The two photons are generated by a physical phenomenon called annihilation, which denotes the collision between a particle and its antiparticle. In the case of PET, positron-emitting short-lived isotopes (typical half-lives 2–110 min) are utilised, and therefore, the detected photons originate from a collision between a positron and an electron (317). It is of note that the emitted positron proceeds a few millimetres in its environment before the annihilation occurs, and this distance is dependent on the used isotope, also affecting the spatial resolution of the imaging slightly (318).

In the PET scanner, the detector elements are made from scintillation crystals, and they are assembled in a ring form around the object being scanned. Further, the opposite detectors are connected to form a pair (316). The detection of the two gamma photons by the pair-connected detectors is called a coincidence event, and the annihilation is assumed to have occurred on the straight line between the two detectors. Millions of coincidence events provide information about the position of the annihilation events in the body (318). It should be pointed out that the detection of the two photons provides a significantly better sensitivity, spatial resolution and quantification of data, as compared to the more common gamma cameras (319). New PET scanners are also equipped with the capability of measuring the time difference between the two photon detections (time-of-flight), providing a better signal-to-noise ratio in PET images (320). Eventually, the PET image is reconstructed on the basis of the detected coincident events. In general, the PET data is corrected for photon attenuation, physical decay, system dead time, scattering photons and random coincidence events (321).

2.6 Preclinical nuclear imaging of brown adipose tissue

This section briefly summarises what is known about factors affecting nuclear imaging of BAT. BAT in rodents has been shown to be metabolically active by using a number of different radioactive tracers, but here, only studies that demonstrate the accumulation of a tracer in BAT via imaging, have been included. PET is the most widely used imaging modality for visualising BAT in rodents.

At first, it was shown by scintigraphy of sacrificed rats that interscapular BAT has a marked uptake of ^{123}I- and ^{125}I-labelled metaiodobenzylguanidine (MIBG), indicating rich sympathetic innervation (322). Thereafter, it has been shown using non-invasive [^{18}F]FDG-PET/CT that both ketamine-anaesthesia and cold exposure increase and that propranolol decreases BAT activity in rats, while diazepam has no apparent effect (323). It is of note that measured [^{18}F]FDG activity reflects glucose uptake in the tissue.

Currently, many physiological and pharmacological experiments have been performed to study the characteristics of the metabolism of rodent BAT. In order to reliably assess BAT function in mice using [^{18}F]FDG-PET/CT, an imaging protocol for BAT imaging has been described (324). Mice kept under fasting conditions on a heating pad have been shown to have lower [^{18}F]FDG uptake in BAT than do freely-fed mice kept at normal room temperature (325). Further, NA and cold exposure have a synergistic effect on BAT glucose metabolism as expected (326), and β_3-agonists (327–328), the AC activator forskolin (328) and the NA reuptake inhibitor atomoxetine (328–329) can increase BAT metabolism, as shown using [^{18}F]FDG-PET/CT. Blood flow in BAT has also been shown to be increased after β_3-agonist administration, as estimated using ^{99m}Tc-methoxyisobutylisonitrile-SPECT/CT showing blood flow-related tracer accumulation (281). SNS activity in BAT can also be studied with the help of an NA analogue (330), and NA transporters of BAT can be visualised with PET, using a selective ligand in rodents (331). Further, by using single photon emission computed tomography (SPECT), a ^{125}I-labelled 1-benzazepin-2-one analogue, which is a voltage-gated sodium channel blocker used to study neurotransmission, has been shown to bind to the BAT of mice (332). The effects of insulin on the BAT glucose uptake of rats have been demonstrated using [^{18}F]FDG-PET/CT in conjunction with a hyperinsulinaemic-euglycaemic clamp (333) and insulin administration into the POA (215). Interestingly, nicotine seems to have a more profound augmenting effect on BAT [^{18}F]FDG uptake than does ephedrine, while caffeine does not seem to have any significant effect in rats (334). Furthermore, stressful situations, such as burn injuries and cutaneous wounds, also increase BAT activity in mice, as visualised with the help of [^{18}F]FDG-PET (335–336). BAT [^{18}F]FDG uptake might also be affected by the circadian rhythm (337–338). However, gastric bypass surgery in rats does not seem to increase BAT metabolism, as measured with [^{18}F]FDG-PET/CT (339).

2.7 Human brown adipose tissue

2.7.1 Early studies on human brown adipose tissue

Even before the presence of the BAT organ in humans was formulated in 1902 (39), distinct cells, at the time called ‘mulberry fat cells’, had been identified by H. Batty Shaw in the axillary, subpleural and perirenal regions of human foetuses and new-borns (340). Later, in 1908, an extremely detailed macroscopic anatomical depiction of cervical BAT in humans was provided by Edmond Bonnot (341). According to Bonnot, cervical BAT is an irregular paired organ in humans, and it is situated between the superior borders of the scapula and clavicle on the shoulder and the side of the neck, comprising a large process that extends towards the temporal bone. Further, cervical BAT was described as being recognisable to the naked eye, not only in infants but also in adult humans. However, at the time, it was not clear whether cervical BAT tissue was different from the BAT-like tissues found other regions in the body. Furthermore, despite the elaborate anatomical descriptions, the functional aspect of this special tissue was still to be revealed.

According to the classical autopsy study by Juliet M. Heaton in 1972, BAT is found less commonly in adults as compared with infants (342). According to Heaton, BAT is found in the neck and mediastinum, and close to the kidneys, adrenal glands and aorta in adult humans (342). A few years later, it was suggested that the prevalence of perirenal BAT decreases with age in humans, as post-mortem samples from adults demonstrate BAT histology less frequently (343).

UCP1 was isolated from BAT mitochondria and subsequently detected by a specific antibody in human infants in the 1980s (344). Furthermore, in an autopsy series, lower UCP1 protein contents were observed in adults and stillborn infants than in children (345), suggesting that the uncoupling capacity of BAT is physiologically most pronounced in childhood. Staining with a UCP1-specific antibody has also been demonstrated in histological human samples obtained from autopsies (346). On the basis of UCP1 and D2 contents in the interscapular BAT, it has further been suggested that BAT activity develops during the first half of the last trimester of gestation in humans (347).

Although BAT can also be found in humans constantly living in a warm environment (348), increased amounts of BAT have been linked in post-mortem studies to chronic cold exposure. It was in fact demonstrated that BAT is found in samples, mainly taken from adipose tissue around the carotid arteries in seven out of eleven outdoor workers in the Northern Finland, while it could not be detected in the control samples taken from indoor workers (66). Interestingly, on the basis of post-mortem samples, it has also been shown that the cervical BAT percentage is negatively correlated with waist circumference in men, even after adjusting for age (349).

2.7.2 Confounding factor in nuclear imaging

Already in the mid-1990s, a characteristic pattern of symmetrical uptake of the glucose analogue [^{18}F]FDG in the cervical region had been identified in conjunction with clinical PET imaging. At the time, this occasionally occurring metabolic activity was considered to be a manifestation of contraction of the cervical skeletal muscles, which was thought to be related to the anxiety of some patients undergoing diagnostic PET studies (350). Supporting this view, oral diazepam pre-medication seemed to lower the incidence of this confounding metabolic activity in diagnostic imaging (350). In the 1990s, it was also observed that one of the physiological uptake sites of ^{123}I-MIBG is symmetrically located in the upper thoracic regions, and that this phenomenon was more intense in children, although no speculation on BAT-related uptake was presented at the time (351).

However, when combined PET/CT devices became more common in the early 2000s, it was realised that the distinct pattern of increased [^{18}F]FDG uptake in the cervical region was actually situated in adipose tissue, not in skeletal muscle (11). The precise co-registration of metabolic and anatomic data with PET/CT enables more accurate interpretation of imaging results than stand-alone PET devices (352).

In 2002, it was postulated for the first time that the incidentally occurring metabolic activity in nuclear imaging of the cervical region might involve BAT (12). However, the true nature of this metabolic activity was not clarified until 2009, when conclusive evidence was provided through PET/CT-guided biopsies from supraclavicular adipose tissue that showed intense glucose uptake as response to cold exposure (**I**). Moreover, it was also shown that functional BAT is present in healthy adults (**I**), and thus BAT in humans is not exclusively related to malignancies or other pathological conditions, which are indications for using PET/CT. By the end of 2013, over 70 studies relating to incidentally detected putative human BAT in conjunction with clinical nuclear imaging had been published and listed in the PubMed search. The main conclusions of each of these studies are listed in Table 3.

Table 3. Studies on incidentally detected BAT in clinical nuclear imaging

The clinical nuclear imaging studies on detectable BAT in patients are listed in chronological order. Most studies are either retrospective analyses of PET images or case reports. If applicable, the frequency of BAT detection is reported, and it denotes prevalence or incidence of BAT in conjunction with clinical imaging. Studies on hibernomas and pheochromocytoma- or paraganglioma-related BAT are excluded from the listing.

Reference	Main imaging method(s)	BAT-positive (%)	Principal conclusion(s)
Hany et al., 2002 (12)	[^{18}F]FDG-PET/CT	2.5	The first postulation of human BAT visualisation is published; symmetrical cervical uptake.
Okuyama et al., 2002 (322)	^{123}I-MIBG-SPECT	10.4	Apparent BAT is found more often in children.
Cohade et al., 2003 (353)	[^{18}F]FDG-PET/CT	4.0	Supraclavicular uptake is distinct from skeletal muscle and malignancies.
Cohade et al., 2003 (354)	[^{18}F]FDG-PET/CT	4.1–13.7	Supraclavicular adipose tissue uptake is more common during winter months.
Okuyama et al., 2003 (355)	^{123}I-MIBG-gamma/SPECT	12.0	Symmetrical uptake in the cervical region of children might be BAT.
Fukuchi et al., 2003 (356)	^{99m}Tc-tetrofosmin-gamma	16.9	Uptake in the interscapular region of children 0–2 years old is sometimes observed.
Yeung et al., 2003 (41)	[^{18}F]FDG-PET/CT	2.3	Uptakes in paravertebral, perinephric and mediastinal fat are associated with the cervical fat uptake pattern. Cervical uptake is more common in females and in children.
Minotti et al., 2004 (357)	[^{18}F]FDG-PET/CT	-	Four case reports: hypermetabolic cervical adipose tissue.
Döbert et al., 2004 (294)	[^{18}F]FDG-PET/CT	17.3	BMI and age are lower in lymphoma patients with symmetrical supraclavicular uptake.
Bar-Shalom et al., 2004 (358)	[^{18}F]FDG-PET/CT	0.7	Infradiaphragmatic foci of adipose tissue uptake are found in 0.7% of patients.
Higuchi et al., 2004 (359)	[^{18}F]FDG-PET/CT, ^{201}Tl- / ^{99m}Tc-SPECT	-	A case report: increased ^{99m}Tc-sestamibi uptake, but no ^{201}Tl uptake in areas corresponding to [^{18}F]FDG uptake in presumed BAT.
Truong et al., 2004 (360)	[^{18}F]FDG-PET/CT	1.8	Presumed BAT is found in the paratracheal, -esophageal, and pericardial regions in 1.8% of patients.
Garcia et al., 2004 (361)	[^{18}F]FDG-PET/CT	-	Two case reports: control of temperature abolishes supraclavicular uptake.
Reddy et Ramaswamy, 2005 (362)	[^{18}F]FDG-PET/CT	-	A case report: supraclavicular uptake together with an adrenal region focus, both of which are eliminated after diazepam administration.
Gelfand et al., 2005 (363)	[^{18}F]FDG-PET	46.6	Uptake in BAT is reduced by intravenous fentanyl pre-medication in children and adolescents.
Castellucci et al., 2005 (364)	[^{18}F]FDG-PET/CT	0.7	Only 22.6% of increased non-malignant uptake was considered to relate to active BAT in patients treated for lymphoma.
Jacobsson et al., 2005 (365)	[^{18}F]FDG-PET	-	A case report: propranolol 2 h before [^{18}F]FDG injection reduces BAT uptake.
Heiba et al., 2005 (366)	[^{18}F]FDG-PET/CT	-	A case report: PET/CT helps to separate BAT from metastatic breast tumour.
Garcia et al., 2006 (367)	[^{18}F]FDG-PET	-	Controlling temperature reduces BAT activity in 10 patients.
Kim et al., 2006 (42)	[^{18}F]FDG-PET	2.8	Almost all mediastinal and periadrenal activity is related to supraclavicular and paravertebral BAT uptake, respectively.
Christensen et al., 2006 (368)	[^{18}F]FDG-PET	-	Warming manoeuvre reverses BAT activity in 9 out of 10 cases.
Rousseau et al., 2006 (369)	[^{18}F]FDG-PET/CT	45.4	Supraclavicular uptake is not associated with age or outdoor temperature in breast cancer patients.
Belhocine et al., 2006 (370)	^{99m}Tc-sestamibi-SPECT/CT	-	A case report: supraclavicular BAT uptake in a patient with primary hyperparathyroidism.
Söderlund et al., 2007 (371)	[^{18}F]FDG-PET	-	All 11 patients show complete or almost complete disappearance of BAT activity after a propranolol pre-

			medication when studied a second time.
Parysow et al., 2007 (372)	[^{18}F]FDG-PET	-	A significant reduction of uptake in BAT following propranolol administration in 26 cancer patients.
Wehrli et al., 2007 (373)	[^{18}F]FDG-PET	-	Dual-time point PET imaging method demonstrates increasing [^{18}F]FDG uptake in various apparent BAT regions.
Clarke et al., 2007 (44)	[^{18}F]FDG-PET/CT	4.5	2.1 and 2.4% of patients have limited and extensive BAT activity, respectively. Atypical uptake in the subcutaneous adipose tissue of thighs, abdomen, and pelvis in 2 men.
Kim et al., 2007 (374)	[^{18}F]FDG-PET	2.8	BAT is detected more often as an acute response to cold weather rather than to prolonged periods of cold weather.
Goetze et al., 2008 (375)	^{99m}Tc-MIBG-SPECT/CT	6.3	Uptake of ^{99m}Tc-MIBG in BAT in adults undergoing imaging for parathyroid diseases.
Wong et al., 2008 (376)	^{99m}Tc-sestamibi-SPECT/CT	-	A case report: cervical BAT in a 55-year-old woman imaged for suspected primary hyperparathyroidism.
Williams et Kolodny, 2008 (377)	[^{18}F]FDG-PET/CT	6.3–2.8	A high-fat, very-low-carbohydrate diet on the night before and on the morning of imaging lowers uptake in BAT.
Alkhawaldeh et Alavi, 2008 (378)	[^{18}F]FDG-PET	-	SUVmax for BAT ranges from 0.8 to 12.4 and BAT SUVmean is 4.6 ± 1.6.
Hyun et Kim, 2008 (379)	[^{18}F]FDG-PET/CT	-	A case report: uptake in apparent parahepatic BAT in a child.
Zukotynski et al., 2008 (380)	[^{18}F]FDG-PET	31.1–5.0	Room temperature at 24 ºC half an hour prior to and during the uptake, significantly decreases BAT activity in children.
Agrawal et al., 2009 (381)	[^{18}F]FDG-PET	-	BAT is not detected in 90% of patients after propranolol.
Sturkenboom et al., 2009 (382)	[^{18}F]FDG-PET	28.6–25.0	No significant effect of pre-medication with diazepam on the uptake of [^{18}F]FDG in the neck and upper chest regions in patients aged between 18 and 40 years.
Cypess et al., 2009 (14)	[^{18}F]FDG-PET/CT	7.5–3.1	Prevalence of BAT is higher in females (7.5 vs. 3.1%), and BAT activity is inversely correlated with age, outdoor temperature and beta-blocker use.
Cheng et al., 2009 (383)	[^{18}F]FDG-PET/CT	3.8	BAT-positive patients have lower male/female ratio, younger age, and lower BMI than BAT-negative patients.
Au-Yong et al., 2009 (384)	[^{18}F]FDG-PET/CT	4.6	Study suggests a strong seasonal variation in BAT activity, which is more closely associated with photoperiod than with ambient temperature.
Huang et al., 2009 (385)	^{67}Ga -SPECT/CT	-	A case report: a SPECT/CT scan shows Ga-67 uptake in supra- and subclavicular adipose tissue of a 10-year-old boy.
Baba et al., 2010 (386)	[^{18}F]FDG-PET/CT	-	A series of 23 patients: Hounsfield units in CT are increased in active BAT.
Hairil Rashmizal et al., 2010 (387)	[^{18}F]FDG-PET/CT	-	Based on one case, the authors state that dual time-point imaging may not be a reliable method to assess BAT activity.
Aukema et al., 2010 (388)	[^{18}F]FDG-PET/CT	16.0–3.6	Prevalence of BAT can be reduced from 16.0 to 3.6% by diazepam combined with controlled room temperature in breast cancer patients.
Pfannenberg et al., 2010 (389)	[^{18}F]FDG-PET/CT	-	BAT activity moderately declines with increasing age in females, but a stronger effect is found in males. Impact of BAT on adiposity decreases with aging in males.
Zukotynski et al., 2010 (390)	[^{18}F]FDG-PET	26.8–8.6	A constant 24 ºC for 30 min prior to and 1 h after tracer administration decreases BAT activity in children.
Lee et al., 2010 (391)	[^{18}F]FDG-PET/CT	8.5	BAT inversely correlates with BMI and blood glucose.
Esen Akkas et al., 2010 (392)	[^{18}F]FDG-PET/CT	-	In cases of atypical BAT uptake, CT helps to avoid false positive findings.
Ouellet et al., 2010 (393)	[^{18}F]FDG-PET/CT	6.8	Outdoor temperature, age, sex, BMI, and diabetes status are determinants of the prevalence, mass, and activity of BAT.
Lebron et al., 2010 (394)	[^{18}F]FDG-PET/CT	-	Two patients with Horner syndrome and one with surgical sympathectomy; unilateral uptake in BAT contralateral to the affected side is demonstrated.

Garcia et al., 2010 (395)	[^{18}F]FDG-PET	-	Controlling temperature reduces BAT uptake in 30 patients.
Gilsanz et al., 2010 (396)	[^{18}F]FDG-PET/CT	42.3	Paediatric BAT-positive patients have greater muscle volume than BAT-negative patients.
Hu et al., 2011 (397)	[^{18}F]FDG-PET/CT	47.5	In a paediatric population, higher Hounsfield units of CT image are associated with BAT activity.
Lee et al., 2011 (398)	[^{18}F]FDG-PET/CT	-	BAT is also found in biopsies from BAT-negative patients.
Yilmaz et al., 2011 (399)	[^{18}F]FDG-PET/CT	1.6	The presence of BAT in adults is associated with a lower frequency of non-alcoholic fatty liver disease.
Drubach et al., 2011 (400)	[^{18}F]FDG-PET	44.2	BAT activity increases from childhood into adolescence and it correlates inversely with BMI.
Ichimiya et al., 2011 (401)	[^{18}F]FDG-PET/CT	-	Subcutaneous fat necrosis is associated with lower [^{18}F]FDG uptake, and biopsies show brown adipocytes in 2 infants.
Pace et al., 2011 (402)	[^{18}F]FDG-PET/CT	8.6	In clinical imaging, the magnitude of BAT in the first scan and outdoor temperature are the strongest determinants of persistence of BAT in repeated scans.
Gilsanz et al., 2011 (403)	[^{18}F]FDG-PET/CT	58.9	The presence and volume of BAT increase during puberty.
Jacene et al., 2011 (404)	[^{18}F]FDG-PET/CT	6.2	BAT activity, blood glucose, BMI, sex, and age might be interrelated.
Huang et al., 2011 (405)	[^{18}F]FDG-PET/CT	1.7	Active neoplasm is associated with BAT activity.
Chalfant et al., 2012 (406)	[^{18}F]FDG-PET/CT	59.4	Based on PET imaging after successful treatment of cancer, the children with active BAT gain less weight during the follow-up.
Gilsanz et al., 2012 (407)	[^{18}F]FDG-PET/CT	9.7–77.4	In children, active BAT is found more often after recovering from lymphoma.
Huang et al., 2012 (408)	[^{18}F]FDG-PET/CT	1.9	The prevalence of BAT decreases by one percentage point for each 5 °C increase in outdoor temperature.
Skillen et al., 2012 (409)	[^{18}F]FDG-PET/CT	15.3–3.3	Thermal control reduces the incidence of BAT by 78%.
Vogel et al., 2012 (410)	[^{18}F]FDG-PET/CT	24.5–5.9	An audio-visual intervention lowers anxiety during tracer uptake, and thus it can lower confounding uptake in BAT.
Ponrartana et al., 2012 (411)	[^{18}F]FDG-PET/CT	-	BAT is positively associated with the amount of bone and the cross-sectional size of the femur in patients successfully treated for paediatric malignancies.
Cronin et al., 2012 (412)	[^{18}F]FDG-PET/CT	4.3	BAT-positive patients are more often females and leaner than BAT-negative patients.
Perkins et al., 2013 (413)	[^{18}F]FDG-PET/CT	9.8	BAT uptake is higher during the winter months in a subtropical climate but there are no differences with respect to patient ethnicity (black vs. white).
Persichetti et al., 2013 (414)	[^{18}F]FDG-PET/CT	3.5	Day length, outdoor temperature, age, sex, BMI, and plasma glucose are major determinants of the prevalence of detectable BAT in clinical imaging.
Harris et al., 2013 (415)	[^{11}C]MET-PET/CT	-	Low uptake of methionine in the BAT of children and young adults.
Cypess et al., 2013 (281)	^{99m}Tc-MIBI-SPECT/CT	5.4	Increased retention is found in cervical and supraclavicular BAT regions of patients imaged for parathyroid disorders.
Ahmadi et al., 2013 (416)	[^{18}F]FDG-PET/CT	-	Hounsfield units from -10 to -87 or from -88 to -190 indicate active BAT or WAT, respectively.

Note: ^{99m}Tc, technetium-99m; ^{201}Tl, thallium-201; SUV, standardised uptake value; ^{67}Ga, gallium-67; [^{11}C]MET, carbon-11-labelled methionine; MIBI, methoxyisobutylisonitrile.

On the basis of the studies listed in Table 3, some conclusions relating to human BAT can be drawn. Firstly, activated BAT is mostly found in the supraclavicular region and parallel to the thoracic spine, but mediastinal and infradiaphragmatic foci also exist in some individuals. Secondly, retrospective studies suggest that active BAT is more abundant in females and children than in males and adults, respectively. Thirdly, the probability of detecting putative BAT also seems to be higher in the winter than in the summer months, and that a warm

temperature during imaging procedures reduces BAT activity. Besides [^{18}F]FDG-PET/CT, metabolically active BAT can also be detected by other nuclear imaging methods, such as SPECT. The unselective beta-blocker propranolol decreases BAT activity, but diazepam may not have a significant effect on BAT activity in humans. The presence of detectable BAT also seems to be inversely associated with BMI and plasma glucose.

Although the clinical patient studies on BAT have given new information, they also contain significant weaknesses. First, studies involving patients with a known or suspected disease as an indication for a PET scan do not necessarily reflect normal human physiology. In fact, many of the studies currently available focus on BAT only as a confounding factor in the diagnostic imaging of cancer and metastases. Second, no cold exposure has been applied, albeit the principal function of BAT is to defend body temperature in a cold environment. Indeed, the lack of designed cold exposure easily leads to the conclusion that the activation of BAT is a sporadic and rare phenomenon in adult humans, and thus the true prevalence of BAT cannot be determined. Furthermore, it has been shown that BAT-negative patients also possess BAT in their cervical region (398) and that the preadipocytes from both BAT-negative and BAT-positive patients can give rise to BAT *in vitro* (417). Third, interpretation of images has usually been qualitative, although semi-quantitative methods, such as the standardised uptake value (SUV) (418), have sometimes been applied. However, fully quantitative modelling has not been utilised in patient studies on BAT, and thus the metabolic rate and metabolic effects of human BAT cannot be determined accurately.

2.7.3 Hibernoma

A tumour of brown adipocyte origin was first described in 1906 (419) and later named hibernoma (420). Hibernomas are extremely rare; they constitute one per cent of all adipose tissue tumours (421). Hibernomas are most commonly found in the thighs, followed by the shoulder and back regions (422). Surprisingly, cervical hibernomas are uncommon (422–423). Hibernomas can be detected with different imaging modalities; for instance, ^{99m}Tc-lymphoscintigraphy (424), [^{18}F]FDG-PET/CT (425), CT (426), magnetic resonance imaging (MRI) (427) and ultrasound (428) have been used.

As being composed of BAT, hibernomas may have a significant impact on body weight in humans. At least case reports in the literature suggest such a role (429). For instance, a report demonstrates a 16 kg weight loss in four months that was followed by weight gain after surgical removal of a hibernoma (430). Another study reports unchanged whole-body EE but a 15 kg weight gain one year after a resection of a hibernoma (431). It is not fully clear why patients with hibernoma seem to lose weight. It is not likely that the weight reduction related to hibernomas stems from paraneoplastic factors, since hibernomas are benign per se (422, 432). Thus, it is possible that they have a significant augmenting effect on whole-body EE. However, typical hibernomas weigh approx. 250 g (433), and therefore, one could expect massive weight loss, but the reported weight-reducing impacts of hibernomas seem to be much lower. This could be due to the fact that hibernomas are mixed tumours that also contain some WAT (433). Further, it is also likely that hibernomas are not subject to the same efficient sympathetic stimulation as BAT, which may reduce their thermogenic capacity.

2.7.4 Pheochromocytoma

Pheochromocytoma is a rare catecholamine-secreting neuroendocrine tumour that derives from the chromaffin cells in the adrenal medulla (434). The extra-adrenal manifestations of this catecholamine-secreting tumour appear as paragangliomas of the sympathetic trunk (435).

BAT is physiologically activated by the NA released from the sympathetic nerve endings as a response to cold exposure, and thus it is not surprising to find increased amounts of BAT in patients with pheochromocytomas (e.g. 436–438). Further, a few case reports on cervical BAT activation in conjunction with these catecholamine-secreting tumours, as detected mainly by [^{18}F]FDG-PET/CT, have also been published (439–446). Interestingly, a retrospective study suggests that cervical BAT is metabolically active in half of the pheochromocytoma patients and that BAT can also be demonstrated by visualising its adrenergic innervation with [^{18}F]-6-fluorodopamine-PET/CT, in patients both with and without pheochromocytoma (447).

Overall, BAT activity seems to be positively associated with circulating catecholamines (448). The stimulation of adjacent periadrenal (449) and mesenteric (43, 450–451) BAT regions by pheochromocytoma-derived catecholamines has also been suggested. Further, increased gene expression of UCP1, PRDM16 and β_3-adrenoreceptor has been described in the omentum of patients with a pheochromocytoma (18).

2.7.5 Involvement of BAT in various medical conditions

BAT has also been implicated as having a role in a number of miscellaneous medical disorders in the literature, including lipodystrophy, i.e., the degeneration of SCWAT, mainly in the face, extremities, buttocks and abdominal region, and gain of visceral adipose tissue (VAT), and sometimes also SCWAT over the dorsocervical spine. Lipodystrophy is also associated with the antiretroviral therapy of human immunodeficiency virus (HIV) infection (452). Studies have shown BAT-like features in the lipodystrophic dorsocervical adipose tissue of HIV patients (453–455), but this view is not shared by all observations (456–457). Further, BAT activity seems to be an unlikely cause of the increased EE in patients with HIV-associated lipodystrophy (457).

BAT has also been observed in atherosclerotic coronary vessels (458), but its role in the development of coronary artery disease has not been clarified in humans. Interestingly, a rather wild hypothesis has also been presented, according to which BAT recruitment over the winter exposes to a greater risk of suicide in the spring – it is suggested that impaired heat tolerance may worsen anxiety (459–460). BAT in adults has also been implicated in the pathophysiology of cancer cachexia, and indeed, a post-mortem study suggests that the prevalence of periadrenal BAT is increased in weight-losing cancer patients (293). By contrast, anorexia nervosa patients have a reduced BAT capacity (461). This is in line with a finding that shows lipid depletion in the BAT of malnourished young children (462). A paediatric case report relating to extreme failure to thrive, which was accompanied by increased whole-body EE, hypoglycaemia and increased amounts of BAT, suggests a role for BAT in the energy and glucose homeostasis of young children (463). Further, the necrosis of BAT in human infants is a well-established condition, which is thought to be caused by diminished blood flow in conjunction with severe hypotension (464). The related calcifications can be detected in plain x-ray images (465).

2.7.6 Obesity and markers of brown adipose tissue

Studies looking for associations between obesity and related disorders with the different alleles of the UCP1 and the β_3-adrenoceptor genes have been carried out extensively, in the effort to understand the role of BAT in the development of obesity in humans.

Indeed, polymorphisms in the UCP1 gene have been linked to obesity in humans in numerous studies (e.g. 466–475), albeit such a connection has not been found in all studies (476–477).

Further, UCP1 polymorphisms have also been linked directly with decreased EE and SNS activity in females (478), and subsequently, to reduced weight loss (479). However, polymorphisms in the UCP1 may not be independently associated with type 2 diabetes (480). Interestingly, polymorphisms of the β_3-adrenoceptor gene have also been linked to obesity (e.g. 468, 481–483) and impaired glucose tolerance (e.g. 484–487), suggesting that a malfunction of the BAT-activating adrenergic pathway may predispose to obesity in humans. Further, a synergistic effect of the polymorphisms in UCP1 and β_3-adrenoceptor genes on the development of obesity has been suggested (477, 488). It has also been demonstrated that β_3-adrenoceptor gene polymorphism is related to fat oxidation (489) and that the genotypes of both the UCP1 and the β_3-adrenoceptor genes could influence exercise-induced enhanced glucose tolerance (490). However, the link between obesity and β_3-adrenoceptor polymorphism has not been established in all studies, for instance, in children and adolescents (491).

Studies have also been conducted comparing gene and protein expressions of the UCP1 in lean and obese humans. It has been shown that morbidly obese humans have a lower expression level of the UCP1 gene in their intraperitoneal adipose tissue compared to lean subjects (2). Further, cervical BAT, as defined by the UCP1-positive cells in cervical biopsies, is found in greater amounts in subjects who are both younger and leaner (492). In addition to UCP1, gene expression of other BAT-related genes, for instance PGC-1α, has been found to correlate with a metabolically beneficial phenotype in humans (493).

Presently, only one study using PET has assessed BAT metabolism in relation to polymorphisms in the UCP1 and β_3-adrenoceptor genes. This study suggests that specific alleles in both genes may increase the age-related decline in BAT activity (494). It should also be pointed out that, although alterations in the sequences of UCP1 and β_3-adrenoceptor genes seem to promote obesity, it is not clear how these varieties affect the function of the proteins at molecular level, and thus influence thermogenesis in brown adipocytes.

2.7.7 Glucose uptake by BAT in lean and obese healthy humans

Glucose uptake by human BAT has been measured *in vivo* only by [^{18}F]FDG-PET. [^{18}F]FDG is a glucose analogue that is transported into cells by the same transporters as glucose, but after being phosphorylated by hexokinase, unlike glucose, it cannot be further metabolised by most cells. Therefore, [^{18}F]FDG is trapped inside the cells (495).

Most studies on human BAT only measure or visualise [^{18}F]FDG activity, or apply SUV as a measure of glucose metabolism in the tissue. However, using [^{18}F]FDG-PET, the glucose uptake rate can also be determined precisely. The glucose uptake rate is determined using the model of Gjedde-Patlak for irreversible uptake and multiple time graphical analysis (496–497). The fractional uptake rate (FUR) can also be calculated, but it provides a robust estimation of glucose uptake only when PET imaging is performed after a significant period of tracer uptake into tissues (498–499).

An inverse correlation between the cold-induced BAT glucose metabolism and BMI has been shown in multiple studies in healthy humans (e.g. 13, 40, 500–501). Further, an inverse relationship between cold-induced BAT activity and age has also been established (501), and the polymorphisms in UCP1 and β_3-adrenoceptor genes may affect this age-related decline in BAT activity (494). In under-weight healthy young women, BAT seems to be active even under thermoneutral conditions (461). BAT activity has also been shown be to be associated with lower glycosylated haemoglobin A_{1c} (HbA_{1c}) (502) and plasma insulin (503) in healthy adults.

Weight reduction might also increase human BAT glucose uptake, at least after bariatric surgery; in a study by Vijgen et al., only two out of ten morbidly obese subjects demonstrated active BAT at baseline, but a year after the surgery, there were five BAT-positive subjects among the ten (504). However, only [^{18}F]FDG activity was measured, instead of using SUV, for instance. On the other hand, a preclinical study on rats does not provide support for increased BAT activity after bariatric surgery (339). In line with the study by Vijgen et al., a trend towards increased BAT glucose uptake rate has been shown after a five-month conventional weight loss period (**III**).

Currently, on the basis of [^{18}F]FDG-PET/CT measurements, evidence of increased postprandial BAT metabolism in healthy humans is weak. Firstly, ingestion of a standardised meal 90 min before the uptake period resulted in lower SUV values of supraclavicular BAT than under fasting conditions, although both measurements were carried out during mild cold exposure (505). Secondly, overeating 24 hours preceding PET measurements did not increase BAT activity (506). However, meal-induced BAT metabolism in humans has been postulated, mainly because BAT showed higher activity as compared to WAT after a meal, although the postprandial BAT SUV was lower than under cold conditions (507). Increased uptake was seen in skeletal muscle as response to the meal in both studies (505, 507), which at least partly explains the decreased uptake values in BAT, since the applied modelling failed to take into account differences in the plasma clearance of [^{18}F]FDG between postprandial and fasting conditions.

Currently, three [^{18}F]FDG-PET/CT studies have shown that repeated cold exposure can increase human BAT activity. After a six-week period of two-hour daily cold exposure at 17 ºC, healthy lean males exhibited decreased body fat mass and also markedly elevated BAT activity, as defined by an increase in the SUV of supraclavicular BAT (67). The six-week cold acclimation also resulted in enhanced cold-induced thermogenic capacity (67). Further, a more pronounced daily cold exposure (six hours at 15–16 °C) for only ten days resulted in increased SUV and volume of active BAT in healthy lean males and females (68). However, BAT glucose uptake rate was only quantified in the latter study, and it was not significantly increased (68). It was also demonstrated that the cold acclimation did not lead to browning of abdominal SCWAT or to enhanced mitochondrial uncoupling in skeletal muscle, suggesting that the measured elevation in BAT activity caused increased non-shivering thermogenesis after cold acclimation (68). However, in a study by Blondin et al., a 4-week, 2-hour daily cold exposure at 10 °C in a liquid-conditioned suit was shown to increase cold-induced fractional glucose uptake by BAT (69).

Interestingly, cold-activated [^{18}F]FDG uptake in BAT has also been linked to higher bone mineral density in females (508–510). Human studies also provide evidence for dense SNS innervation of BAT, since a correlation between BAT activities in [^{18}F]FDG-PET/CT and ^{123}I-MIBG-SPECT/CT scans has been shown in healthy humans (511). Further, by using these two imaging methods, no significant difference could be found in the cold-induced activity of BAT between young lean men of South-Asian and European origin (512).

2.7.8 Blood flow in human brown adipose tissue

Studies measuring blood flow in the putative human BAT had already been performed in the 1980s, but in the light of current knowledge, a major problem of the earlier studies was the erroneous anatomical location of the measurements. Astrup et al. showed that ephedrine slightly induces blood flow in the human interscapular subcutaneous adipose tissue, but the blood flow there still remained lower than in the lumbar SCWAT that served as a control tissue

(513). Astrup et al. also found that ephedrine induces blood flow in the perirenal adipose tissue, which was presumed to contain BAT, in only one out of five tested subjects (514).

Whether human supraclavicular BAT also has intense blood flow, similarly to BAT in rodents, remained an open question until demonstrated using kinetic [^{15}O]H_2O-PET/CT imaging (**II**). The method of measuring tissue blood flow with [^{15}O]H_2O is based on the principle of exchange of inert gas between two compartments, blood and tissue (515). With [^{15}O]H_2O-PET, either kinetic modelling or the autoradiography method can be applied to determine blood flow in the tissue.

2.7.9 Energy expenditure by human brown adipose tissue

Instead of measuring oxygen consumption by BAT directly, BAT metabolism in healthy humans has mainly been assessed by measuring [^{18}F]FDG activity. Fortunately, whole-body EE measurements have been included in most studies.

It has been shown that, without affecting spontaneous physical activity, mild cold exposure at a room temperature of 19 ºC can significantly increase whole-body EE, which is accompanied by a rise in circulating catecholamines (516). However, the association between a cold-induced rise in whole-body EE and [^{18}F]FDG activity in BAT was first demonstrated in lean and obese healthy men, studied at an ambient temperature of 16 ºC (13). Nevertheless, further evidence suggests that EE at a room temperature of 19 ºC and BAT activity are indeed associated, suggesting that this small reduction in ambient temperature is also sufficient to activate BAT with a significant energy-consuming effect in adult humans (111). Further support for the positive association between active BAT and whole-body EE was provided by using cold exposure, which involved intermittent immersion of the lower legs in cold water, although EE was not measured during the uptake period of [^{18}F]FDG (517). Further, an inverse correlation between measured BAT activity and changes in body fat during the next six months has been found (506).

Despite the fact that BAT activity is most often measured using [^{18}F]FDG in humans, the role of glucose as an energy source for BAT thermogenesis is somewhat controversial. Namely, [^{18}F]FDG uptake by BAT is significantly reduced by the non-selective beta blocker propranolol (e.g. 371–372), although propranolol does not seem to decrease cold-induced thermogenesis (102). This suggests that glucose uptake by BAT is an unlikely principal energy source for cold-induced thermogenesis in humans. On the other hand, it is possible that under the influence of propranolol other tissues have a more pronounced thermogenetic response to cold exposure than under normal conditions.

In addition to the measurements of [^{18}F]FDG activity within BAT, a positive association between whole-body EE and BAT blood flow has also been demonstrated in healthy humans (**II**). As expected on the basis of rodent studies, cold-activated human supraclavicular BAT also has the capacity to take up fatty acids, as shown using [^{18}F]fluoro-6-thia-heptadecanoic acid ([^{18}F]FTHA) combined with PET/CT (103). Further, Ouellet et al. also showed retention of [^{11}C]Acetate in cold-activated BAT, which was accompanied by a monoexponential decay slope from tissue peak activity, suggesting a tissue oxidative metabolism (103). Furthermore, the authors demonstrated increased Hounsfield units in the CT images of cold-activated BAT, which indicates a decrease in lipid content in the tissue (103). Finally, whole-body EE was also increased in this sample of six healthy men, all of whom showed cold-activated BAT (103). Intriguingly, it has also been demonstrated that BAT oxidative metabolism, as assessed by [^{11}C]Acetate retention, is increased in lean men after a 4-week, 2-hour daily (five times a week)

period of cold exposure at 10 °C in a liquid-conditioned suit (69). Another study demonstrated that in thyroid patients, the supraclavicular adipose tissue, as compared to cervical SCWAT, has a higher basal capacity to consume oxygen *in vitro* (518).

A method of measuring brain oxygen consumption combining the use of oxygen-15-labelled water ($[^{15}O]H_2O$), carbon monoxide ($[^{15}O]CO$) and oxygen ($[^{15}O]O_2$) tracers and PET has been developed (519). This method was first applied to human BAT by Muzik et al., who showed that, despite similar oxygen extractions between BAT-positive and -negative participants, the calculated metabolic rate of oxygen was increased in the humans with active BAT (520). This was due to the increased blood flow in the detectable BAT (520). However, Muzik et al. also estimated that cold-activated BAT is responsible for only a small proportion (approx. 1%) of whole-body EE during the short cooling (20 minutes) that was applied in the study (521).

2.7.10 Substances capable of stimulating human brown adipose tissue

Direct evidence on the pharmacological manipulation of human BAT is very limited. Although there are currently no studies assessing human BAT metabolism after selective β_3-agonist administration, it has been shown that treatment with a β_3-agonist increases insulin action and lipid oxidation in lean humans (522). The treatment with β_3-agonists also seems to enhance glucose tolerance in both rodents and in humans (523). Moreover, *in vitro* experiments suggest that β_3-agonists induce UCP1 gene expression in human perirenal adipocytes (524), indicating enhanced thermogenic capacity of BAT or browning of WAT. It is worth noting that chronic treatment with a β_3-agonist may also cause desensitisation of the beta-adrenergic pathway in humans, as shown *in vitro* (525). Interestingly, it has been shown that treatment with caffeine and ephedrine causes an elevation of β_3-adrenoceptors in the WAT of obese humans (300).

Nevertheless, it is still unclear whether β_3-adrenoceptor agonists significantly increase BAT thermogenesis with beneficial metabolic effects in humans, but evidence of BAT induction by these drugs has been obtained in primates. In rhesus monkeys, treatment with a β_3-adrenoceptor agonist has been shown to increase lipolysis and whole-body EE in short-term, and chronic treatment has been shown to increase UCP1 expression in BAT (526).

On the basis of early blood flow studies on putative perirenal BAT in humans, only a minor role was proposed for BAT in the whole-body EE increment induced by ephedrine (514). On the other hand, recent studies involving precise determination of human BAT metabolism using [^{18}F]FDG-PET/CT have been contradictory. In fact, it has been shown that intramuscular injection of ephedrine does not stimulate BAT (114), while ingested ephedrine has a stimulating effect on BAT in lean but not in obese young men (527). This discrepancy might be explained by the fact that, in the latter study (527), a larger dose of ephedrine was given, and that the lean subjects were slightly younger and had lower BMI than the subjects in the former study (114). Further, infusion of the non-selective β-agonist, isoprenaline, does not increase BAT metabolism, as measured with [^{18}F]FDG-PET/CT, even though whole-body EE is significantly elevated (528).

Interestingly, it has been demonstrated that after a single dose of an oral non-pungent capsaicin analogue (capsinoid), whole-body EE is increased only in the subjects with cold-activated BAT, suggesting BAT-mediated thermogenesis as a response to the capsinoid (529). Further, daily ingestion of capsinoids for six weeks increased cold-induced thermogenesis, although BAT metabolism was not directly measured in this experiment (67). Besides capsinoids, other spices have been proposed as activating BAT in humans. Although BAT metabolism was only measured after cold exposure, it has indeed been suggested that Grains of Paradise, a spice

belonging to the ginger family, can increase BAT metabolism, since the whole-body EE of the BAT-positive subjects increased significantly more than that of the BAT-negative subjects, after ingesting Grains of Paradise extract (530).

2.7.11 Additional methods for imaging of human brown adipose tissue

Besides PET, other imaging modalities have also been applied to the study of human BAT (Table 4). MRI of human BAT has been proposed as an excellent alternative to PET. As compared to PET, the appeal of MRI is based on its better spatial resolution, feasibility and lack of ionising radiation. Various techniques for functional imaging are also currently available for use in MRI scanners. Alternatively, an extremely feasible infrared thermal imaging method has also been proposed (531–532). However, it is evident that MRI offers a more quantitative approach and also enables the study of those BAT depots that are located deeper in the body.

Table 4. Imaging modalities used to study human BAT non-invasively

Modality	Concept	First described, reference
PET/CT	Co-registration of anatomy (CT) and metabolic activity (PET). Short-lived positron-emitting isotopes are coupled to molecules that are close analogues of natural substances, for instance glucose. Enables good quantification of the metabolic data.	Hany et al., 2002 (12)
SPECT	Co-registration of anatomy and metabolic activity. Applied tracers have longer half-lives, but the resolution of imaging and quantification of data is weaker as compared to PET/CT.	Okuyama et al., 2002 (322)
CT	Hounsfield units are increased in active BAT, implying reduced intracellular triglyceride storages.	Baba et al., 2010 (386)
MRI	BAT is separated from WAT on the basis of lower fat-signal fractions and T2* values on chemical-shift MRI.	Hu et al., 2013 (533)
fMRI	Measures haemodynamic changes linked to oxygenation demand, and this signal is increased in active BAT.	Chen et al., 2013 (534)
Near-infrared spectroscopy	Measures oxygenated haemoglobin mainly in the veins, and reduction in regional blood oxygen saturation reflects increased tissue oxygen use.	Muzik et al., 2013 (521)
Infrared thermal imaging	Demonstrates a localised increase in skin temperature within the supraclavicular region.	Symonds et al., 2012 (531)

All currently available non-invasive techniques for human BAT imaging are briefly described.

Although BAT has been studied extensively in rodents using various MRI techniques (e.g. 535–539), besides two case reports on BAT associated either with a pheochromocytoma (441) or with a deceased infant (540), only a few studies on the MRI of human BAT have been published.

The first systematic study on the MRI detection of human BAT included a post-mortem body and eight patients (533). In addition to MRI, the BAT status was evaluated using [^{18}F]FDG-PET/CT in some patients, and the presence of BAT was confirmed in the post-mortem body (533). By using the chemical-shift water-fat 3-T MRI technique, it was shown that fat-signal fractions and T2* times were shorter in the supraclavicular adipose tissue as compared to SCWAT, but a large range of fat-signal fraction values was observed in the supraclavicular adipose tissue (533). It can be speculated that the variation in fat-signal fractions is caused by the differences in the functional status of BAT (541). Interestingly, the MRI of one PET-negative patient also suggested the presence of BAT (533). Later, it has been shown that infants have lower supraclavicular fat-signal fractions than children, and that lean children

have shorter supraclavicular fat-signal fractions and T2* values than overweight children (542). In adults, the inverse correlation between BMI and the presence of BAT has been found by measuring the non-linear MR signals generated by intermolecular zero-quantum coherences (543). It has also been shown in healthy adults that cold-activated supraclavicular BAT has a lower fat-signal fraction than SCWAT (544). Furthermore, in a series of four participants, the [^{18}F]FDG-PET/CT-detectable volume of cold-activated BAT has been shown to correlate well with a water-saturation-based MRI measurement of BAT volume under thermoneutral conditions (534). Further, the authors also demonstrated an increased fMRI signal from BAT as a response to cold exposure in three subjects (534).

2.7.12 Closing words on the review of the literature

There is a marked resurgence of interest in the biology of BAT after the BAT of healthy adult humans was shown to be functional using PET imaging in 2009. The most important findings on the BAT of healthy humans achieved so far by means of nuclear imaging are summarised in Table 5. Many old studies on the physiology of BAT have also gained new appeal as their findings may have significant value in the lengthy process of investigating the unique metabolism of human BAT. However, it should be emphasised that findings on animals must also be tested on human subjects *in vivo*, in order to decide the true relevance of the discoveries in rodents. Nevertheless, it is already clear that human BAT provides an extremely intriguing target in order to find new ways of combating the obesity pandemic, as discussed in this review of the literature. It is certain that many fascinating imaging techniques will be developed for the study of human BAT in even more detail in the future.

Table 5. Milestones in nuclear imaging of BAT in healthy adult humans

Reference	Imaging method(s)	Principal finding(s)
Virtanen et al., 2009 (**I**)	[^{18}F]FDG-PET/CT	Healthy adult humans have functional BAT, as shown conclusively by PET imaging and biopsies from the corresponding supraclavicular region.
van Marken Lichtenbelt et al., 2009 (13)	[^{18}F]FDG-PET/CT	BMI and whole-body EE have significant negative and positive correlations, respectively, with the BAT activity in healthy men.
Saito et al., 2009 (40)	[^{18}F]FDG-PET/CT	The cold-activated BAT metabolism is increased in winter compared with summer, and it is also inversely associated with age, BMI and total and visceral fat areas at the umbilical level in healthy adults.
Orava et al., 2011 (**II**)	[^{18}F]FDG- / [^{15}O]H_2O-PET/CT	BAT in lean adult humans is a highly insulin-sensitive tissue. Blood flow in the BAT of adult humans is also increased as response to cold exposure.
Ouellet et al., 2012 (103)	[^{18}F]FTHA- / [^{11}C]Acetate-PET/CT	Cold-activated BAT has a capacity to take up fatty acids, and acetate is also accumulated in BAT.
Muzik et al., 2012 (520)	[^{15}O]H_2O- / [^{15}O]CO- / [^{15}O]O_2-PET/CT	Blood flow but not oxygen extraction is increased in cold-activated BAT.
Cypess et al., 2012 (114)	[^{18}F]FDG-PET/CT	Intramuscular injection of ephedrine (1 mg • kg^{-1}) does not stimulate BAT glucose uptake.
Carey et al., 2012 (527)	[^{18}F]FDG-PET/CT	Ingested ephedrine (2.5 mg • kg^{-1}) increases BAT glucose uptake in lean but not in obese young men.
Admiraal et al., 2013 (511)	^{123}I-MIBG-SPECT/CT and [^{18}F]FDG-PET/CT	^{123}I-MIBG-SPECT/CT, a marker of sympathetic activity, and [^{18}F]FDG-PET/CT identify the same BAT regions in lean men.
Orava et al., 2013 (**III**)	[^{18}F]FDG- / [^{15}O]H_2O-PET/CT	Insulin-stimulated glucose uptake rate and cold-induced blood flow in BAT are attenuated in obese subjects as compared with lean subjects. Females have higher cold-induced BAT glucose uptake rate.
Chen et al., 2013 (111)	[^{18}F]FDG-PET/CT	A slight decrease in ambient temperature (19 ºC) is sufficient to activate BAT with a significant energy-consuming impact in healthy males and females.
Yoneshiro et al., 2013 (67)	[^{18}F]FDG-PET/CT	A 6-week, 2-hour daily cold exposure at 17 ºC decreases body fat mass and increases BAT activity, as defined by an increase in [^{18}F]FDG-SUV, in healthy lean men.
van der Lans et al., 2013 (68)	[^{18}F]FDG-PET/CT	A 10-day, 6-hour daily cold exposure at 15–16 °C increases both SUV and volume of BAT in healthy lean males and females.
Blondin et al., 2014 (69)	[^{18}F]FDG- / [^{11}C]Acetate-PET/CT	A 4-week, 2-hour daily cold exposure at 10 °C in a liquid-conditioned suit results in a 45% increase in BAT volume of activity and a 2.2-fold increase in cold-induced BAT oxidative metabolism.

Important studies designed to investigate the BAT of healthy adult humans are listed in chronological order.

3 OBJECTIVES OF THE STUDY

1) According to the initial hypothesis of this doctoral work, healthy lean adult humans have functional BAT, whose glucose uptake and blood flow are increased as a response to cold exposure, and the testing of this hypothesis was set as a primary aim of the dissertation.
2) Secondly, as indicated by studies on rodents, it was postulated that the BAT of healthy lean adult humans also has a role in energy homeostasis, and that it is a highly insulin-sensitive tissue. These hypotheses would be studied if the presence of functional BAT in healthy adults could be shown.
3) Thirdly, since the BAT in rodents has a fundamental impact on whole-body metabolism, a subsequent objective of the thesis was to study whether cold- and insulin-stimulated glucose uptake and blood flow responses are altered in the BAT of obese adult humans, and whether weight loss affects cold-activated glucose uptake in human BAT.
4) Finally, it was hypothesised that certain cerebral regions could be closely linked to BAT activation and cold exposure in adult humans, and that lean and obese adult humans may have different cerebral responses to cold exposure. Thus, the fourth objective was to assess cerebral activity in relation to the BAT function, and to determine whether cerebral glucose metabolism is affected by cold exposure both in lean and in obese humans.

4 SUBJECTS AND METHODS

4.1 Study subjects (I–IV)

This study includes 27 lean (Group 1) and 16 obese subjects (Group 2), and an additional 20 obese subjects, who participated in a weight loss programme (Group 3) (Table 6).

All subjects from the three recruitments were screened for medical history and metabolic status, as assessed on the basis of a physical examination, routine blood tests (i.e., complete blood count, liver and thyroid function tests, creatinine, K, Na, lipids, C-reactive protein), a two-hour oral glucose tolerance test (2h-OGTT), electrocardiograms and measured BP. The subjects' ages ranged from 20–52 years. The included subjects did not have any significant medical conditions. All the subjects were euthyroid and non-diabetic. The final decision on a subject's inclusion in the study was conducted by a licenced physician. The main exclusion criteria applied in the study were:

1. Regular smoking
2. Cardiovascular or neurological disease, or psychiatric disorder
3. Pregnancy or lactation
4. Diabetes mellitus, hypo- or hyperthyroidism
5. Malignancies
6. Medication (antihypertensive and -diabetic drugs, lipid lowering drugs, antidepressants, corticosteroids)
7. Presence of any ferromagnetic objects in the body that would contraindicate MRI imaging
8. Previous participation in PET imaging

The study protocols were approved by the ethics committees of the hospital districts of Southwest Finland and Helsinki and Uusimaa (the weight loss programme), and the studies were conducted in accordance with the Declaration of Helsinki (545). Written informed consent was obtained from all subjects.

The recruitment of most study subjects was arranged by the investigators at the Turku PET Centre (Groups 1 and 2), but the participants in the weight loss programme (Group 3) were recruited at the Obesity Research Unit of Helsinki University Central Hospital.

Table 6. Subjects and PET imaging in the sub-studies I–IV

Participation of subject groups in the sub-studies			Sub-study (I–IV)	No. of subjects in the sub-studies	BMI ($kg \cdot m^{-2}$)	Cold 1 $[^{15}O]H_2O$ / $[^{18}F]FDG$	Warm $[^{15}O]H_2O$ / $[^{18}F]FDG$	Insulin $[^{15}O]H_2O$ / $[^{18}F]FDG$	Cold 2 $[^{18}F]FDG$
Group 1			I	5	23 ± 4	-/5	-/5	-/-	-
			II	27	23 ± 2	27/27	12/12	14/14	-
	Group 2	Group 3	III	27	23 ± 2	27/27	12/12	14/14	-
				16	33 ± 5	16/16	7/7	9/9	-
				20	35 ± 3	-/20	-/-	-/-	18
			IV	24	22 ± 2	-/24	-/8	-/-	-
				17	33 ± 6	-/24	-/7	-/-	-

The study includes 63 subjects from three different subject groups. The numbers of subjects and the usage of the two PET tracers, $[^{15}O]H_2O$ and $[^{18}F]FDG$, in the sub-studies are shown. Subjects participated in two PET imaging sessions. One imaging session was always under cold conditions (Cold 1), and the other under either warm or insulin-clamp conditions, or in conjunction with the weight loss programme, under cold conditions (Cold 2).

4.2 The weight loss programme (III)

Twenty out of 36 obese subjects (Group 3) participated in a five-month weight loss programme, which consisted of individual and group-based diet and exercise counselling bi-monthly, starting with a six-week modified very-low-calorie diet (Nutrilett, Allevo) phase. During the first six weeks, the subjects were instructed to eat 0.5 kg vegetables for additional sources of fibre and vitamins, and protein-rich food snacks such as lean meat and milk products to yield a total of 70–90 g of protein daily. After the very-low-calorie diet phase, a protein intake of 1.2–1.5 g/kg was prescribed for the subjects. Multivitamins (Multi-Tabs, Orion Pharma) were provided daily to ensure nutritional needs, and physical activity was recommended according to Finnish weight loss guidelines (546).

Inclusion criteria of the weight loss programme:

1. Age 20–40 years
2. BMI > 30 kg • m^{-2}
3. Total body weight < 120 kg
4. Weight stability for ≥ three months
5. Lifetime weight loss attempts less than two
6. Plasma triglyceride concentration < 2.0 mmol • l^{-1}
7. Concentration of plasma high-density lipoprotein (HDL) cholesterol > 1.0 mmol • l^{-1} in males, and > 1.3 mmol • l^{-1} in females

4.3 Anthropometry (I–IV)

Fasting weight was measured barefoot and in light underwear to the nearest 0.1 kg using a digital scale, and height was measured using a stadiometer to the nearest 0.1 cm. Body composition (fat percentage) was assessed in a fasting state after voiding by a bioimpedance method (Omron BF400, Omron Healthcare). Waist circumference was measured midway between the anterior superior iliac spine and the lower rib margin, and hip circumference at the level of the greater trochanters. Skeletal muscle mass was estimated by multiplying the measured FFM by a factor of 0.38 (547).

4.4 Study design (I–IV)

The subjects were scanned twice, and at least one scan was performed during cold exposure in order to identify functional BAT. The numbers of subjects in the sub-studies **I–IV** are shown in Table 6.

Sub-study I:
Glucose uptake was measured in five lean healthy subjects (Group 1) using [^{18}F]FDG as a tracer in the cervical BAT and SCWAT, under warm and cold conditions. Corresponding BAT and SCWAT biopsies were obtained in three subjects in order to verify the identities of the tissues studied. Subsequently, the tissue samples were analysed for histology and expressions of genes and proteins characteristic for BAT.

Sub-study II:
Cold-induced glucose uptake in BAT, skeletal muscle and various WAT depots were measured using [^{18}F]FDG as a tracer, in 27 healthy lean subjects (Group 1). In addition, cold-induced blood flow was measured with [^{15}O]H_2O as a tracer in the cervical BAT, SCWAT and skeletal muscle. Furthermore, glucose uptake and blood flow were also studied under either warm (n = 12) or insulin-clamp (n = 14) (548) conditions in these subjects. One subject attended only the

cold exposure PET study. BAT and SCWAT biopsies were studied from seven subjects in order to measure the expression of genes relevant to insulin signalling and glucose transport.

Sub-study III:
Cold-induced glucose uptake in BAT, skeletal muscle and various WAT depots was measured with [^{18}F]FDG as a tracer in 16 obese subjects (Group 2). In these subjects, cold-induced blood flow was also measured with [^{15}O]H_2O as a tracer in the cervical BAT, SCWAT and skeletal muscle. Glucose uptake and blood flow were also studied under either warm (n = 7) or insulin-clamp (n = 9) (548) conditions in these subjects.

An additional 20 obese subjects participated in a five-month weight loss programme (Group 3), in which cold-induced glucose uptake in BAT and various WAT depots was measured using [^{18}F]FDG as a tracer both before and after the weight loss. Two of the 20 subjects in the weight programme withdrew from the study before cold-induced glucose uptake had been measured a second time by PET.

The lean subjects (Group 1) served as a control group.

Sub-study IV:
Cold-induced glucose uptake in the brain, BAT, WAT and skeletal muscle were studied using [^{18}F]FDG as a tracer in 24 lean and 17 obese subjects, who participated in sub-studies **I–III** (Groups 1–2). From these subjects, eight lean and seven obese participants also underwent PET scans under warm conditions in order to generate control values. Subsequently, regional cerebral glucose uptake was investigated in relation to BAT glucose uptake which was measured during the same imaging session (**I–III**). Furthermore, the pattern of cerebral glucose uptake was compared between the lean and the obese subjects.

4.5 Cold exposure (I–IV)

On the cold exposure day, subjects spent two hours wearing light clothing in a room with an ambient temperature of 17 ºC before PET imaging. The transition to the PET imaging room, which had an air temperature of 23 ºC, was carried out using a wheelchair to minimise skeletal muscle activity. During the PET imaging, the cold exposure was induced by intermittent immersion (5 min in / 5 min out) of the right foot in water at a temperature of 8 ºC (549). The foot was always placed in the water by investigators in order to minimise excess skeletal muscle activity. Interindividual variation in the insulating SCWAT layer is generally small in this anatomical region.

4.6 PET imaging (I–IV)

4.6.1 Production of PET tracers

The isotope ^{15}O (physical $t_{½}$ 123 s) was produced with a low-energy deuteron accelerator, Cyclone 3 (IBA Molecular). [^{15}O]H_2O was synthesised in a continuously operating water module (Hidex) using a diffusion membrane technique to trap radioactive water vapour in the sterile saline (550) (**II–III**). [^{18}F]FDG (physical $t_{½}$ 110 min) was synthesised with a computer-controlled apparatus in accordance with the standard manufacturing procedure of the Turku PET Centre (551) (**I–IV**).

4.6.2 PET acquisition

PET imaging was performed after overnight fasting. The subjects were instructed to avoid strenuous physical activity the day before imaging. Before entering the PET scanning room, a catheter was inserted into antecubital vein of both arms for the bolus injection of the PET tracers, blood sampling, and in conjunction with an insulin-clamp (548), for infusion of insulin and glucose. When an insulin-clamp was not applied, isotonic saline was infused. Subjects were scanned in a supine position with the arms beside the body. The outline of the PET protocol is provided in Fig. 4.

PET scanning began from the cervical region. Before the imaging of the [^{18}F]FDG emission, a 900 MBq bolus of [^{15}O]H_2O was administered intravenously, and a dynamic emission scan with variable frame lengths (6x5 s, 6x15 s, 8x30 s) was performed to determine blood flow in the cervical region (**II–III**). A 185 MBq bolus of the glucose analogue, [^{18}F]FDG, was administered intravenously in conjunction with all the PET studies, and a dynamic emission scan with variable frame lengths (1x1 min, 6x0.5 min, 1x1 min, 3x5 min, 2x10 min) was performed in the cervical region (**I–IV**). Next, the axial-field-of-view (AFOV) was placed on the lower thoracic region, followed by the abdominal region, and dynamic emission scans with constant frame lengths (5x3 min) were performed in both regions (**II–IV)**. A dynamic brain scan (5x3 min) was performed last (**IV**).

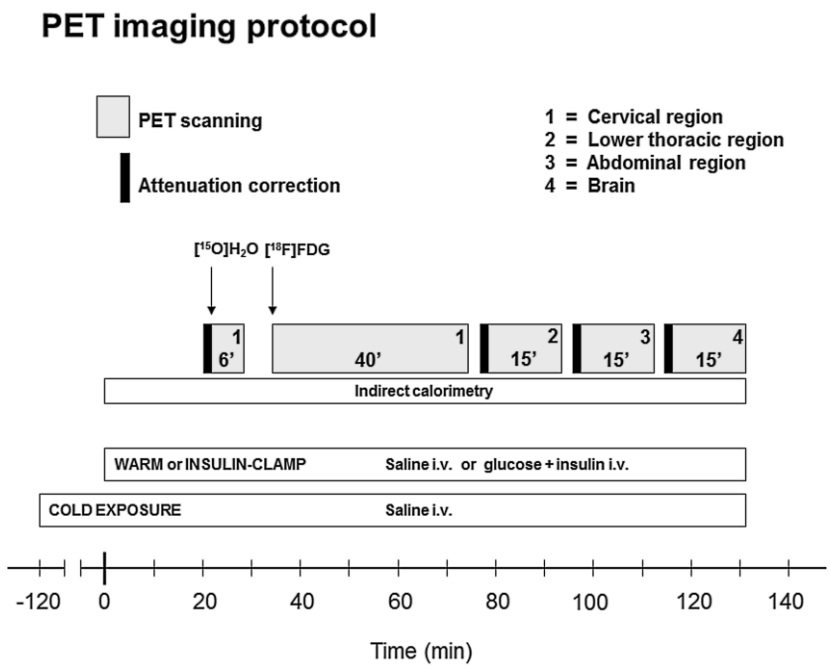

Figure 4. PET imaging protocol
First, tissue blood flow was measured with [^{15}O]H_2O as a tracer, and next, tissue glucose uptake was measured using [^{18}F]FDG. EE was simultaneously determined using an indirect calorimeter. Cold exposure was started two hours before PET imaging. PET imaging was also performed under either warm or hyperinsulinaemic euglycaemic conditions to generate control values and to study the effects of insulin, respectively. It is of note that blood flow and cerebral glucose uptake were not investigated in all subjects in this study (Table 6). Modified from Orava et al., 2013 (**III**).

Dynamic PET data were always corrected for photon attenuation, physical decay, dead time, scatter and random coincidences, and PET images were reconstructed with a matrix size of 128x128 (**I–IV)**. Subjects in Group 1 were scanned using a GE Discovery VCT scanner (General Electric Medical Systems) with 3D acquisition mode. A low-dose CT image was used for attenuation correction, and the PET images were reconstructed using the VUE point algorithm (GE Healthcare) with two iterations and 28 subsets (**I–IV)**. Subjects in Groups 2 and 3 were scanned with an ECAT EXACT HR+ scanner (Siemens/CTI), and transmission scans with a germanium-68 source were performed before acquisition of emission data. Acquisition of [^{15}O]H_2O and [^{18}F]FDG emission data were carried out in 2D and 3D modes, respectively, using iterative reconstruction with six iterations and 16 subsets (**III–IV)**.

4.7 Magnetic resonance imaging (III–IV)

A 1.5-T MRI scanner (Gyroscan Intera CV Nova Dual system, Philips Medical Systems) equipped with an internal body coil was used to obtain T1-weighted anatomical reference images for obese subjects (n = 36) (**III–IV**). MRI scans were performed in a separate session. In the weight loss programme (**III**), MRI was performed both before and after weight loss. Subjects were in a supine position with the arms beside the body, and they were instructed to avoid unnecessary movement during the MRI.

4.8 PET analyses

4.8.1 Regions-of-interest: adipose tissue and skeletal muscle (I–IV)

Regions-of-interest (ROIs) were manually outlined on 2–3 transaxial planes in a fusion-image, composed of a summed dynamic [^{18}F]FDG-PET image and a CT or magnetic resonance (MR) image. Vinci 2.54.0 software (Max-Planck Institute, Cologne) was applied in the image analysis. ROIs were drawn on both lateral aspects of deltoid muscle and supraclavicular adipose tissue to define glucose uptake rates in skeletal muscle and BAT, respectively. Cervical SCWAT was outlined posteriorly in the midline, and abdominal SCWAT and VAT at the level of the umbilicus. Perirenal adipose tissue was outlined around both kidneys. Subsequently, regional [^{18}F]FDG time-activity curves (TACs) were generated.

4.8.2 Regional cerebral glucose uptake rate (IV)

Statistical parametric mapping (SPM) of cerebral glucose uptake was performed with SPM8 (http://www.fil.ion.ucl.ac.uk/spm/). Parametric glucose uptake images were calculated voxel-by-voxel. First, dynamic brain PET images were summed and normalised into standard space. Next, these parameters were applied to the parametric glucose uptake images. Spatially normalised glucose uptake images were smoothed with 12-mm full width at a half-maximum Gaussian kernel. The data were analysed using random effects models, contrasting glucose uptake rate in warm versus cold conditions, and for lean versus obese subjects, separately under warm and cold conditions. To quantify the relationship between glucose uptake in the brain and BAT, cerebral glucose uptake rate was regressed with BAT glucose uptake rate separately for warm and cold conditions. Age was introduced as a nuisance covariate for all between-subject comparisons. A statistical threshold of $P < 0.05$, false discovery rate-corrected at cluster-level was applied in all analyses. To quantify regional glucose uptake values, ROIs were generated in the frontal cortex, parietal cortex, temporal cortex, occipital cortex, limbic lobe, pons, sub-lobar regions, hypothalamus and cerebellum using the WFU Pickatlas tool (552). Subsequently, subject-wise glucose uptake rate values were computed for each region.

4.8.3 Image-derived input functions (I–IV)

Image-derived-input-functions (IDIF) for [^{15}O]H_2O and [^{18}F]FDG were created by drawing multiple ROIs in the aortic arch in the time frame with the highest first-pass concentration of the tracer, after which blood TACs were calculated for each ROI (553). The TAC with high peak concentration and low noise in the tail was selected. In conjunction with abdominal region glucose uptake analysis, ROIs were also drawn in the left ventricle or descending aorta in the second AFOV to extend the blood TAC of [^{18}F]FDG. To determine the plasma TAC of [^{18}F]FDG, rather than image-derived whole-blood TAC, an additional conversion taking account of haematocrit and continuing accumulation of [^{18}F]FDG in red blood cells was applied (554). [^{18}F]FDG-IDIFs were extrapolated by fitting a line to the logarithm-transformed TACs to extend them to the abdominal and cerebral regions.

4.8.4 Quantification of blood flow (II–III)

Kinetic modelling was applied, and subsequently, a two-compartment model including fractional arterial blood volume (555) was linearised and fitted with the whole-blood input function to PET data voxel-by-voxel using the Lawson-Hanson non-negative least-squares technique to produce parametric blood flow images. ROIs of regional glucose uptake rate analyses were employed to determine blood flow in the tissues.

4.8.5 Quantification of glucose uptake rate and BAT mass (I–IV)

The influx rate constant (K_i) of [^{18}F]FDG for the supraclavicular BAT, cervical and abdominal SCWAT, VAT, skeletal muscle and cerebral regions were determined using the model of Gjedde-Patlak and graphical analysis (496–497, 556). FUR was calculated for abdominal subcutaneous, perirenal and visceral adipose tissues in obese subjects (Groups 2 and 3) (499). A lumped constant (LC) value of 1.14 was used for all adipose tissues (557), 1.20 for skeletal muscle (558), and 0.52 for brain tissue (559). Glucose uptake rate was calculated as follows: plasma glucose concentration • K_i • LC^{-1}. The glucose extraction was determined by dividing the glucose uptake rate with the corresponding rate of blood flow. For the estimation of BAT mass, additional parametric cold-exposure K_i images were calculated voxel-by-voxel to determine the metabolic rate in the supraclavicular and upper thoracic regions. Activation of BAT was defined as a glucose uptake rate higher than 3 µmol • $(100\ g)^{-1}$ • min^{-1}, which was chosen after visual interpretation of PET images and determination of the BAT glucose uptake rate under warm conditions, where it was always lower than 1.7 µmol • $(100\ g)^{-1}$ • min^{-1}. The PET images were then fused with the CT or MR images. Thereafter, the mass of active BAT was assessed manually.

4.9 Indirect calorimetry (II–III)

Whole-body EE was measured with an indirect calorimeter (Deltatrac II, Datex-Ohmeda) during the PET sessions. Measurements were started 15–20 minutes before the PET imaging. The gas fractions of O_2 and CO_2 were measured in inspired and expired air, and $\dot{V}O_2$ and $\dot{V}CO_2$ were calculated using the Haldane transformation. The calorimeter was equipped with a canopy, i.e., a ventilated hood, through which a constant air flow was generated. In the data analyses, transient spikes due to irregular breathing that exceeded 1.5 x the standard deviation, were excluded from the $\dot{V}O_2$, $\dot{V}CO_2$, respiratory quotient (RQ) and EE signals. The EE values were normalised by adding residuals of the linear regression of the measured EE and FFM to the mean EE value.

4.10 Assessment of sympathetic tone (II–IV)

In order to assess the tonus of the sympathetic nervous system during PET scanning, BP, HR (n = 63) and plasma catecholamines were measured (n = 27). BP and HR were recorded using an electronic sphygmomanometer (Omron 711 Automatic IS, Omron Healthcare). The concentrations of NA and dihydroxyphenylglycol (DHPG) in EDTA plasma were determined by high performance liquid chromatography and coulometric electrochemical detection (Coulochem 5100A, ESA Inc.) (560). cAMP was measured with a commercial DELFIA assay kit (PerkinElmer DELFIA cAMP kit 4003-0010).

4.11 Oral glucose tolerance test (I–IV)

2h-OGTT was performed in all subjects in a separate session, after overnight fasting. The subjects were instructed to avoid strenuous exercise the day before. The study subjects drank 330 ml of liquid containing 75 g glucose. Venous blood samples for the determination of plasma glucose and insulin at 0, 15, 30, 45, 60, 90 and 120 min were obtained. Areas under the curve (AUC) for plasma glucose and plasma insulin were determined by the trapezoidal rule. The Matsuda index (561) was applied to estimate whole-body insulin sensitivity in conjunction with the weight loss programme (**III**).

4.12 Hyperinsulinaemic-euglycaemic clamp (II–III)

In the hyperinsulinaemic-euglycaemic clamp, plasma insulin was increased for approx. 160 min using a primed-continuous (1 mU • kg^{-1} • min^{-1}) infusion of insulin (Actrapid, Novo Nordisk A/S) (548). Normoglycaemia was maintained using a variable infusion rate of 20% glucose, based on venous plasma glucose measurements. Subsequently, insulin-stimulated whole-body glucose uptake (*M* value) was calculated. Plasma insulin concentrations were similar in lean and obese subjects (64 ± 11 vs. 68 ± 15 mU • l^{-1}, $P = 0.27$).

4.13 Blood measurements (I–IV)

Plasma glucose was determined by a glucose oxidase method (Analox GM9 Analyzer, Analox Instruments). HbA_{1c} was determined using high-performance liquid chromatography (Variant II, Bio-Rad Laboratories). Plasma insulin, TSH, free plasma T4 and free plasma T3 concentrations were measured using the electrochemiluminescence immunoassay technique (Modular E180 automatic analyser, Roche Diagnostics GmbH). Plasma concentrations of total cholesterol, HDL cholesterol and triglycerides were determined photometrically (Modular P800, Roche Diagnostics GmbH). The concentration of plasma low-density lipoprotein (LDL) was calculated using the Friedewald equation (562). Concentrations of serum FFAs were determined photometrically (NEFA C, ACS-ACOD, Wako Chemicals GmbH; Modular P800, Roche Diagnostics GmbH).

4.14 Biopsy procedure (I–II)

Nine lean subjects provided an additional written informed consent for supraclavicular biopsies. The site for incision was decided by the cold exposure [^{18}F]FDG-PET/CT image indicating glucose uptake by BAT. A superficial SCWAT sample was collected from the same incision. The biopsies were obtained under local lidocaine-adrenaline anaesthesia by a plastic surgeon. Immediately after removal, the tissue samples were snap-frozen in liquid nitrogen.

4.14.1 Histology (I)

Cervical BAT and SCWAT samples (n = 3) were kept in formalin until moulding in paraffin and staining with haematoxylin-eosin, and they were subsequently imaged using an Eclipse E800 microscope (Nikon) with a 40X/0.75 Plan Fluor objective (Nikon).

4.14.2 Quantitative Real-time PCR (I–II)

RNA was isolated from nine BAT and SCWAT biopsies using the RNeasy Lipid Tissue Mini Kit (Qiagen) according to the manufacturer's protocol. The 1st Strand DNA Synthesis Kit for reverse transcriptase polymerase chain reaction (PCR) (AMV) (Roche) was used for complementary DNA synthesis. Complementary DNA synthesis reactions without the addition of reverse transcriptase were used to exclude unspecific amplification. Gene expression studies were carried out in the Department of Medical and Clinical Genetics at the University of Gothenburg. The primers used are shown in Table 7. Real-time PCRs were performed using the Power SYBR Green PCR Master Mix (Applied Biosystems), and the final analyses were carried out on the ABI PRISM 7900HT machine (Applied Biosystems). Samples were analysed and subsequently normalised to the expression level of β-actin.

Table 7. Primer sequences used in the sub-studies I–II

Gene name	Primer sequence
β-actin *(n = 9)*	GAGCTACGAGCTGCCTGACG GTAGTTTCGTGGATGCCACAG
UCP1 *(n = 9)*	CTGGAATAGCGGCGTGCTT AATAACACTGGACGTCGGGC
D2 *(n = 3)*	CCTCCTCGATGCCTACAAAC GCTGGCAAAGTCAAGAAGGT
PGC-1α *(n = 3)*	GCCAAACCAACAACTTTATCTCTTC CACACTTAAGGTGCGTTCAATAGTC
PRDM16 *(n = 3)*	GAGGAGGACGATGAGGACAG CGGCTCCAAAGCTAACAGAC
β_3-adrenoceptor *(n = 3)*	TTTGCCAACGGCTCGAC CGTCAGGTTCTGGAGGGTAG
GLUT1 *(n = 7)*	ACGCTGTCTTCTATTACTCCACGA GCCACGATGCTCAGATAGGAC
GLUT4 (*n = 7)*	CCGCTACCTCTACATCATCC TTCCGCTTCTCATCCTTCAG
IR *(n = 7)*	GCTGCCACCAGTACGTCATT CACCGAGTCGATGGTCTTCTC
IRS1 *(n = 7)*	GAGGATTTAAGCGCCTATGCCA TGCATCGTACCATCTACTGATGAG
IRS2 *(n = 7)*	CCAGCATTGACTTCTTGTCC GTTGGTGCCTCATCTAACAG

Modified from Virtanen et al., 2009 (**I**), and Orava et al., 2011 (**II**).

4.14.3 Western blot (I)

Protein extracts (n = 3) from BAT and SCWAT were prepared from the organic phases obtained during the RNA extraction according to the manufacturer's recommendations for TRI Reagent (Sigma-Aldrich). Protein concentrations were determined using the BCA Protein Assay Kit (Pierce), and 25 μg protein fractions were separated by SDS-PAGE (4-12% or 10% gels, NuPage, Invitrogen), blotted onto a PVDF membrane (Immobilon P, Millipore) and detected by anti-human-UCP1 (U6382, Sigma), anti-human Cytochrome C (#4272, Cell Signaling) and anti-human-GAPDH (ab9484, Abcam) antibodies. Western blot analysis was

carried out in the Department of Medical and Clinical Genetics at the University of Gothenburg.

4.14.4 Immunofluorescence and -histochemistry (I)

Sections (n = 3) of BAT and SCWAT were subjected to heat-induced antigen retrieval by boiling for 10 min in a pressure cooker in a Tris-EDTA buffer (10 mM Tris, 1 mM EDTA, pH 9). After washing in PBS, the sections for immunofluorescence were blocked for 1 h in 1% BSA, 0.1% Tween20 in PBS and subsequently incubated with primary antibody in a dilution buffer (0.5% BSA, 0.05% Tween20 in PBS) for 2 h. This was followed by 3 x 10 min washes in PBS and incubation with secondary antibody, mitochondrial and nuclear markers in a dilution buffer for 1 h. After washing 3 x 10 min in PBS, the sections were mounted in ProLong Gold Antifade (Invitrogen, Molecular probes P-36934) and photographed. The VECTASTAIN Elite ABC Kit (Vector Laboratories, PK-6101) was used according to the manufacturer's protocol. Slides were mounted with DPX Mountant for Histology (Sigma, 44581) and photographed. The specific antibodies used were rabbit anti-UCP1 (1:500, Sigma U6382), Alexa594 conjugated mouse anti-OxPhos Complex IV subunit I (1:200, Invitrogen, Molecular Probes A21297) and Cy2 conjugated donkey anti-rabbit immunoglobulin G (1:100, Jackson Immunoresearch, 711-225-152). Topro3 (1:1000, Invitrogen, Molecular Probes T3605) was used as a nuclear marker. The immunochemistry studies were carried out in the Department of Medical and Clinical Genetics at the University of Gothenburg.

4.15 Statistical analyses (I–IV)

Results are expressed as means ± SD, and a two-tailed *P* value less than 0.05 was considered significant. Differences between lean and obese subjects and subjects with and without detectable cold-activated BAT were evaluated by the unpaired t-test, after adjusting for age and gender (residuals from linear regression analyses). The *P* value of gender difference was calculated using the Chi-Square test. The Mann–Whitney U test was used to assess differences in BAT mass between lean and obese subjects. Paired and unpaired t-tests were applied to test the statistical significance between the PET results recorded under warm, cold and insulin-clamp conditions. Partial Pearson correlations adjusted for age and gender were used to study associations between different metabolic responses. Multiple linear regression analysis was applied to test independent determinants of cold-activated detectable BAT (dependent variables were waist circumference, fat percentage, age and gender). Differences in gene expression between SCWAT and BAT were evaluated either by the t-test or the Wilcoxon matched pairs signed ranks test. The following variables were log10-transformed before statistical testing: BAT glucose uptake rate, BAT blood flow, *M* value, AUC of plasma insulin, plasma TSH and free plasma T4. Statistical analyses were performed using SPSS 20.0. (563) and Stata 11.0. (564).

5 RESULTS

5.1 BAT, WAT and muscle metabolism in lean subjects (I–II)

Metabolic activation of BAT was detected in 19 out of 27 lean subjects (70%) under cold conditions, as defined by BAT glucose uptake rate. Active BAT was most often found bilaterally in the supraclavicular area, but in conjunction with the supraclavicular uptake, also in the paraspinal and -aortic regions, axillary depots, mediastinum, intercostal spaces and close to the adrenal glands in some subjects. Only the subjects with activated BAT were included in the analysis of BAT metabolism in lean subjects in order to define values for pure BAT.

The glucose uptake rate in BAT increased on average by a factor of 12 in response to cold, but no effects were seen in SCWAT, VAT or skeletal muscle (Fig. 5A). The mean mass of detectable cold-activated BAT was 34 ± 22 g in lean subjects. Under insulin-clamp conditions, the BAT glucose uptake rate was five times higher than under warm conditions (Fig. 5A), and did not significantly differ from the skeletal muscle glucose uptake rate (P = 0.19). Lower insulin-stimulated glucose uptake rates were seen in various WAT depots (Fig. 5A).

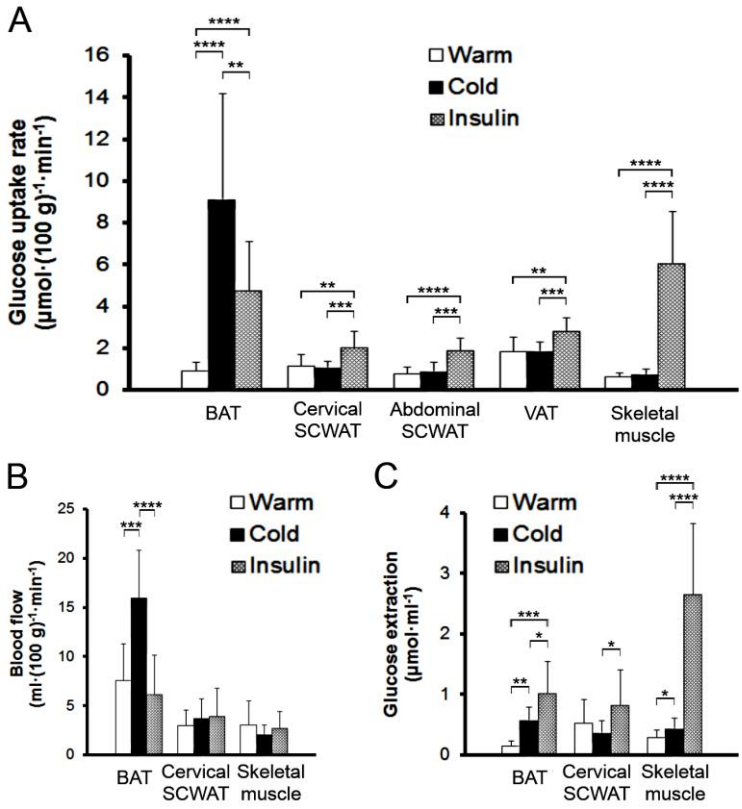

Figure 5. PET measurements under warm, cold, and insulin-clamp conditions in lean subjects
(**A**) Glucose uptake rates in various tissues. (**B**) Blood flow and corresponding (**C**) glucose extraction values in the cervical tissues. Results are expressed as means ± SD. *P < 0.05, **P < 0.01, ***P < 0.001, and ****P < 0.0001. Modified from Orava et al., 2011 (**II**).

The estimated amount of glucose taken up by the BAT depot was 1.1 ± 1.0 g • d^{-1} and 0.4 ± 0.4 g • d^{-1} under cold and insulin-clamp conditions, respectively, while altogether the skeletal muscles took up glucose 32 ± 11 g • d^{-1} and 290 ± 111 g • d^{-1} under cold and insulin-clamp conditions, respectively.

Blood flow in BAT increased 2-fold in response to cold exposure, but no changes were observed in cervical SCWAT or skeletal muscle (Fig. 5B). Subsequently, glucose extractions were determined (Fig. 5C). Cold exposure markedly increased glucose extraction in BAT, and slightly in skeletal muscle, but not in cervical SCWAT. However, insulin had the most significant effect on glucose extraction in BAT, cervical SCWAT and skeletal muscle (Fig. 5C).

5.2 Comparison of cervical BAT and SCWAT biopsies (I–II)

5.2.1 Gene expression (I–II)

In order to verify that apparent human BAT has the molecular signature of BAT, the levels of five BAT-characteristic genes were measured in three subjects (**I**). All the samples were analysed twice in triplicate, and subsequently, all the BAT versus SCWAT comparisons turned out to be statistically significant (*P* value of t-test < 0.05), except for the expression of PRDM16 in one subject. In the two other subjects, however, PRDM16 was 3–8 times more highly expressed in BAT than in SCWAT. Importantly, UCP1 was extremely highly expressed in the BAT samples of all three subjects, its expression in BAT varying from 3 000-folds to 13 000-folds to that in SCWAT. The expression of D2 was 2–30 times higher in BAT than in SCWAT. The expression levels of PGC-1α in BAT varied between 3–13 times to that in SCWAT, and finally, the gene of the β_3-adrenoceptor was expressed 4–60 times more highly in BAT than in the adjacent SCWAT.

In order to clarify the mechanism of higher insulin sensitivity of human BAT, the expression levels of five genes related to insulin signalling and glucose transport were compared between BAT and SCWAT in seven lean subjects using the Wilcoxon matched pairs signed ranks test (**II**). GLUT4 was more highly expressed in BAT than in SCWAT (*P* = 0.047), but no significant differences could be found in the expression levels of GLUT1 (*P* = 0.11), IRS1 (*P* = 0.078), IRS2 (*P* = 0.81) and IR (*P* = 0.94).

5.2.2 Histology and detection of BAT-characteristic proteins (I)

In the BAT samples from three subjects, typical brown adipocytes with multilocular lipid droplets could be identified, whereas in the SCWAT samples, these cells were absent. Staining with a UCP1-specific antibody was also seen in BAT but not in SCWAT. Further, Western blot analyses clearly revealed the presence of UCP1 and cytochrome c in all three BAT samples, while these proteins were not detected in the SCWAT samples. Finally, immunofluorescence staining showed the colocalisation of UCP1 and cytochrome oxidase subunit I in BAT but not in SCWAT, showing that UCP1 is, indeed, found in the BAT mitochondria in adult humans.

5.3 Comparison of BAT metabolism between lean and obese subjects (III)

Cold activation of BAT was detected in only 11 out of 36 (31%) obese subjects, but the cold-induced glucose uptake rate in BAT depot was high in some obese subjects (range: 0.3–19.1 μmol • (100 g)$^{-1}$ • min^{-1}). However, the mean BAT depot glucose uptake rates between warm and cold exposure did not differ significantly (P = 0.27). The characteristics of the lean and obese subjects are shown in Table 8.

Table 8. The characteristics of lean (n = 27) and obese (n = 36) subjects

Variable	Lean subjects	Obese subjects	*P* value[a]
Age (yr)	39.6 ± 9.8	38.1 ± 8.7	0.52
Proportion of males (ratio, %)	7/27, 26	11/36, 31	0.69
BMI (kg • m^{-2})	22.7 ± 2.3	34.0 ± 4.1	<0.001
Weight (kg)	66 ± 11	96 ± 15	<0.001
Waist circumference (cm)	76.0 ± 8.1	108.6 ± 13.2	<0.001
Fat percentage (%)	27.6 ± 6.2	40.8 ± 8.9	<0.001
Fat-free mass (kg)	47.8 ± 10.9	57.3 ± 13.3	<0.001
FFM-adjusted whole-body EE in cold (MJ • d^{-1})	6.9 ± 1.0	7.5 ± 1.0	0.024[b]
RQ in cold	0.82 ± 0.14	0.79 ± 0.03	0.10
FFM-adjusted whole-body EE in warm (MJ • d^{-1})	5.8 ± 0.4	6.2 ± 0.5	0.056[b]
RQ in warm	0.80 ± 0.03	0.80 ± 0.01	0.87
FFM-adjusted whole-body EE in insulin-clamp (MJ • d^{-1})	6.3 ± 0.6	6.7 ± 0.6	0.11[b]
RQ in insulin-clamp	0.92 ± 0.03	0.88 ± 0.04	0.008
Change in serum FFAs in cold (%)	85 ± 90	52 ± 47	0.20
Change in plasma insulin in cold (%)	-41 ± 32	-45 ± 20	0.66
2h-OGTT glucose AUC 0-120 min (mmol • l^{-1} • min)	849 ± 144	940 ± 172	0.028
2h-OGTT insulin AUC 0-120 min (mU • l^{-1} • min)	4138 ± 2067	8443 ± 4628	<0.001
Blood HbA_{1c} (%)	5.3 ± 0.3	5.6 ± 0.3	<0.001
Plasma TSH (mU • l^{-1})	2.6 ± 1.6	2.0 ± 0.9	0.19
Plasma free T4 (pmol • l^{-1})	14.9 ± 2.3	14.1 ± 2.4	0.12

Values are means ± SD. [a]Unpaired two-tailed t-test after adjusting for age and gender. [b]Whole-body EE was adjusted for fat-free mass (FFM). Modified from Orava et al., 2013 (**III**).

The mass of BAT was greater in the lean than in the obese subjects (24 ± 24 vs. 14 ± 29 g, P = 0.009; BAT-negative subjects included), and ranged from 0–102 g in all subjects. The BAT depot glucose uptake rate was also significantly higher in lean than in obese subjects under cold and insulin-clamp conditions (Fig. 6A).

To test whether the disparity in the effect of insulin was unique to BAT, other tissues were compared between the lean and the obese, and similar but less pronounced differences were found for the insulin-stimulated glucose uptake rates of cervical (P = 0.019) and abdominal (P = 0.024) SCWAT, and for skeletal muscle (P = 0.006), but not for VAT (P = 0.42). Further, the insulin-stimulated glucose uptake rate in the BAT depot of obese subjects was not significantly different from the insulin-stimulated glucose uptake rates in cervical (P = 0.18) and abdominal SCWAT (P = 0.065), and VAT (P = 0.076), whereas it was lower than the glucose uptake rate in skeletal muscle (P < 0.001). We also found an association between cold-induced and insulin-stimulated BAT depot glucose uptake rates (Fig. 6B).

Blood flow in the BAT depot was twice as high in the lean as in the obese subjects during cold exposure (Fig. 6C). Further, a positive correlation was found between glucose uptake rate and blood flow in the supraclavicular BAT depot during cold exposure (Fig. 6D). However, blood flow in BAT showed no difference between lean and obese subjects under warm or insulin-clamp conditions (Fig. 6C). Glucose extraction was higher in the BAT depot of lean subjects only during insulin stimulation (0.9 ± 0.5 vs. 0.4 ± 0.2 μmol • ml^{-1}, P = 0.003).

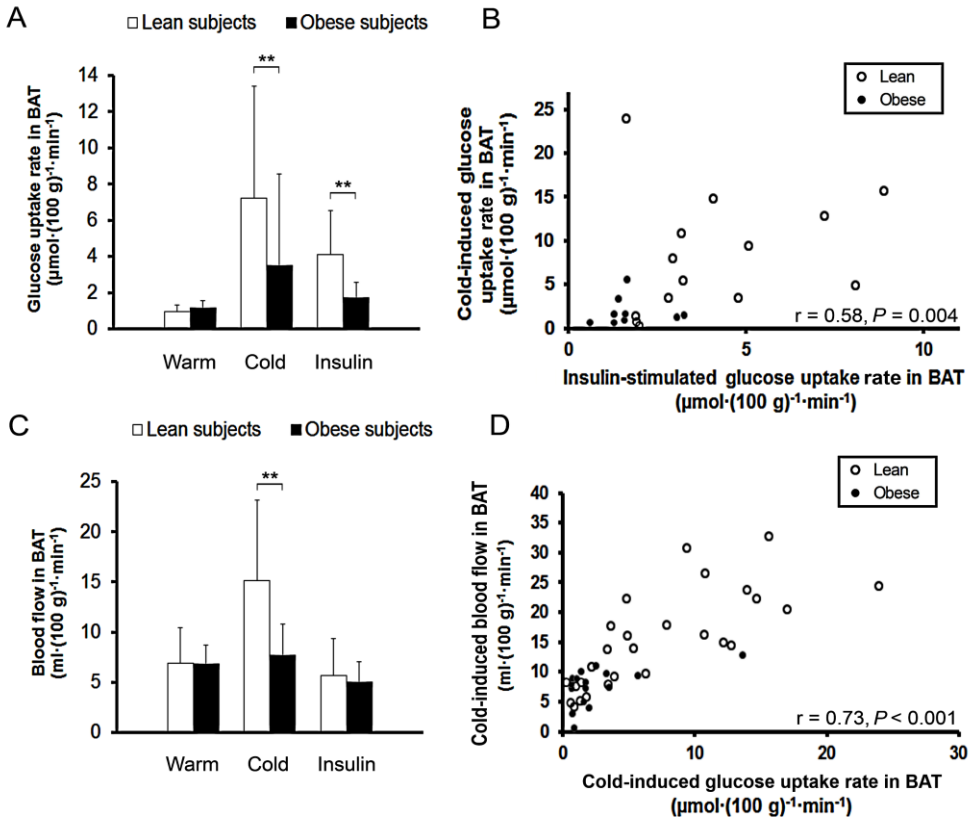

Figure 6. Comparison of supraclavicular BAT depot metabolism between lean and obese subjects
(**A**) BAT depot glucose uptake rates under warm, cold, and insulin-clamp conditions are shown. (**B**) The association between insulin- and cold-induced glucose uptake rates of BAT depot. The Pearson's correlation coefficient for all subjects is shown, and the corresponding coefficients were 0.47 (P = 0.092) and 0.28 (P = 0.46) in lean and obese subjects, respectively. (**C**) Blood flow in the BAT depot under warm, cold, and insulin-clamp conditions. The Pearson's correlation coefficient for all subjects is shown, and the corresponding coefficients were 0.82 (P < 0.001) and 0.40 (P = 0.12) in lean and obese subjects, respectively. (**D**) The association between glucose uptake rate and blood flow in BAT depot under cold conditions. Results are expressed as means ± SD. **P < 0.01. Modified from Orava et al., 2013 (**III**).

5.4 WAT and muscle metabolism in obese subjects (III)

The glucose uptake rates in cervical and abdominal SCWAT, visceral and perirenal adipose tissues, and skeletal muscle were unaffected by cold exposure, with insulin increasing glucose uptake significantly only in skeletal muscle (Fig. 7A).

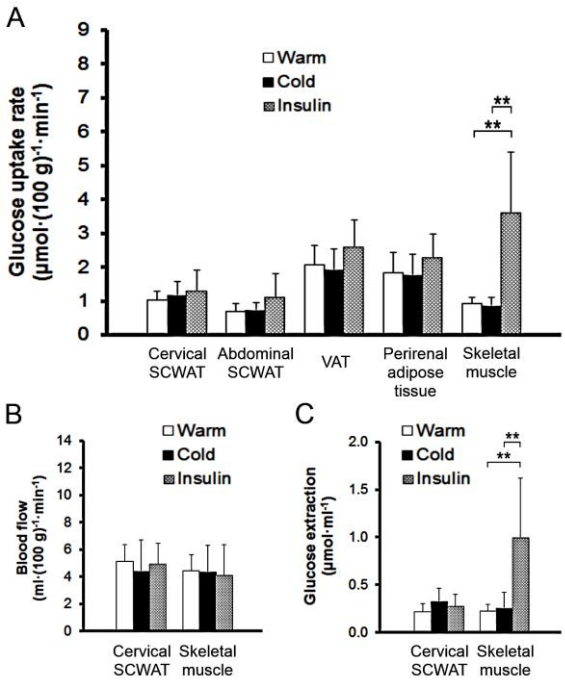

Figure 7. WAT and muscle metabolism under warm, cold, and insulin-clamp conditions in obese subjects
(**A**) Glucose uptake rates in various tissues are shown. (**B**) Blood flow and (**C**) corresponding glucose extraction values in the cervical SCWAT and skeletal muscle. Results are expressed as means ± SD. ***P* < 0.01. Modified from Orava et al., 2013 (**III**).

Compared to warm conditions, blood flow did not change in response to cold or insulin stimulation in the cervical SCWAT or skeletal muscle of the obese subjects (Fig. 7B), while insulin increased glucose extraction substantially in skeletal muscle (Fig. 7C).

5.5 Characteristics associated with detectable BAT activation (III)

Females had a higher cold-induced BAT glucose uptake rate than did males (3.1 ± 5.9 vs. 5.9 ± 5.6 µmol • (100 g)$^{-1}$ • min^{-1}, age-adjusted $P < 0.001$). The cold activation of BAT was also negatively associated with age. Subsequently, subjects with and without cold-activated BAT, as defined by the increased glucose uptake rate, were compared (Table 9).

Table 9. Characteristics of BAT-positive (n = 30) and BAT-negative (n = 33) subjects

Variable	BAT-positive	BAT-negative	*P* value[a]
Age (yr)	36 ± 11	41 ± 7	0.026
Proportion of females (ratio, %)	26/30, 87	19/33, 58	0.011
Proportion of obese (ratio, %)	11/30, 37	25/33, 76	0.002
BMI ($kg \cdot m^{-2}$)	26.6 ± 5.8	31.5 ± 6.6	0.0015
Weight (kg)	73 ± 15	93 ± 20	<0.001
Waist circumference (cm)	85 ± 15	103 ± 19	0.0015
Fat percentage (%)	34 ± 10	36 ± 11	0.0076
Whole-body EE in cold ($MJ \cdot d^{-1}$)	6.9 ± 1.4	7.5 ± 1.2	0.07[b]
FFM-adjusted whole-body EE in cold ($MJ \cdot d^{-1}$)	7.3 ± 1.1	7.1 ± 0.9	0.53[c]
RQ in cold	0.81 ± 0.14	0.80 ± 0.03	0.34
2h-OGTT glucose AUC 0-120 min ($mmol \cdot l^{-1} \cdot min$)	857 ± 143	941 ± 176	0.21
2h-OGTT insulin AUC 0-120 min ($mU \cdot l^{-1} \cdot min$)	5739 ± 4486	7379 ± 4035	0.16
***M* value** ($\mu mol \cdot kg^{-1} \cdot min^{-1}$)	45 ± 22	31 ± 18	0.017
Blood HbA_{1c} (%)	5.4 ± 0.3	5.5 ± 0.3	0.17
Plasma total cholesterol ($mmol \cdot l^{-1}$)	4.6 ± 0.8	4.8 ± 0.8	0.99
Plasma HDL cholesterol ($mmol \cdot l^{-1}$)	1.7 ± 0.5	1.5 ± 0.4	0.30
Plasma LDL cholesterol ($mmol \cdot l^{-1}$)	2.5 ± 0.8	2.8 ± 0.7	0.58
Plasma triglycerides ($mmol \cdot l^{-1}$)	1.0 ± 0.8	1.1 ± 0.5	0.95
Plasma TSH ($mU \cdot l^{-1}$)	2.5 ± 1.6	2.0 ± 0.9	0.024
Plasma free T4 ($pmol \cdot l^{-1}$)	14.5 ± 2.1	14.4 ± 2.6	0.69
Change in serum FFAs in cold (%)	102 ± 90	43 ± 46	0.012
Change in plasma insulin in cold (%)	-48 ± 19	-38 ± 33	0.30

Values are means ± SD. [a]Unpaired 2-tailed t-test after adjusting for age and gender, starting from BMI. [b]Whole-body EE is reported without any corrections or as [c]adjusted for fat-free mass (FFM). Modified from Orava et al., 2013 (**III**).

Further, the cold-induced BAT depot glucose uptake rate correlated negatively with BMI, fat percentage, waist and hip circumferences (partial correlation adjusted for gender and age r = -0.39–(-0.50), $P < 0.002$). The negative correlation between glucose uptake rate in the BAT depot and waist circumference remained, even after adjustment for fat percentage (r = -0.37, $P = 0.0035$). The cold-induced BAT depot glucose uptake rate also correlated with the *M* value (r = 0.35, $P = 0.030$) and AUC of glucose in 2h-OGTT (r = -0.30, $P = 0.021$) before, but not after, further adjustment for fat percentage. In a multivariate regression model, age (β = -0.33, 95% CI -0.47–(-0.19) years, $P < 0.001$) and waist circumference (β = -0.18, 95% CI -0.33–(-0.03) cm, $P < 0.017$) remained significantly associated with the cold-induced BAT depot glucose uptake rate, independent of gender and fat percentage (whole model $R^2 = 0.36$, $P < 0.001$).

The *M* value correlated with the insulin-stimulated glucose uptake rate of the BAT depot (gender- and age-adjusted r = 0.57, $P = 0.007$) and slightly more modestly with insulin-stimulated glucose uptake rates in other adipose tissues (gender- and age-adjusted r = 0.48–0.52, $P < 0.05$). The insulin-stimulated glucose uptake rate in skeletal muscle was, as expected, highly associated with the *M* value (gender- and age-adjusted r = 0.82, $P < 0.001$). The glucose uptake rates of BAT and skeletal muscle correlated significantly during insulin stimulation (gender- and age-adjusted r = 0.50, $P = 0.022$).

5.6 Weight loss and metabolism in BAT, WAT and muscle (III)

The cold-induced BAT depot glucose uptake rate was not significantly different ($P = 0.058$) after a mean of 12.5% (range: 3.5–24.5%) weight loss, and no differences could be detected in other tissues either (Fig. 8). The mass of BAT was not increased as a result of weight loss (19 ± 32 vs. 18 ± 29 g, $P = 0.72$). As expected, whole-body glucose tolerance and insulin sensitivity, which was estimated using the Matsuda index, improved after weight loss (Table 10).

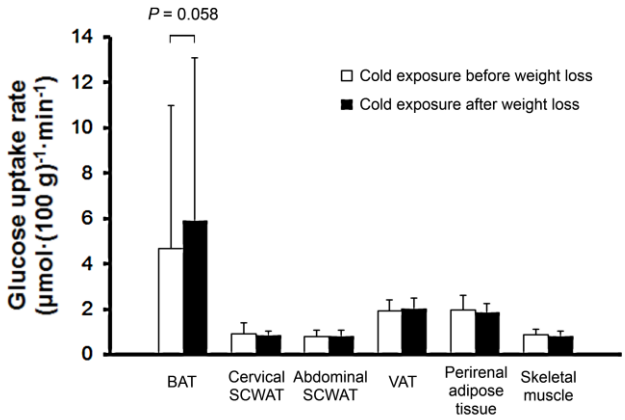

Figure 8. Cold-induced glucose uptake rates before and after five-month weight loss
Cold-induced glucose uptake rates in various tissues of 18 obese subjects after a mean of 12.5% weight loss are shown. Only the supraclavicular BAT depot showed a trend towards higher cold-induced glucose uptake after the weight loss. Results are expressed as means ± SD. Modified from Orava et al., 2013 (**III**).

Table 10. Characteristics of obese subjects before and after weight loss

Variable	Before weight loss	After weight loss	*P* value[a]
Age (yr)	35.2 ± 8.0	35.6 ± 8.0	-
Proportion of males (ratio, %)	6/18, 33	6/18, 33	-
BMI (kg • m^{-2})	35.0 ± 2.6	30.8 ± 3.4	<0.001
Weight (kg)	99 ± 14	87 ± 14	<0.001
Waist circumference (cm)	112.5 ± 10.1	100.3 ± 10.0	<0.001
Fat percentage (%)	41.2 ± 8.8	37.0 ± 9.3	<0.001
Fat-free mass (kg)	58.9 ± 14.9	55.0 ± 13.1	<0.001
FFM-adjusted whole-body EE in cold (MJ • d^{-1})	8.1 ± 1.1	7.3 ± 0.8	<0.001
RQ in cold	0.78 ± 0.02	0. 79 ± 0.02	0.063
2h-OGTT glucose AUC 0-120 min (mmol • l^{-1} • min)	903 ± 181	808 ± 164	0.007
2h-OGTT insulin AUC 0-120 min (mU • l^{-1} • min)	7929 ± 4997	4894 ± 3258	<0.001
Matsuda index	5.0 ± 2.9	7.7 ± 4.2	<0.001
Blood HbA_{1c} (%)	5.6 ± 0.3	5.5 ± 0.3	0.077
Plasma TSH (mU • l^{-1})	1.8 ± 0.6	-	-
Plasma free T4 (pmol • l^{-1})	12.9 ± 1.4	-	-

Values are means ± SD. [a]Paired two-tailed t-test. Modified from Orava et al., 2013 (**III**).

Interestingly, in the six subjects with the largest elevation in their BAT depot metabolism, defined as an increase of more than 1 µmol • $(100\ g)^{-1}$ • min^{-1} in the supraclavicular glucose uptake rate after weight loss, the glucose uptake rate also increased in their perirenal adipose tissue (1.7 ± 0.5 vs. 2.0 ± 0.4 µmol • $(100\ g)^{-1}$ • min^{-1}, $P = 0.042$), while no higher glucose uptake was observed in the other WAT depots or skeletal muscle. Weight loss also affected HR, systolic and diastolic BP, all of which were lower in cold conditions after weight loss. Before weight loss, the BAT non-activators showed significant increases in both systolic ($P < 0.001$) and diastolic BP ($P = 0.0038$) as a response to cold, whereas in the BAT activators, BP did not change from warm to cold conditions. After weight loss, the increase was less pronounced and was only seen for systolic BP ($P = 0.017$) in the BAT non-activators.

5.7 Whole-body energy expenditure and BAT metabolism (II–III)

As compared to measurements made under warm conditions, cold exposure increased whole-body EE (5.9 ± 0.9 vs. 6.8 ± 1.2 MJ • d^{-1}, *P* = 0.005) but not RQ (0.80 ± 0.02 vs. 0.81 ± 0.11, *P* = 0.24). However, despite their lower BAT activity, obese subjects had higher FFM-adjusted EE under cold conditions (Table 8). Further, when lean and obese subjects were divided into two groups, BAT-positive and BAT-negative, FFM-adjusted EE did not differ significantly between the groups (Table 9). On the other hand, under cold conditions, blood flow in the supraclavicular BAT depot was found to be positively associated with FFM-adjusted EE in lean but not in obese subjects (Fig. 9). Interestingly, glucose uptake rate in the BAT depot was not significantly associated with FFM-adjusted EE under cold conditions (r = 0.22, *P* = 0.272; r = 0.26, *P* = 0.128, lean and obese subjects, respectively).

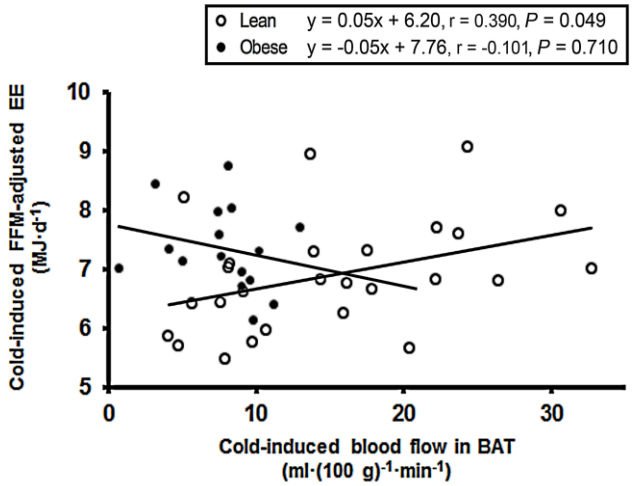

Figure 9. Association of FFM-adjusted EE and BAT depot blood flow under cold conditions
Lean and obese subjects are indicated separately. The linear regression equations of non-log10-transformed values are shown in both lean and obese subjects.

5.8 Cerebral glucose uptake (IV)

5.8.1 Cerebral glucose uptake in lean and obese subjects (IV)

Cold-induced cerebral glucose uptake was investigated in 24 lean and 17 obese subjects (Table 11), and eight lean and seven obese subjects were also studied under warm control conditions. As a response to cold exposure, the cerebral glucose uptake increased all over the neocortex as well as in the subcortical regions and the cerebellum (Fig. 10A). The greatest cold-driven glucose uptake elevation was observed in the parietal and frontal lobes, but glucose uptake rate was not altered by cold exposure in the limbic system, the pons or the hypothalamus.

Table 11. Characteristics of lean (n = 24) and obese (n = 17) subjects whose cerebral glucose metabolism was studied under cold conditions

Variable	Lean subjects	Obese subjects	*P* value[a]
Proportion of males (ratio, %)	5/24, 21 %	5/17, 29 %	0.53
Age (yr)	39 ± 10	40 ± 9	0.80
Body mass index, BMI (kg • m^{-2})	22 ± 2	33 ± 6	< 0.001
Weight (kg)	64 ± 9	92 ± 15	< 0.001
Waist circumference (cm)	75 ± 7	103 ± 15	< 0.001
Hip circumference (cm)	90 ± 6	111 ± 14	< 0.001
Fat percentage (%)	27 ± 6	40 ± 10	< 0.001
Blood HbA_{1c} (%)	5.3 ± 0.3	5.5 ± 0.3	0.01
Plasma total cholesterol (mmol • l^{-1})	4.8 ± 0.7	4.8 ± 0.9	0.82
Plasma HDL cholesterol (mmol • l^{-1})	1.9 ± 0.4	1.4 ± 0.3	< 0.001
Plasma LDL cholesterol (mmol • l^{-1})	2.5 ± 0.6	2.7 ± 0.8	0.42
Plasma triglycerides (mmol • l^{-1})	0.8 ± 0.3	1.5 ± 1.0	0.01
Plasma TSH (mU • l^{-1})	2.6 ± 1.7	2.5 ± 1.0	0.88
Plasma free T4 (pmol • l^{-1})	14.7 ± 2.3	15.8 ± 2.4	0.13
Plasma free T3 (pmol • l^{-1})	4.7 ± 0.6	5.0 ± 0.5	0.03

Data are mean ± SD. **P* values are from two-tailed unpaired t-tests. Modified from Orava et al., in press (**IV**).

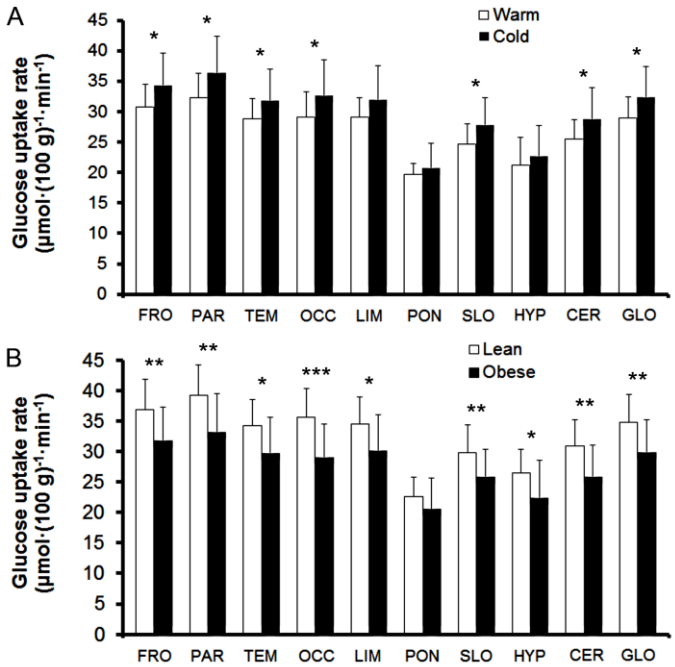

Figure 10. Cerebral glucose uptake in lean and obese subjects
(**A**) Cerebral glucose uptake rates of the eight lean and seven obese subjects whose cerebral glucose uptake was measured under both warm and cold conditions. (**B**) Cold-induced cerebral glucose uptake rates are shown separately for lean and obese subjects. Results are expressed as means ± SD. **P* < 0.05, ***P* < 0.01, ****P* < 0.001. Note: FRO, frontal lobe; PAR, parietal lobe; TEM, temporal lobe; OCC, occipital lobe; LIM, limbic lobe; PON, pons; SLO, sub-lobar regions; HYP, hypothalamus; CER, cerebellum; GLO, mean cortex. Modified from Orava et al., in press (**IV**).

Under cold conditions, cerebral glucose uptake rates were higher in most regions in the lean than in the obese subjects (Fig. 10B), while no such differences could be established under warm conditions.

5.8.2 BAT metabolism in relation to cerebral glucose uptake (IV)

SPM analysis showed that supraclavicular BAT depot glucose uptake rate was positively associated with the glucose uptake rates of the cerebellum, thalamus, temporo-parietal, lateral frontal and cingulate cortices under cold conditions (Fig. 11A), while no significant connections could be found under warm conditions. During cold exposure, the association was stronger in lean than in obese subjects (Fig. 11B). No negative associations were observed under warm or cold conditions. It is of note that the glucose uptake rates of SCWAT, VAT and skeletal muscle were not associated with cerebral glucose uptake rates under either warm or cold conditions.

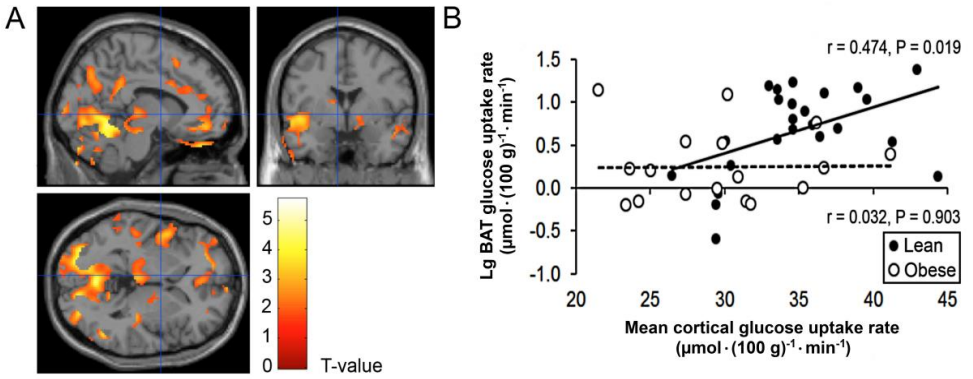

Figure 11. Association between glucose uptake rates of the brain and of BAT
(**A**) Lean participants' brain regions whose glucose uptake rate was associated significantly with that of BAT under cold conditions. (**B**) The scatterplots show the relationship between mean cortical cerebral and BAT glucose uptake rates under cold conditions in lean and obese subjects. Modified from Orava et al., in press (**IV**).

6 DISCUSSION

6.1 Identification of functional brown adipose tissue in adult humans (I)

Since the first convincing hypothesis regarding active brown adipose tissue in adult humans (12), this study has provided the next step forward in the field of human BAT research. The study showed conclusively that healthy adult humans have cold-activated BAT by demonstrating increased glucose uptake in the supraclavicular adipose tissue under cold conditions in healthy lean adults and by combining these imaging findings with corresponding tissue sample analyses that clearly indicated the histology and expression of genes and proteins characteristic of BAT. Of note, the anatomical location of the newly discovered functional BAT in the PET/CT images showed a strikingly similar pattern as had already been described one hundred years ago in a classical dissection study (341). Now, however, the function of this unique tissue was also identified unequivocally.

Previous studies related to putative human BAT in imaging were either case reports or retrospective patient studies, and thus no profound conclusions could have had drawn on the presence or function of BAT as part of the normal physiology in adult humans. This is due to the fact that various underlying medical conditions, such as malignancies, may have an impact on BAT metabolism, and that controlled cold exposures had not been applied, even though the ultimate function of BAT is to defend core body temperature in a cold environment. Further, in previous studies, the true identity of increased metabolic activity in imaging had not been verified by means of biopsies.

One other report on BAT in healthy humans was also published at the same time as the first sub-study of this dissertation (13) and another a few weeks later (40), both of which studies did involve controlled cold exposure. However, neither of these two studies was unequivocally able to demonstrate that the cold-induced glucose metabolic activity in the supraclavicular adipose tissue was related to BAT function – the biopsies demonstrated were not obtained from healthy subjects who had been studied using PET/CT. On the other hand, these two studies showed for the first time that the assumed BAT activity in healthy adults was inversely associated with BMI, suggesting a role for BAT in human energy homeostasis.

After the identification of functional BAT in healthy adult humans, a clear target was set to elucidate the role of BAT in energy homeostasis and to clarify whether the insulin sensitivity of BAT differs from that of WAT and skeletal muscle in healthy lean adults. These aims were considered important since, on the basis of numerous studies on rodents, BAT is known to be a metabolically highly active and insulin-sensitive tissue. Subsequently, the BAT of obese adult humans was also studied, since BAT in rodents has been shown to have a fundamental impact on body-weight. Finally, it was hypothesised that, being regulated by the CNS, the BAT function and the activity of specific cerebral regions might be linked. Further, it was also postulated that lean and obese adult humans may have differences in their cerebral responses to cold exposure, which could contribute to the possible disparities in BAT metabolism.

6.2 Glucose uptake by human brown adipose tissue (I–III)

In this study, BAT glucose uptake rate was quantified using the model of Gjedde-Patlak, as it provides an accurate metabolic uptake rate of glucose independently of the size of the subject, the plasma glucose concentration and the administered dose and plasma clearance of the [^{18}F]FDG (496–497). Therefore, we could reliably compare lean and obese subjects and study

different conditions. With semi-quantitative methods, such as the SUV, the risk of bias would have been considerable.

Here, the stimulatory effects of both cold exposure and insulin on human BAT glucose uptake are clearly demonstrated. Furthermore, both these effects were found to be significantly impaired by obesity. No other studies have so far been conducted on the effect of insulin on human BAT *in vivo*.

The insulin sensitivity of BAT in lean subjects was not significantly different from that found in skeletal muscle, showing that human BAT is a highly insulin-sensitive tissue. A possible mechanism behind the marked insulin sensitivity could be the higher abundance of GLUT4 in BAT than in SCWAT, as was indicated by the elevated GLUT4 gene expression levels. However, it should be noted that the supraclavicular biopsies were obtained under warm conditions and without insulin stimulation, and that, in general, gene expression does not verify the presence of functional proteins in the tissue.

The low cold-induced glucose uptake was linked to reduced blood flow in the BAT of obese subjects, whereas glucose extraction was similar between lean and obese subjects. By contrast, the blunted insulin action in obesity was associated with decreased glucose extraction in BAT. Further, a trend suggesting increased cold-induced glucose uptake by BAT after conventional weight loss was found, while no significant changes or trends could be found in the various WAT depots or skeletal muscle.

Plasma NA was measured in lean subjects, and it was found to be increased in response to cold, indicating elevated overall sympathetic tone. It was also demonstrated that BP increased in response to cold more before than after weight loss, and that HR decreased during cold exposure, after but not before, weight loss in obese subjects. Based on these findings, it can be hypothesised that sympathetic overactivity in obese humans is linked to impaired BAT glucose uptake.

This study shows for the first time in a prospective setting that BAT activity is higher in females than in males, as judged by the cold-induced glucose uptake rate in the supraclavicular BAT depot. This is in line with the conclusions based on retrospective patient studies and on a study according to which abdominal SCWAT in females shows higher levels of UCP1 mRNA as compared to males (565). Taken together, these observations suggest a more brownish phenotype of the adipose tissue in females as compared to males. Besides the gender-based difference, it was also shown that cold-induced BAT glucose uptake rate decreases with age. Subsequently, after correcting for gender and age, the cold activation of BAT was also associated with slightly elevated baseline plasma TSH concentration. Interestingly, TSH-Rs are found in adipose tissue (249), and their activation has been associated with increased UCP1 expression in preadipocytes (250). Although no causality has been proven, it can be speculated that TSH may promote brown adipogenesis. In addition, circulating FFAs were also found to be elevated in BAT-positive subjects under cold conditions. The cold-induced increase in circulating FFAs has also been shown in previous studies (122), but those studies did not assess BAT activity. The increase in circulating FFAs probably results from increased sympathetic stimulation and decreased insulin action in WAT under cold conditions. It has been shown in rodents that FFAs are the main source of energy in BAT thermogenesis (189). Therefore, the increase in circulating FFAs can also be interpreted to mean that the lipolytic physiological signals to WAT might have the same origin as the BAT-activating signals, since concurrent release of fatty acids provide fuel for thermogenesis, or they are utilised in the refuelling of BAT in humans (103).

Here, it is suggested that a lifestyle change with weight loss over a five-month period increases the cold-induced glucose uptake rate by human BAT. The finding is in line with a study indicating that morbidly obese subjects may increase their BAT activity after bariatric surgery (504). Moreover, we showed that the subjects with the greatest increase in their BAT glucose uptake rate also had an increase in the glucose uptake rate in perirenal adipose tissue. BAT is known to be present within perirenal adipose tissue in adult humans (566). Taking these observations into account, it seems reasonable to conclude that weight loss can increase cold-induced glucose uptake in perirenal BAT, although the supraclavicular region is clearly the main BAT depot of adult humans.

6.3 Blood flow in human brown adipose tissue (II–III)

Kinetic modelling was applied for quantifying tissue blood flow. The kinetic modelling allows precise quantification of blood flow despite blood flow heterogeneity and an unknown partition coefficient of water in the tissue, both of which are characteristic of both white and brown adipose tissue.

BAT in rodents is known to be a highly vascularised tissue. Here, it was shown for the first time that blood flow in human BAT is significantly increased as a response to cold exposure, and that this response is attenuated in obesity. Increased cold-induced blood flow in human BAT has subsequently been confirmed by others (520–521). Moreover, the actual blood flow values of BAT were rather similar in the published studies, even though different cold exposure protocols have been applied.

BAT blood flow and glucose uptake rate were associated under cold conditions. In general, blood flow is closely related to oxygen demand in the tissues (286), and it has been shown in rodents that changes in BAT blood flow reflect changes in the oxygen-consuming thermogenic metabolism in BAT (288). Taken together, both the decreased glucose uptake rate and the attenuated blood flow in the BAT of obese subjects under cold conditions argue for a blunted thermogenic capacity of BAT in obese humans, although BAT thermogenesis was not directly measured.

It was also shown that insulin stimulation does not increase blood flow in human BAT, albeit glucose uptake by BAT is significantly enhanced by insulin. The results suggest that, unlike cold exposure, insulin does not induce thermogenesis in human BAT, since insulin failed to increase blood flow in BAT. This interpretation is in line with the findings of rodent studies, which indicate that insulin inhibits lipolysis and, thus, also thermogenesis (567). Further, the concentration of plasma NA was substantially increased only during cold exposure, suggesting that insulin did not ignite NA-driven BAT thermogenesis. Insulin has been shown to increase plasma NA when infused at a 15-fold concentration compared to the protocol used here (568), while plasma insulin concentrations comparable to those used in this study have been shown to increase the sympathetic tone in skeletal muscle (569). In conclusion, although significantly elevated sympathetic tone in BAT caused by insulin probably did not occur, it cannot be excluded, since the BAT-specific sympathetic tone was not measured in this study.

6.4 Impact of human BAT on metabolism at whole-body level (III)

The cold-induced glucose uptake rate in BAT was inversely associated with BMI, fat percentage and waist circumference, even after corrections for gender and age. The association of low BAT activity to large waist circumference remained after adjusting for overall adiposity. This suggests that the causes that promote detrimental abdominal fat accumulation may partly

be the same as those favouring impaired BAT metabolism, or that the presence of central adiposity is a sign of a metabolically harmful status, for instance inflammation, which could deactivate BAT (570). In summary, these findings argue that a phenotype rich in cold-activated BAT is beneficial for adipose tissue distribution and energy homeostasis.

In rodents, increased amounts of BAT provide improved glucose tolerance (217), and the role of insulin-sensitive human BAT was therefore assessed at whole-body level. Subsequently, a positive correlation with the insulin-stimulated BAT glucose uptake rate and the *M* value was found. Interestingly, the presence of cold-activated BAT was also associated with a higher *M* value. Further, other investigators have found negative associations between BAT glucose uptake and blood glucose and HbA_{1c} in healthy adult humans (502). However, the role of BAT in glucose disposal in humans can still be disputed. On the basis of this study, it can be estimated that, in the subjects who were not cold-acclimated, glucose uptake at whole-body level is, on average, 30 and 700 times higher in skeletal muscle than in BAT during cold and insulin stimulation, respectively. Furthermore, it is suggested that the impacts of weight loss on cold- and insulin-stimulated glucose disposal are not associated. Whole-body insulin sensitivity was markedly enhanced, although, with the exception of the trend towards a higher cold-induced BAT glucose uptake rate, no significant changes in the cold-induced glucose uptake rates were found in the tissues studied after weight loss. On the other hand, it has been shown that transplanted BAT improves glucose homeostasis by increasing the insulin sensitivities of WAT and the myocardium in mice (219), suggesting an endocrine role for BAT. Whether BAT truly improves the insulin sensitivity of other tissues in humans remains to be discovered.

Unlike the glucose uptake rate of BAT, blood flow in the BAT of lean subjects was positively associated with whole-body EE under cold conditions. No such associations were found under warm or insulin-clamp conditions. The metabolism in various WAT depots and skeletal muscle was not significantly affected by cold exposure. However, cerebral glucose uptake was increased by cold exposure, which might affect whole-body EE. The brain utilises glucose as a predominant energy substrate to satisfy its high metabolic needs (571). The proportion of brain of whole-body EE is approximately 20% under resting conditions, and the brain metabolic rate can have implication on whole-body EE (572). We measured an 11% mean rise in the mean cortical glucose uptake rate due to cold exposure, and on the basis of EE measurements under warm (resting) and cold conditions, it can be estimated that mean brain EE was elevated by at most 0.13 MJ • d^{-1} by cold exposure. However, mean whole-body EE was increased by 0.48 MJ • d^{-1} at the same time, suggesting that the brain was responsible for only a quarter of the cold-induced increment in whole-body EE. However, the contributions of all the various organs in the body to whole-body EE are currently undetermined, and thus the proportion of BAT in the cold-induced increment of whole-body EE cannot be fully clarified. Nevertheless, from all the tested parameters, BAT blood flow showed the most significant positive correlation with whole-body EE, suggesting a marked role for BAT in cold-induced thermogenesis in humans. However, it should be pointed out that BAT oxygen consumption can also be measured directly by PET, and these measurements indicate a minor role for BAT in cold-induced thermogenesis in humans who are not cold-acclimated (520–521).

6.5 Cold-induced glucose uptake in brain and BAT (IV)

Regional cerebral glucose uptake reflects focal neural activity (573). The close relationship between the glucose metabolism of specific cerebral regions and the BAT function shows that BAT thermogenesis involves diverse activation of the human brain. Neither of the previous studies on the human CNS mechanisms of BAT activation involved cold exposure, which

might partly explain the differences between the present and previous findings. Also, the previous studies only estimated cerebral glucose metabolism, by measuring [^{18}F]FDG activity or SUVs.

The positive association that was found between BAT glucose uptake rate and the cingulate cortex metabolism may be related to the regulation of the sympathetic response (574). Increased activity was also detected in the cerebellum. The cerebellum is known to process sensory input (575), which might partly explain its activity in conjunction with cold exposure. On the other hand, the cerebellum is also involved in the coordination of sympathetic and parasympathetic information, since lesions of the cerebellum have a fundamental impact on autonomic functions, for instance, the regulation of the cardiovascular system (576). Interestingly, increased metabolic activity in the cerebellum has also been shown in hyperthermia, suggesting a thermoregulatory function for the cerebellum in humans (577). This study suggests an additional role for the cerebellum in the regulation of BAT function.

In accordance with prior studies (143, 146), we observed that cold exposure elicited activation of the somatosensory cortex. Interestingly, increased cold-induced cerebellar [^{18}F]FDG activity was also indicated in the only previous report on the brain glucose metabolism of healthy humans under cold conditions (149). However, in the present study no decreased metabolism in either insula was observed during cold exposure. The reason for such a discrepancy could stem from the fact that the study subjects, cold exposure and quantification of [^{18}F]FDG-PET data were very different.

Although the hypothalamus has a key role in controlling BAT function and body temperature (126), we did not detect any change in its metabolism due to cold exposure. Neither could we observe any association between BAT metabolism and the hypothalamic glucose uptake rate. However, it was found that the glucose uptake rate in the hypothalamus was higher in lean than in obese subjects during cold exposure, suggesting that hypothalamic thermoregulation was functioning less actively in obese humans. Further, the cold-induced response was attenuated in many cerebral regions in obese subjects as compared to lean subjects, perhaps explaining why active BAT is detected less frequently in obese humans under cold conditions.

On the other hand, the results show that, besides the hypothalamus, other cerebral regions also have a role in regulating physiological responses to cold exposure in humans. It seems that basic research with animals has almost completely focused on hypothalamus and a few nuclei in the medulla (Fig. 2). Considering the complex nature of cold exposure, which includes, e.g., afferent thermal signals, various efferent signals of insulative response and facultative thermogenesis, and also affects cognition (localisation of cold stimulus, stress etc.), it is very probable that the neocortex and the cerebellum are also active in controlling the body's response to cold exposure in humans. Thus, the findings presented in this study regarding cold-induced cerebral activity, should not be ignored or disregarded as unorthodox.

6.6 Limitations of the study

In this study, only the BAT glucose uptake rate and blood flow were measured, although fatty acids are the main fuel source of activated BAT (189), and BAT has a key role in overall fatty acid handling, as shown in rodents (178). Further, substantial fatty acid uptake and oxidation have been shown to occur in humans, too (103), and thus differences in fatty acid consumption may contribute to the variation observed in the BAT glucose uptake rate. It is also possible that some BAT-negative subjects, as defined by the glucose uptake rate, had a significant fatty acid

metabolism within their BAT. However, because of the limitations on radiation dose, additional PET measurements of fatty acid metabolism could not be performed on the study subjects.

The tissue samples of human BAT usually show multilocular cells interspersed within WAT. Therefore, it is likely that the human BAT measurements carried out by PET always include both BAT and, to some extent, WAT. Thus, the so-called partial volume effect may lead to a decrease in the level of detected BAT activity, if the diameters of BAT regions are smaller than the resolution of the scanner. This might, at least partly, explain why some metabolic parameters show significantly lower values in humans as compared to rodents. For instance, markedly higher blood flow values have been measured in rodents (278). It should also be pointed out that, for the quantification of BAT glucose uptake rate, an LC value of 1.14, which accounts for the differences between uptake of [^{18}F]FDG and glucose, was used, although this value is derived from experiments on abdominal SCWAT (557). Albeit all the validated LC values of different tissues have been close to 1.00, the lack of correct LC for BAT slightly influences the accuracy of the reported BAT glucose uptake rate values.

Currently, no feasible method is available for assessing the sympathetic outflow to human BAT. Plasma catecholamines provide a good estimation of the overall sympathetic tone, but they were only measured in lean subjects, and the evaluation of the sympathetic tone between lean and obese subjects was therefore performed by comparing BP and HR measurements. However, BP and HR only estimate the sympathetic responses of the cardiovascular system, and thus these measurements have a limited power to determine the sympathetic stimulation of BAT.

It should also be pointed out that two different PET scanners were used, although both the scanners have relatively similar spatial resolutions (578–579). The utilisation of two scanners was a practical solution, since the PET/CT scanner was in great clinical demand at the time of our investigations. Importantly, all PET analyses were performed using the same software, and ROIs were systematically outlined using a similar technique in all images, substantially reducing the risk of bias. Nevertheless, minor differences between the scanners cannot be completely excluded.

It can also be argued that the cooling was not optimal for all subjects, resulting in false negatives in respect to BAT activity. However, it has been demonstrated that most morbidly obese humans fail to activate BAT even after a personalised cooling protocol has been utilised (500), which argues against the view that the method of cold exposure is of vital importance when BAT metabolism is studied. Further, although electromyography was not applied in the study, shivering was not generally encountered under cold conditions, as assessed by inspecting and questioning of the subjects, suggesting that the "cold exposure window" included mostly the phase of non-shivering thermogenesis. It is nevertheless possible that protocols applying cold exposure to large skin area, such as the use of water-perfused suits (96) or vests (114), would have led to minor variation in the measured parameters of BAT activity. It must be noted that, due to the use of kinetic modelling, PET imaging was started simultaneously with the administration of the tracers, and for this reason whole-body cooling could not be applied easily during the imaging.

Taken together, despite some disadvantages or parts of the study that could have been improved, the findings of the study are genuine, and thus the conclusions presented are valid, providing novel insights into the function of human BAT.

6.7 Key areas of future research

Currently, the most sensitive method for detecting functional human BAT is [^{18}F]FDG-PET/CT. However, there is a clear demand for alternative methods, since the availability of PET is limited in many parts of the world, and moreover PET imaging is rather expensive. The use of ionising radiation also sets limits to the experiments that can be carried out with human subjects. Promising results have been obtained with MRI (533–534), which has better spatial resolution than PET and also enables functional imaging. In the future, MRI technology should be developed in close collaboration with physicians, who have a clear view of the metabolic aspect of BAT, and also with physicists, who have the best knowledge of the possibilities and limitations of various MRI techniques. As PET/MRI scanners become more common, it is probable that MRI methods for human BAT imaging will be developed more intensively. MRI imaging could also provide significantly preciser evaluation of the cerebral processes related to BAT function. Especially the hypothalamus, which is a small structure and is thought to be the key site of the thermoregulatory network, can be more reliably studied with MRI.

Little is known about the role of BAT in certain common diseases. For instance, the role of BAT in hypothyroidism-related weight gain needs elucidation. In addition, it is not clear whether BAT is involved in cancer-cachexia or febrile reaction in humans.

Nevertheless, PET also provides many untapped features for human BAT imaging. For instance, the sympathetic activity of human BAT can also be studied using PET, and in fact, current evidence for the sympathetic innervation of human BAT has been provided using semi-quantitative ^{123}I-MIBG-SPECT/CT (511) or qualitative [^{18}F]-6-fluorodopamine-PET/CT (447). BAT in humans is presumed to be under the direct control of the peripheral SNS, and thus, better understanding of this innervation could offer new ways to activate human BAT.

Further, it is yet to be shown, whether sympathomimetics induce BAT metabolism in humans. Results on ephedrine are contradictory (114, 527), and a study shows that isoprenaline does not induce BAT metabolism (528). Further, there are currently no PET studies published on the effect of selective β_3-agonists on human BAT. It is also unresolved whether the promotion of BAT has a weight-lowering effect in humans, although studies suggest that repeated cold exposure increases BAT activity (67–69). In fact, additional studies on human BAT recruitment are also needed, since the capacity of the BAT depot to increase glucose uptake after cold-acclimation has not been shown unequivocally. Importantly, it is also not known whether chronic cold exposure, i.e., inhabiting cold climate regions, can increase the volume and activity of BAT in humans. Furthermore, investigators should think out of the box, and innovatively look for completely new methods of promoting BAT in humans.

7 CONCLUSIONS

1 Healthy lean adult humans have functional BAT, as assessed by the intense cold-induced glucose uptake rate and blood flow, the distinct multilocular cells, and the expression of BAT-characteristic genes and proteins in the tissue.

2 BAT in healthy lean adult humans is a highly insulin-sensitive tissue. Further, both the glucose uptake rate and blood flow in the BAT of healthy lean adult humans are increased in response to cold exposure, suggesting active thermogenesis. Cold-induced BAT blood flow is also positively associated with whole-body EE, suggesting a role for BAT in energy homeostasis.

3 The effects of cold exposure and insulin stimulation are decreased in the BAT of obese adult humans, as compared to lean subjects, but the glucose uptake capacity of cold-activated BAT may be restored after weight loss in adult humans. The presence of cold-activated BAT in the body may contribute to a metabolically healthy status.

4 Metabolic activation of BAT is accompanied by the activity of specific cerebral regions in adult humans. The cold-induced increment in cerebral activity is attenuated in obese adult humans as compared to lean adult humans, suggesting a possible mechanism for decreased cold-induced BAT activity in obesity.

8 ACKNOWLEDGEMENTS

This study was conducted within the Finnish Centre of Excellence in Molecular Imaging in Cardiovascular and Metabolic Research supported by the Academy of Finland, the University of Turku, the Hospital District of Southwest Finland and Åbo Akademi University.

First and most importantly, I wish to express my sincere acknowledgements to my supervisors, Docent Kirsi A. Virtanen and Professor Pirjo Nuutila, who gave me the opportunity to carry out this doctoral work in the Turku PET Centre and introduced me to the world of PET imaging. I also appreciate the support of Professor Juhani Knuuti, who as Director of Turku PET Centre provided excellent facilities for the studies of the doctorate. I also wish to express my appreciation to Professor Jaakko Hartiala, Head of the Department of Clinical Physiology and Nuclear Medicine, and Professor Jorma Viikari, Head of the Department of Medicine, for approving this study to be carried out in their departments. I also express my sincere thanks to Professor Markku Koulu and Docent Eriika Savontaus for their encouraging support for the project.

I also wish to thank the reviewers, Aaron M. Cypess and Atso Raasmaja, for their constructive comments that helped me to improve the thesis and Heikki A. Koistinen, for accepting the role of dissertation opponent.

This study was supported by personal grants from the Finnish Medical Foundation, Instrumentarium Science Foundation, the Finnish Cultural Foundation, The National Graduate School of Clinical Investigation, The Turku Doctoral Programme of Clinical Sciences and by the Elias Tillandz prize awarded by BioCity Turku. The study was also supported by grants from The Diabetes Research, Novo Nordisk and Paulo Foundations, and by the European Union (EU FP7 project 278373; DIABAT).

I am very grateful to Sven Enerbäck, Martin E. Lidell, Mikael Heglind and Rickard Westergren in the Department of Medical and Clinical Genetics, Institute of Biomedicine, Sahlgrenska Academy, University of Göteborg, for their vital contribution to the analysis of biopsies. I also thank Tarja Niemi for her surgical skills, placing the unique biopsies at our disposal, Markku Taittonen for anaesthesiological guidance during the biopsy procedures and Jukka Laine for the histological analysis of the tissue samples. I also appreciate Lauri Nummenmaa's input to the statistical parametric mapping of cerebral metabolism. A great deal of guidance has also been provided by Vesa Oikonen, who has helped me with many PET modelling issues over the years. I also owe my thanks to Tommi Noponen, who assessed the calorimetric raw data and helped me with image reconstructions. Further, I appreciate Kirsi H. Pietiläinen and Aila Rissanen for their excellent contributions, which helped me to better understand the various metabolic phenomena related to weight loss in humans. I also wish to thank Mika Teräs, Tuula Tolvanen and Jarkko Johansson for their assistance in PET image reconstruction issues, and Mika Scheinin for his expertise related to catecholamines. I acknowledge Riitta Parkkola for her assistance in radiological and anatomical issues. I also thank Nina-Johanna Savisto and Tapio Viljanen for their efforts in the radiochemistry of [^{18}F]FDG and Hannu Sipilä for the [^{15}O]H_2O equipment. I acknowledge Jacqueline Välimäki and Robert M. Badeau for the linguistic edition of the manuscripts, and Rosemary Mackenzie for the linguistic revision of the thesis.

I am also very much indebted to Patricia Iozzo, Ronald Borra, Jarna Hannukainen, Iina Laitinen and Saila Kauhanen for all the fruitful discussions we have had, and to Marko

Laaksonen and Kari Kalliokoski for providing insight into the physiology of exercising skeletal muscle. I also acknowledge Marco Bucci, Miikka Honka, Sergey Nesterov, Ilkka Heinonen and Anna Karmi for helping me with the modelling computer programs, and Markus Lindroos for his advice on the analyses of OGTT data. I also like to thank Riikka Lautamäki for the discussions related to blood flow measurements, and Minna Lahesmaa and Teemu Saari for their challenging questions relating to PET and BAT.

Acknowledgements are also due to Rami Mikkola and Marko Tättäläinen, who have helped me numerous times with computer issues. I also thank Mirja Jyrkinen and Tarja Marttila for helping me with many practical issues over the years. Further, I am grateful for the contributions of Helena Kortelainen, Eija Salo, Mia Koutu, Minna Aatsinki, Heidi Betlehem, Tarja Keskitalo, Marjo Tähti, and all the staff at the Turku PET Centre, whose efforts enabled us to carry out these studies.

I also owe a great debt of gratitude to the study subjects for their participation, which was vital for all the studies included in this doctoral thesis.

Finally, I owe an immeasurable debt of appreciation to my family and relatives for all the support they have provided over the years.

Turku, March 2014

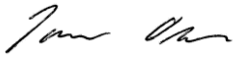

9 REFERENCES

1. **Cinti S.** *The adipose organ.* Prostaglandins Leukot Essent Fatty Acids. 2005;73(1):9-15.

2. **Oberkofler H, Dallinger G, Liu YM, Hell E, Krempler F, Patsch W.** *Uncoupling protein gene: quantification of expression levels in adipose tissues of obese and non-obese humans.* J Lipid Res. 1997;38(10):2125-33.

3. **Cinti S.** *Transdifferentiation properties of adipocytes in the adipose organ.* Am J Physiol Endocrinol Metab. 2009;297(5):E977-86.

4. **Klaus S, Casteilla L, Bouillaud F, Ricquier D.** *The uncoupling protein UCP: a membraneous mitochondrial ion carrier exclusively expressed in brown adipose tissue.* Int J Biochem. 1991;23(9):791-801.

5. **Heaton GM, Wagenvoord RJ, Kemp A Jr, Nicholls DG.** *Brown-adipose-tissue mitochondria: photoaffinity labelling of the regulatory site of energy dissipation.* Eur J Biochem. 1978;82(2):515-21.

6. **Smith RE.** *Thermoregulatory and adaptive behavior of brown adipose tissue.* Science. 1964;146(3652):1686-9.

7. **Morrison SF, Nakamura K, Madden CJ.** *Central control of thermogenesis in mammals.* Exp Physiol. 2008;93(7):773-97.

8. **Lean ME.** *Brown adipose tissue in humans.* Proc Nutr Soc. 1989;48(2):243-56.

9. **Cannon B, Nedergaard J.** *Brown adipose tissue: function and physiological significance.* Physiol Rev. 2004;84(1):277-359.

10. **World Health Organisation.** *Global Health Observatory (GHO) - Obesity.* Accessed 28th August 2013: http://www.who.int/gho/ncd/risk_factors/obesity_text/en/.

11. **Nedergaard J, Bengtsson T, Cannon B.** *Unexpected evidence for active brown adipose tissue in adult humans.* Am J Physiol Endocrinol Metab. 2007;293(2):E444-52.

12. **Hany TF, Gharehpapagh E, Kamel EM, Buck A, Himms-Hagen J, von Schulthess GK.** *Brown adipose tissue: a factor to consider in symmetrical tracer uptake in the neck and upper chest region.* Eur J Nucl Med Mol Imaging. 2002;29(10):1393-8.

13. **van Marken Lichtenbelt WD, Vanhommerig JW, Smulders NM, Drossaerts JM, Kemerink GJ, Bouvy ND, Schrauwen P, Teule GJ.** *Cold-activated brown adipose tissue in healthy men.* N Engl J Med. 2009;360(15):1500-8.

14. **Cypess AM, Lehman S, Williams G, Tal I, Rodman D, Goldfine AB, Kuo FC, Palmer EL, Tseng YH, Doria A, Kolodny GM, Kahn CR.** *Identification and importance of brown adipose tissue in adult humans.* N Engl J Med. 2009;360(15):1509-17.

15. **Cypess AM, White AP, Vernochet C, Schulz TJ, Xue R, Sass CA, Huang TL, Roberts-Toler C, Weiner LS, Sze C, Chacko AT, Deschamps LN, Herder LM, Truchan N, Glasgow AL, Holman AR, Gavrila A, Hasselgren PO, Mori MA, Molla M, Tseng YH.** *Anatomical localization, gene expression profiling and functional characterization of adult human neck brown fat.* Nat Med. 2013;19(5):635-9.

16. **Wu J, Boström P, Sparks LM, Ye L, Choi JH, Giang AH, Khandekar M, Virtanen KA, Nuutila P, Schaart G, Huang K, Tu H, van Marken Lichtenbelt WD, Hoeks J, Enerbäck S, Schrauwen P, Spiegelman BM.** *Beige adipocytes are a distinct type of thermogenic fat cell in mouse and human.* Cell. 2012;150(2):366-76.

17. **Petrovic N, Walden TB, Shabalina IG, Timmons JA, Cannon B, Nedergaard J.** *Chronic peroxisome proliferator-activated receptor gamma (PPARgamma) activation of epididymally derived white adipocyte cultures reveals a population of thermogenically competent, UCP1-containing adipocytes molecularly distinct from classic brown adipoc.*. J Biol Chem. 2010;285(10):7153-64.

18. **Frontini A, Vitali A, Perugini J, Murano I, Romiti C, Ricquier D, Guerrieri M, Cinti S.** *White-to-brown transdifferentiation of omental adipocytes in patients affected by pheochromocytoma.* Biochim Biophys Acta. 2013;1831(5):950-9.

19. **Tang W, Zeve D, Suh JM, Bosnakovski D, Kyba M, Hammer RE, Tallquist MD, Graff JM.** *White fat progenitor cells reside in the adipose vasculature.* Science. 2008;322(5901):583-6.

20. **Cinti S.** *The role of brown adipose tissue in human obesity.* Nutr Metab Cardiovasc Dis. 2006;16(8):569-74.

21. **Gesta S, Tseng YH, Kahn CR.** *Developmental origin of fat: tracking obesity to its source.* Cell. 2007;131(2):242-56.

22. **Clockaerts S, Bastiaansen-Jenniskens YM, Runhaar J, Van Osch GJ, Van Offel JF, Verhaar JA, De Clerck LS, Somville J.** *The infrapatellar fat pad should be considered as an active osteoarthritic joint tissue: a narrative review.* Osteoarthritis Cartilage. 2010;18(7):876-82.

23. **Iacobellis G, Corradi D, Sharma AM.** *Epicardial adipose tissue: anatomic, biomolecular and clinical relationships with the heart.* Nat Clin Pract Cardiovasc Med. 2005;2(10):536-43.

24. **Fukai I, Funato Y, Mizuno T, Hashimoto T, Masaoka A.** *Distribution of thymic tissue in the*

mediastinal adipose tissue. J Thorac Cardiovasc Surg. 1991;101(6):1099-102.

25. **Stern N, Marcus Y.** *Perivascular fat: innocent bystander or active player in vascular disease?* J Cardiometab Syndr. 2006;1(2):115-20.

26. **Zakaria E, Shafrir E.** *Yellow bone marrow as adipose tissue.* Proc Soc Exp Biol Med. 1967;124(4):1265-8.

27. **Ilankovan V, Soames JV.** *Morphometric analysis of orbital, buccal and subcutaneous fats: their potential in the treatment of enophthalmos.* Br J Oral Maxillofac Surg. 1995;33(1):40-2.

28. **Montani JP, Carroll JF, Dwyer TM, Antic V, Yang Z, Dulloo AG.** *Ectopic fat storage in heart, blood vessels and kidneys in the pathogenesis of cardiovascular diseases.* Int J Obes Relat Metab Disord. 2004;28 Suppl 4:S58-65.

29. **Schlett CL, Massaro JM, Lehman SJ, Bamberg F, O'Donnell CJ, Fox CS, Hoffmann U.** *Novel measurements of periaortic adipose tissue in comparison to anthropometric measures of obesity, and abdominal adipose tissue.* Int J Obes (Lond). 2009;33(2):226-32.

30. **Phillips DI, Caddy S, Ilic V, Fielding BA, Frayn KN, Borthwick AC, Taylor R.** *Intramuscular triglyceride and muscle insulin sensitivity: evidence for a relationship in nondiabetic subjects.* Metabolism. 1996;45(8):947-50.

31. **Gaborit B, Kober F, Jacquier A, Moro PJ, Cuisset T, Boullu S, Dadoun F, Alessi MC, Morange P, Clément K, Bernard M, Dutour A.** *Assessment of epicardial fat volume and myocardial triglyceride content in severely obese subjects: relationship to metabolic profile, cardiac function and visceral fat.* Int J Obes (Lond). 2012;36(3):422-30.

32. **Ludwig J, Viggiano TR, McGill DB, Oh BJ.** *Nonalcoholic steatohepatitis: Mayo Clinic experiences with a hitherto unnamed disease.* Mayo Clin Proc. 1980;55(7):434-8.

33. **Lindberg O, de Pierre J, Rylander E, Afzelius BA.** *Studies of the mitochondrial energy-transfer system of brown adipose tissue.* J Cell Biol. 1967;34(1):293-310.

34. **Hausberger FX, Widelitz MM.** *Distribution of labeled erythrocytes in adipose tissue and muscle in the rat.* Am J Physiol. 1963;204:649-52.

35. **Gesner K.** *Conradi Gesneri medici Tigurine Historiae Animalium: Lib. I De Quadrupedibus viviparis.* 1551.

36. **Cannon B, Nedergaard J.** *Developmental biology: Neither fat nor flesh.* Nature. 2008;454(7207):947-8.

37. **Smith RE.** *Thermogenic activity of the hibernating gland in the cold-acclimated rat.* Physiologist. 1961;4:113-113.

38. **Horwitz BA, Hamilton JS, Kott KS.** *GDP binding to hamster brown fat mitochondria is reduced during hibernation.* Am J Physiol. 1985;249(6 Pt 2):R689-93.

39. **Hatai S.** *On the presence in human embryos of an interscapular gland corresponding to the so-called hibernating gland of lower mammals.* Anat Anzeiger. 1902;21:369-373.

40. **Saito M, Okamatsu-Ogura Y, Matsushita M, Watanabe K, Yoneshiro T, Nio-Kobayashi J, Iwanaga T, Miyagawa M, Kameya T, Nakada K, Kawai Y, Tsujisaki M.** *High incidence of metabolically active brown adipose tissue in healthy adult humans: effects of cold exposure and adiposity.* Diabetes. 2009;58(7):1526-31.

41. **Yeung HW, Grewal RK, Gonen M, Schöder H, Larson SM.** *Patterns of (18)F-FDG uptake in adipose tissue and muscle: a potential source of false-positives for PET.* J Nucl Med. 2003;44(11):1789-96.

42. **Kim S, Krynyckyi BR, Machac J, Kim CK.** *Concomitant paravertebral FDG uptake helps differentiate supraclavicular and suprarenal brown fat uptake from malignant uptake when CT coregistration is not available.* Clin Nucl Med. 2006;31(3):127-30.

43. **Cheng W, Zhu Z, Jin X, Chen L, Zhuang H, Li F.** *Intense FDG activity in the brown adipose tissue in omental and mesenteric regions in a patient with malignant pheochromocytoma.* Clin Nucl Med. 2012;37(5):514-5.

44. **Clarke JR, Brglevska S, Lau EW, Ramdave S, Hicks RJ.** *Atypical brown fat distribution in young males demonstrated on PET/CT.* Clin Nucl Med. 2007;32(9):679-82.

45. **Timmons JA, Wennmalm K, Larsson O, Walden TB, Lassmann T, Petrovic N, Hamilton DL, Gimeno RE, Wahlestedt C, Baar K, Nedergaard J, Cannon B.** *Myogenic gene expression signature establishes that brown and white adipocytes originate from distinct cell lineages.* Proc Natl Acad Sci U S A. 2007;104(11):4401-6.

46. **Atit R, Sgaier SK, Mohamed OA, Taketo MM, Dufort D, Joyner AL, Niswander L, Conlon RA.** *Beta-catenin activation is necessary and sufficient to specify the dorsal dermal fate in the mouse.* Dev Biol. 2006;296(1):164-76.

47. **Seale P, Bjork B, Yang W, Kajimura S, Chin S, Kuang S, Scimè A, Devarakonda S, Conroe HM, Erdjument-Bromage H, Tempst P, Rudnicki MA, Beier DR, Spiegelman BM.** *PRDM16 controls a brown fat/skeletal muscle switch.* Nature. 2008;454(7207):961-7.

48. **Kajimura S, Seale P, Kubota K, Lunsford E, Frangioni JV, Gygi SP, Spiegelman BM.** *Initiation of myoblast to brown fat switch by a PRDM16-C/EBP-beta transcriptional complex.* Nature. 2009;460(7259):1154-8.

49. **Seale P, Kajimura S, Yang W, Chin S, Rohas LM, Uldry M, Tavernier G, Langin D, Spiegelman BM.** *Transcriptional control of brown fat determination by PRDM16.* Cell Metab. 2007;6(1):38-54.

50. **Hansen JB, Jørgensen C, Petersen RK, Hallenborg P, De Matteis R, Bøye HA, Petrovic N, Enerbäck S, Nedergaard J, Cinti S, te Riele H, Kristiansen K.** *Retinoblastoma protein functions as a molecular switch determining white versus brown adipocyte differentiation.* Proc Natl Acad Sci U S A. 2004;101(12):4112-7.

51. **Tseng YH, Kokkotou E, Schulz TJ, Huang TL, Winnay JN, Taniguchi CM, Tran TT, Suzuki R, Espinoza DO, Yamamoto Y, Ahrens MJ, Dudley AT, Norris AW, Kulkarni RN, Kahn CR.** *New role of bone morphogenetic protein 7 in brown adipogenesis and energy expenditure.* Nature. 2008;454(7207):1000-4.

52. **Schulz TJ, Huang P, Huang TL, Xue R, McDougall LE, Townsend KL, Cypess AM, Mishina Y, Gussoni E, Tseng YH.** *Brown-fat paucity due to impaired BMP signalling induces compensatory browning of white fat.* Nature. 2013;495(7441):379-83.

53. **Sanchez-Gurmaches J, Hung CM, Sparks CA, Tang Y, Li H, Guertin DA.** *PTEN loss in the Myf5 lineage redistributes body fat and reveals subsets of white adipocytes that arise from Myf5 precursors.* Cell Metab. 2012;16(3):348-62.

54. **Shan T, Liang X, Bi P, Zhang P, Liu W, Kuang S.** *Distinct populations of adipogenic and myogenic Myf5-lineage progenitors in white adipose tissues.* J Lipid Res. 2013;54(8):2214-24.

55. **Waldén TB, Hansen IR, Timmons JA, Cannon B, Nedergaard J.** *Recruited vs. nonrecruited molecular signatures of brown, "brite," and white adipose tissues.* Am J Physiol Endocrinol Metab. 2012;302(1):E19-31.

56. **Elabd C, Chiellini C, Carmona M, Galitzky J, Cochet O, Petersen R, Pénicaud L, Kristiansen K, Bouloumié A, Casteilla L, Dani C, Ailhaud G, Amri EZ.** *Human multipotent adipose-derived stem cells differentiate into functional brown adipocytes.* Stem Cells. 2009;27(11):2753-60.

57. **Pisani DF, Djedaini M, Beranger GE, Elabd C, Scheideler M, Ailhaud G, Amri EZ.** *Differentiation of Human Adipose-Derived Stem Cells into "Brite" (Brown-in-White) Adipocytes.* Front Endocrinol (Lausanne). 2011;2:87.

58. **Sharp LZ, Shinoda K, Ohno H, Scheel DW, Tomoda E, Ruiz L, Hu H, Wang L, Pavlova Z, Gilsanz V, Kajimura S.** *Human BAT possesses molecular signatures that resemble beige/brite cells.* PLoS One. 2012;7(11):e49452.

59. **Sacks HS, Fain JN, Bahouth SW, Ojha S, Frontini A, Budge H, Cinti S, Symonds ME.** *Adult epicardial fat exhibits beige features.* J Clin Endocrinol Metab. 2013;98(9):E1448-55.

60. **Svensson PA, Jernås M, Sjöholm K, Hoffmann JM, Nilsson BE, Hansson M, Carlsson LM.** *Gene expression in human brown adipose tissue.* Int J Mol Med. 2011;27(2):227-32.

61. **Jespersen NZ, Larsen TJ, Peijs L, Daugaard S, Homøe P, Loft A, de Jong J, Mathur N, Cannon B, Nedergaard J, Pedersen BK, Møller K, Scheele C.** *A classical brown adipose tissue mRNA signature partly overlaps with brite in the supraclavicular region of adult humans.* Cell Metab. 2013;17(5):798-805.

62. **Lidell ME, Betz MJ, Dahlqvist Leinhard O, Heglind M, Elander L, Slawik M, Mussack T, Nilsson D, Romu T, Nuutila P, Virtanen KA, Beuschlein F, Persson A, Borga M, Enerbäck S.** *Evidence for two types of brown adipose tissue in humans.* Nat Med. 2013;19(5):631-4.

63. **Lim S, Honek J, Xue Y, Seki T, Cao Z, Andersson P, Yang X, Hosaka K, Cao Y.** *Cold-induced activation of brown adipose tissue and adipose angiogenesis in mice.* Nat Protoc. 2012;7(3):606-15.

64. **Rosenwald M, Perdikari A, Rülicke T, Wolfrum C.** *Bi-directional interconversion of brite and white adipocytes.* Nat Cell Biol. 2013;15(6):659-67.

65. **Barbatelli G, Murano I, Madsen L, Hao Q, Jimenez M, Kristiansen K, Giacobino JP, De Matteis R, Cinti S.** *The emergence of cold-induced brown adipocytes in mouse white fat depots is determined predominantly by white to brown adipocyte transdifferentiation.* Am J Physiol Endocrinol Metab. 2010;298(6):E1244-53.

66. **Huttunen P, Hirvonen J, Kinnula V.** *The occurrence of brown adipose tissue in outdoor workers.* Eur J Appl Physiol Occup Physiol. 1981;46(4):339-45.

67. **Yoneshiro T, Aita S, Matsushita M, Kayahara T, Kameya T, Kawai Y, Iwanaga T, Saito M.** *Recruited brown adipose tissue as an antiobesity agent in humans.* J Clin Invest. 2013;123(8):3404-8.

68. **van der Lans AA, Hoeks J, Brans B, Vijgen GH, Visser MG, Vosselman MJ, Hansen J, Jörgensen JA, Wu J, Mottaghy FM, Schrauwen P, van Marken Lichtenbelt WD.** *Cold acclimation recruits human brown fat and increases nonshivering thermogenesis.* J Clin Invest. 2013;123(8):3395-403.

69. **Blondin DP, Labbé SM, Christian Tingelstad H, Noll C, Kunach M, Phoenix S, Guérin B, Turcotte EE, Carpentier AC, Richard D, Haman F.** *Increased brown adipose tissue oxidative capacity in cold-acclimated humans.* J Clin Endocrinol Metab. 2014;99(3):E438–E46.

70. **Betz MJ, Slawik M, Lidell ME, Osswald A, Heglind M, Nilsson D, Lichtenauer UD, Mauracher B, Mussack T, Beuschlein F, Enerbäck S.** *Presence of brown adipocytes in retroperitoneal fat from patients with benign adrenal tumors: relationship with outdoor temperature.* J Clin Endocrinol Metab. 2013;98(10):4097-104.

71. **Tai TA, Jennermann C, Brown KK, Oliver BB, MacGinnitie MA, Wilkison WO, Brown HR, Lehmann JM, Kliewer SA, Morris DC, Graves RA.** *Activation of the nuclear receptor peroxisome proliferator-activated receptor gamma promotes brown adipocyte differentiation.* J Biol Chem. 1996;271(47):29909-14.

72. **Wilson-Fritch L, Nicoloro S, Chouinard M, Lazar MA, Chui PC, Leszyk J, Straubhaar J, Czech MP, Corvera S.** *Mitochondrial remodeling in adipose tissue associated with obesity and treatment with rosiglitazone.* J Clin Invest. 2004;114(9):1281-9.

73. **Ohno H, Shinoda K, Spiegelman BM, Kajimura S.** *PPARγ agonists induce a white-to-brown fat conversion through stabilization of PRDM16 protein.* Cell Metab. 2012;15(3):395-404.

74. **Fisher FM, Kleiner S, Douris N, Fox EC, Mepani RJ, Verdeguer F, Wu J, Kharitonenkov A, Flier JS, Maratos-Flier E, Spiegelman BM.** *FGF21 regulates PGC-1α and browning of white adipose tissues in adaptive thermogenesis.* Genes Dev. 2012;26(3):271-81.

75. **Jiménez-Aranda A, Fernández-Vázquez G, Campos D, Tassi M, Velasco-Perez L, Tan DX, Reiter RJ, Agil A.** *Melatonin induces browning of inguinal white adipose tissue in Zucker diabetic fatty rats.* J Pineal Res. 2013;55(4):416-23.

76. **Boon MR, van den Berg SA, Wang Y, van den Bossche J, Karkampouna S, Bauwens M, De Saint-Hubert M, van der Horst G, Vukicevic S, de Winther MP, Havekes LM, Jukema JW, Tamsma JT, van der Pluijm G, van Dijk KW, Rensen PC.** *BMP7 Activates Brown Adipose Tissue and Reduces Diet-Induced Obesity Only at Subthermoneutrality.* PLoS One. 2013;8(9):e74083.

77. **Hinoi E, Nakamura Y, Takada S, Fujita H, Iezaki T, Hashizume S, Takahashi S, Odaka Y, Watanabe T, Yoneda Y.** *Growth differentiation factor-5 promotes brown adipogenesis in systemic energy expenditure.* Diabetes. 2014;63(1):162-75.

78. **Lee P, Werner CD, Kebebew E, Celi FS.** *Functional thermogenic beige adipogenesis is inducible in human neck fat.* Int J Obes (Lond). 2014;38(2):170-6.

79. **Bordicchia M, Liu D, Amri EZ, Ailhaud G, Dessì-Fulgheri P, Zhang C, Takahashi N, Sarzani R, Collins S.** *Cardiac natriuretic peptides act via p38 MAPK to induce the brown fat thermogenic program in mouse and human adipocytes.* J Clin Invest. 2012;122(3):1022-36.

80. **De Matteis R, Lucertini F, Guescini M, Polidori E, Zeppa S, Stocchi V, Cinti S, Cuppini R.** *Exercise as a new physiological stimulus for brown adipose tissue activity.* Nutr Metab Cardiovasc Dis. 2013;23(6):582-90.

81. **Ringholm S, Grunnet Knudsen J, Leick L, Lundgaard A, Munk Nielsen M, Pilegaard H.** *PGC-1α is required for exercise- and exercise training-induced UCP1 up-regulation in mouse white adipose tissue.* PLoS One. 2013;8(5):e64123.

82. **Boström P, Wu J, Jedrychowski MP, Korde A, Ye L, Lo JC, Rasbach KA, Boström EA, Choi JH, Long JZ, Kajimura S, Zingaretti MC, Vind BF, Tu H, Cinti S, Højlund K, Gygi SP, Spiegelman BM.** *A PGC1-α-dependent myokine that drives brown-fat-like development of white fat and thermogenesis.* Nature. 2012;481(7382):463-8.

83. **Moreno-Navarrete JM, Ortega F, Serrano M, Guerra E, Pardo G, Tinahones F, Ricart W, Fernández-Real JM.** *Irisin is expressed and produced by human muscle and adipose tissue in association with obesity and insulin resistance.* J Clin Endocrinol Metab. 2013;98(4):E769-78.

84. **Raschke S, Elsen M, Gassenhuber H, Sommerfeld M, Schwahn U, Brockmann B, Jung R, Wisløff U, Tjønna AE, Raastad T, Hallén J, Norheim F, Drevon CA, Romacho T, Eckardt K, Eckel J.** *Evidence against a Beneficial Effect of Irisin in Humans.* PLoS One. 2013;8(9):e73680.

85. **Norheim F, Langleite TM, Hjorth M, Holen T, Kielland A, Stadheim HK, Gulseth HL, Birkeland KI, Jensen J, Drevon CA.** *The effects of acute and chronic exercise on PGC-1α, irisin and browning of subcutaneous adipose tissue in humans.* FEBS J. 2014;281(3):739-49.

86. **Hohtola E.** *Shivering Thermogenesis in Birds and Mammals. In: Life in the Cold: Evolution, Mechanisms, Adaptation, and Application. Twelfth International Hibernation Symposium (Barnes BM, Carey HV, eds). Biological Papers of the University of Alaska.* Fairbanks : Institute of Arctic Biology, University of Alaska, 2004;27:241-52.

87. **Cannon B, Nedergaard J.** *Nonshivering thermogenesis and its adequate measurement in metabolic studies.* J Exp Biol. 2011;214(Pt 2):242-53.

88. **van Marken Lichtenbelt WD, Daanen HA.** *Cold-induced metabolism.* Curr Opin Clin Nutr Metab Care. 2003;6(4):469-75.

89. **Dauncey MJ.** *Metabolic effects of altering the 24 h energy intake in man, using direct and indirect calorimetry.* Br J Nutr. 1980;43(2):257-69.

90. **de Jonge L, Nguyen T, Smith SR, Zachwieja JJ, Roy HJ, Bray GA.** *Prediction of energy expenditure in a whole body indirect calorimeter at both low and high levels of physical activity.* Int J Obes Relat Metab Disord. 2001;25(7):929-34.

91. **Frankenfield D, Roth-Yousey L, Compher C.** *Comparison of predictive equations for resting metabolic rate in healthy nonobese and obese adults: a systematic review.* J Am Diet Assoc. 2005;105(5):775-89.

92. **Ravussin E, Lillioja S, Anderson TE, Christin L, Bogardus C.** *Determinants of 24-hour energy*

expenditure in man. Methods and results using a respiratory chamber. J Clin Invest. 1986;78(6):1568-78.

93. **Elia M, Stratton R, Stubbs J.** *Techniques for the study of energy balance in man.* Proc Nutr Soc. 2003;62(2):529-37.

94. **van Marken Lichtenbelt WD, Schrauwen P, van De Kerckhove S, Westerterp-Plantenga MS.** *Individual variation in body temperature and energy expenditure in response to mild cold.* Am J Physiol Endocrinol Metab. 2002;282(5):E1077-83.

95. **Buemann B, Astrup A, Christensen NJ, Madsen J.** *Effect of moderate cold exposure on 24-h energy expenditure: similar response in postobese and nonobese women.* Am J Physiol. 1992;263(6 Pt 1):E1040-5.

96. **Haman F, Péronnet F, Kenny GP, Massicotte D, Lavoie C, Scott C, Weber JM.** *Effect of cold exposure on fuel utilization in humans: plasma glucose, muscle glycogen, and lipids.* J Appl Physiol. 2002;93(1):77-84.

97. **Claessens-van Ooijen AM, Westerterp KR, Wouters L, Schoffelen PF, van Steenhoven AA, van Marken Lichtenbelt WD.** *Heat production and body temperature during cooling and rewarming in overweight and lean men.* Obesity (Silver Spring). 2006;14(11):1914-20.

98. **Vybíral S, Lesná I, Jansky L, Zeman V.** *Thermoregulation in winter swimmers and physiological significance of human catecholamine thermogenesis.* Exp Physiol. 2000;85(3):321-6.

99. **van Ooijen AM, van Marken Lichtenbelt WD, van Steenhoven AA, Westerterp KR.** *Cold-induced heat production preceding shivering.* Br J Nutr. 2005;93(3):387-91.

100. **Vallerand AL, Jacobs I.** *Rates of energy substrates utilization during human cold exposure.* Eur J Appl Physiol Occup Physiol. 1989;58(8):873-8.

101. **van Ooijen AM, van Marken Lichtenbelt WD, van Steenhoven AA, Westerterp KR.** *Seasonal changes in metabolic and temperature responses to cold air in humans.* Physiol Behav. 2004;82(2-3):545-53.

102. **Wijers SL, Schrauwen P, van Baak MA, Saris WH, van Marken Lichtenbelt WD.** *Beta-adrenergic receptor blockade does not inhibit cold-induced thermogenesis in humans: possible involvement of brown adipose tissue.* J Clin Endocrinol Metab. 2011;96(4):E598-605.

103. **Ouellet V, Labbé SM, Blondin DP, Phoenix S, Guérin B, Haman F, Turcotte EE, Richard D, Carpentier AC.** *Brown adipose tissue oxidative metabolism contributes to energy expenditure during acute cold exposure in humans.* J Clin Invest. 2012;122(2):545-52.

104. **Golozoubova V, Hohtola E, Matthias A, Jacobsson A, Cannon B, Nedergaard J.** *Only UCP1 can mediate adaptive nonshivering thermogenesis in the cold.* FASEB J. 2001;15(11):2048-50.

105. **Griggio MA.** *The participation of shivering and nonshivering thermogenesis in warm and cold-acclimated rats.* Comp Biochem Physiol A Comp Physiol. 1982;73(3):481-4.

106. **Budd GM, Warhaft N.** *Body temperature, shivering, blood pressure and heart rate during a standard cold stress in Australia and Antarctica.* J Physiol. 1966;186(1):216-32.

107. **Davis TR.** *Chamber cold acclimatization in man.* J Appl Physiol. 1961;16:1011-5.

108. **Joy RJ.** *Responses of cold-acclimatized men to infused norepinephrine.* J Appl Physiol. 1963;18:1209-12.

109. **Wijers SL, Saris WH, van Marken Lichtenbelt WD.** *Individual thermogenic responses to mild cold and overfeeding are closely related.* J Clin Endocrinol Metab. 2007;92(11):4299-305.

110. **Wijers SL, Schrauwen P, Saris WH, van Marken Lichtenbelt WD.** *Human skeletal muscle mitochondrial uncoupling is associated with cold induced adaptive thermogenesis.* PLoS One. 2008;3(3):e1777.

111. **Chen KY, Brychta RJ, Linderman JD, Smith S, Courville A, Dieckmann W, Herscovitch P, Millo CM, Remaley A, Lee P, Celi FS.** *Brown fat activation mediates cold-induced thermogenesis in adult humans in response to a mild decrease in ambient temperature.* J Clin Endocrinol Metab. 2013;98(7):E1218-23.

112. **Rintamäki H.** *Human responses to cold.* Alaska Med. 2007;49(2 Suppl):29-31.

113. **Granberg PO.** *Human physiology under cold exposure.* Arctic Med Res. 1991;50 Suppl 6:23-7.

114. **Cypess AM, Chen YC, Sze C, Wang K, English J, Chan O, Holman AR, Tal I, Palmer MR, Kolodny GM, Kahn CR.** *Cold but not sympathomimetics activates human brown adipose tissue in vivo.* Proc Natl Acad Sci U S A. 2012;109(25):10001-5.

115. **Goldstein DS, McCarty R, Polinsky RJ, Kopin IJ.** *Relationship between plasma norepinephrine and sympathetic neural activity.* Hypertension. 1983;5(4):552-9.

116. **Leppäluoto J, Korhonen I, Huttunen P, Hassi J.** *Serum levels of thyroid and adrenal hormones, testosterone, TSH, LH, GH and prolactin in men after a 2-h stay in a cold room.* Acta Physiol Scand. 1988;132(4):543-8.

117. **Marino F, Sockler JM, Fry JM.** *Thermoregulatory, metabolic and sympathoadrenal responses to repeated brief exposure to cold.* Scand J Clin Lab Invest. 1998;58(7):537-45.

118. **Vigas M, Martino E, Bukovská M, Langer P.** *Effect of acute cold exposure and insulin hypoglycemia on plasma thyrotropin levels by IRMA in healthy young males.* Endocrinol Exp. 1988;22(4):229-34.

119. **Jessen K.** *The cortisol fluctuations in plasma in relation to human regulatory nonshivering thermogenesis.* Acta Anaesthesiol Scand. 1980;24(2):151-4.

120. **Jacobs I, Romet T, Frim J, Hynes A.** *Effects of endurance fitness on responses to cold water immersion.* Aviat Space Environ Med. 1984;55(8):715-20.

121. **Seitz HJ, Krone W, Wilke H, Tarnowski W.** *Rapid rise in plasma glucagon induced by acute cold exposure in man and rat.* Pflugers Arch. 1981;389(2):115-20.

122. **Doi K, Ohno T, Kurahashi M, Kuroshima A.** *Thermoregulatory nonshivering thermogenesis in men, with special reference to lipid metabolism.* Jpn J Physiol. 1979;29(4):359-72.

123. **Lazarus M, Yoshida K, Coppari R, Bass CE, Mochizuki T, Lowell BB, Saper CB.** *EP3 prostaglandin receptors in the median preoptic nucleus are critical for fever responses.* Nat Neurosci. 2007;10(9):1131-3.

124. **Gupta BN, Nier K, Hensel H.** *Cold-sensitive afferents from the abdomen.* Pflugers Arch. 1979;380(2):203-4.

125. **Greenspan JD, Taylor DJ, McGillis SL.** *Body site variation of cool perception thresholds, with observations on paradoxical heat.* Somatosens Mot Res. 1993;10(4):467-74.

126. **Morrison SF, Madden CJ, Tupone D.** *Central control of brown adipose tissue thermogenesis.* Front Endocrinol (Lausanne). 2012;3(5).

127. **Bratincsák A, Palkovits M.** *Evidence that peripheral rather than intracranial thermal signals induce thermoregulation.* Neuroscience. 2005;135(2):525-32.

128. **Craig AD, Krout K, Andrew D.** *Quantitative response characteristics of thermoreceptive and nociceptive lamina I spinothalamic neurons in the cat.* J Neurophysiol. 2001;86(3):1459-80.

129. **Feil K, Herbert H.** *Topographic organization of spinal and trigeminal somatosensory pathways to the rat parabrachial and Kölliker-Fuse nuclei.* J Comp Neurol. 1995;353(4):506-28.

130. **Li J, Xiong K, Pang Y, Dong Y, Kaneko T, Mizuno N.** *Medullary dorsal horn neurons providing axons to both the parabrachial nucleus and thalamus.* J Comp Neurol. 2006;498(4):539-51.

131. **Nakamura K, Morrison SF.** *A thermosensory pathway that controls body temperature.* Nat Neurosci. 2008;11(1):62-71.

132. **Nakamura K, Morrison SF.** *Preoptic mechanism for cold-defensive responses to skin cooling.* J Physiol. 2008;586(10):2611-20.

133. **Boulant JA.** *Role of the preoptic-anterior hypothalamus in thermoregulation and fever.* Clin Infect Dis. 2000;31 Suppl 5:S157-61.

134. **Cao WH, Morrison SF.** *Glutamate receptors in the raphe pallidus mediate brown adipose tissue thermogenesis evoked by activation of dorsomedial hypothalamic neurons.* Neuropharmacology. 2006;51(3):426-37.

135. **Nakamura K, Morrison SF.** *Central efferent pathways mediating skin cooling-evoked sympathetic thermogenesis in brown adipose tissue.* Am J Physiol Regul Integr Comp Physiol. 2007;292(1):R127-36.

136. **Chao PT, Yang L, Aja S, Moran TH, Bi S.** *Knockdown of NPY expression in the dorsomedial hypothalamus promotes development of brown adipocytes and prevents diet-induced obesity.* Cell Metab. 2011;13(5):573-83.

137. **Tupone D, Madden CJ, Cano G, Morrison SF.** *An orexinergic projection from perifornical hypothalamus to raphe pallidus increases rat brown adipose tissue thermogenesis.* J Neurosci. 2011;31(44):15944-55.

138. **Mano-Otagiri A, Ohata H, Iwasaki-Sekino A, Nemoto T, Shibasaki T.** *Ghrelin suppresses noradrenaline release in the brown adipose tissue of rats*. J Endocrinol. 2009;201(3):341-9.

139. **Vijgen GH, Bouvy ND, Leenen L, Rijkers K, Cornips E, Majoie M, Brans B, van Marken Lichtenbelt WD.** *Vagus nerve stimulation increases energy expenditure: relation to brown adipose tissue activity.* PLoS One. 2013;8(10):e77221.

140. **Tanaka M, Owens NC, Nagashima K, Kanosue K, McAllen RM.** *Reflex activation of rat fusimotor neurons by body surface cooling, and its dependence on the medullary raphe.* J Physiol. 2006;572(Pt 2):569-83.

141. **Fabjan A, Musizza B, Bajrović FF, Zaletel M, Strucl M.** *The effect of the cold pressor test on a visually evoked cerebral blood flow velocity response.* Ultrasound Med Biol. 2012;38(1):13-20.

142. **Casey KL, Minoshima S, Morrow TJ, Koeppe RA.** *Comparison of human cerebral activation pattern during cutaneous warmth, heat pain, and deep cold pain.* J Neurophysiol. 1996;76(1):571-81.

143. **Tracey I, Becerra L, Chang I, Breiter H, Jenkins L, Borsook D, González RG.** *Noxious hot and cold stimulation produce common patterns of brain activation in humans: a functional magnetic resonance imaging study.* Neurosci Lett. 2000;288(2):159-62.

144. **Davis KD, Kwan CL, Crawley AP, Mikulis DJ.** *Functional MRI study of thalamic and cortical*

activations evoked by cutaneous heat, cold, and tactile stimuli. J Neurophysiol. 1998;80(3):1533-46.

145. **Craig AD, Chen K, Bandy D, Reiman EM.** *Thermosensory activation of insular cortex.* Nat Neurosci. 2000;3(2):184-90.

146. **Egan GF, Johnson J, Farrell M, McAllen R, Zamarripa F, McKinley MJ, Lancaster J, Denton D, Fox PT.** *Cortical, thalamic, and hypothalamic responses to cooling and warming the skin in awake humans: a positron-emission tomography study.* Proc Natl Acad Sci U S A. 2005;102(14):5262-7.

147. **Kanosue K, Sadato N, Okada T, Yoda T, Nakai S, Yoshida K, Hosono T, Nagashima K, Yagishita T, Inoue O, Kobayashi K, Yonekura Y.** *Brain activation during whole body cooling in humans studied with functional magnetic resonance imaging.* Neurosci Lett. 2002;329(2):157-60.

148. **McAllen RM, Farrell M, Johnson JM, Trevaks D, Cole L, McKinley MJ, Jackson G, Denton DA, Egan GF.** *Human medullary responses to cooling and rewarming the skin: a functional MRI study.* Proc Natl Acad Sci U S A. 2006;103(3):809-13.

149. **Fechir M, Klega A, Buchholz HG, Pfeifer N, Balon S, Schlereth T, Geber C, Breimhorst M, Maihöfner C, Birklein F, Schreckenberger M.** *Cortical control of thermoregulatory sympathetic activation.* Eur J Neurosci. 2010;31(11):2101-11.

150. **Huang YC, Hsu CC, Huang P, Yin TK, Chiu NT, Wang PW, Huang SH, Huang YE.** *The changes in brain metabolism in people with activated brown adipose tissue: a PET study.* Neuroimage. 2011;54(1):142-7.

151. **Miao Q, Zhao XL, Zhang QY, Zhang ZY, Guan YH, Ye HY, Zhang S, Zeng MF, Zuo CT, Li YM.** *Stability in brain glucose metabolism following brown adipose tissue inactivation in chinese adults.* AJNR Am J Neuroradiol. 2012;33(8):1464-9.

152. **Depocas F, Behrens WA.** *Levels of noradrenaline in plasma during thermogenesis induced by cold-exposure or by noradrenaline infusion in warm- and in cold-acclimated rats.* Experientia Suppl. 1978;32:135-46.

153. **McCorry LK.** *Physiology of the autonomic nervous system.* Am J Pharm Educ. 2007;71(4):78.

154. **Zilberfarb V, Piétri-Rouxel F, Jockers R, Krief S, Delouis C, Issad T, Strosberg AD.** *Human immortalized brown adipocytes express functional beta3-adrenoceptor coupled to lipolysis.* J Cell Sci. 1997;110 (Pt 7):801-7.

155. **Arch JR, Ainsworth AT, Cawthorne MA, Piercy V, Sennitt MV, Thody VE, Wilson C, Wilson S.** *Atypical beta-adrenoceptor on brown adipocytes as target for anti-obesity drugs.* Nature. 1984;309(5964):163-5.

156. **Zhao J, Unelius L, Bengtsson T, Cannon B, Nedergaard J.** *Coexisting beta-adrenoceptor subtypes: significance for thermogenic process in brown fat cells.* Am J Physiol. 1994;267(4 Pt 1):C969-79.

157. **Bronnikov G, Bengtsson T, Kramarova L, Golozoubova V, Cannon B, Nedergaard J.** *beta1 to beta3 switch in control of cyclic adenosine monophosphate during brown adipocyte development explains distinct beta-adrenoceptor subtype mediation of proliferation and differentiation.* Endocrinology. 1999;140(9):4185-97.

158. **Bengtsson T, Cannon B, Nedergaard J.** *Differential adrenergic regulation of the gene expression of the beta-adrenoceptor subtypes beta1, beta2 and beta3 in brown adipocytes.* Biochem J. 2000;347 Pt 3:643-51.

159. **Bourová L, Pesanová Z, Novotný J, Bengtsson T, Svoboda P.** *Differentiation of cultured brown adipocytes is associated with a selective increase in the short variant of g(s)alpha protein. Evidence for higher functional activity of g(s)alphaS.* Mol Cell Endocrinol. 2000;167(1-2):23-31.

160. **Patel TB, Du Z, Pierre S, Cartin L, Scholich K.** *Molecular biological approaches to unravel adenylyl cyclase signaling and function.* Gene. 2001;269(1-2):13-25.

161. **McKnight GS, Cummings DE, Amieux PS, Sikorski MA, Brandon EP, Planas JV, Motamed K, Idzerda RL.** *Cyclic AMP, PKA, and the physiological regulation of adiposity.* Recent Prog Horm Res. 1998;53:139-59; discussion 160-1.

162. **Thonberg H, Fredriksson JM, Nedergaard J, Cannon B.** *A novel pathway for adrenergic stimulation of cAMP-response-element-binding protein (CREB) phosphorylation: mediation via alpha1-adrenoceptors and protein kinase C activation.* Biochem J. 2002;364(Pt 1):73-9.

163. **Puigserver P, Wu Z, Park CW, Graves R, Wright M, Spiegelman BM.** *A cold-inducible coactivator of nuclear receptors linked to adaptive thermogenesis.* Cell. 1998;92(6):829-39.

164. **Cao W, Medvedev AV, Daniel KW, Collins S.** *beta-Adrenergic activation of p38 MAP kinase in adipocytes: cAMP induction of the uncoupling protein 1 (UCP1) gene requires p38 MAP kinase.* J Biol Chem. 2001;276(29):27077-82.

165. **Briscini L, Tonello C, Dioni L, Carruba MO, Nisoli E.** *Bcl-2 and Bax are involved in the sympathetic protection of brown adipocytes from obesity-linked apoptosis.* FEBS Lett. 1998;431(1):80-4.

166. **Zhao J, Cannon B, Nedergaard J.** *alpha1-Adrenergic stimulation potentiates the thermogenic action of beta3-adrenoreceptor-generated cAMP in brown fat cells.* J Biol Chem. 1997;272(52):32847-56.

167. **Collins S, Yehuda-Shnaidman E, Wang H.** *Positive and negative control of Ucp1 gene transcription*

and the role of β-adrenergic signaling networks. Int J Obes (Lond). 2010;34 Suppl 1:S28-33.

168. **Ye L, Wu J, Cohen P, Kazak L, Khandekar MJ, Jedrychowski MP, Zeng X, Gygi SP, Spiegelman BM.** *Fat cells directly sense temperature to activate thermogenesis.* Proc Natl Acad Sci U S A. 2013;110(30):12480-5.

169. **Fredriksson JM, Thonberg H, Ohlson KB, Ohba K, Cannon B, Nedergaard J.** *Analysis of inhibition by H89 of UCP1 gene expression and thermogenesis indicates protein kinase A mediation of beta(3)-adrenergic signalling rather than beta(3)-adrenoceptor antagonism by H89.* Biochim Biophys Acta. 2001;1538(2-3):206-17.

170. **Chaudhry A, Granneman JG.** *Differential regulation of functional responses by beta-adrenergic receptor subtypes in brown adipocytes.* Am J Physiol. 1999;277(1 Pt 2):R147-53.

171. **Krintel C, Mörgelin M, Logan DT, Holm C.** *Phosphorylation of hormone-sensitive lipase by protein kinase A in vitro promotes an increase in its hydrophobic surface area*. FEBS J. 2009;276(17):4752-62.

172. **Zimmermann R, Strauss JG, Haemmerle G, Schoiswohl G, Birner-Gruenberger R, Riederer M, Lass A, Neuberger G, Eisenhaber F, Hermetter A, Zechner R.** *Fat mobilization in adipose tissue is promoted by adipose triglyceride lipase.* Science. 2004;306(5700):1383-6.

173. **Daikoku T, Shinohara Y, Shima A, Yamazaki N, Terada H.** *Dramatic enhancement of the specific expression of the heart-type fatty acid binding protein in rat brown adipose tissue by cold exposure.* FEBS Lett. 1997;410(2-3):383-6.

174. **Yamamoto T, Yamamoto A, Watanabe M, Kataoka M, Terada H, Shinohara Y.** *Quantitative evaluation of the effects of cold exposure of rats on the expression levels of ten FABP isoforms in brown adipose tissue.* Biotechnol Lett. 2011;33(2):237-42.

175. **Vergnes L, Chin R, Young SG, Reue K.** *Heart-type fatty acid-binding protein is essential for efficient brown adipose tissue fatty acid oxidation and cold tolerance.* J Biol Chem. 2011;286(1):380-90.

176. **Champe PC, Harvey RA, Ferrier DR.** *Lippincott's illustrated reviews: biochemistry, third edition.* Baltimore : Lippincott Williams & Wilkins, 2005.

177. **Carneheim C, Nedergaard J, Cannon B.** *Beta-adrenergic stimulation of lipoprotein lipase in rat brown adipose tissue during acclimation to cold.* Am J Physiol. 1984;246(4 Pt 1):E327-33.

178. **Bartelt A, Bruns OT, Reimer R, Hohenberg H, Ittrich H, Peldschus K, Kaul MG, Tromsdorf UI, Weller H, Waurisch C, Eychmüller A, Gordts PL, Rinninger F, Bruegelmann K, Freund B, Nielsen P, Merkel M, Heeren J.** *Brown adipose tissue activity controls triglyceride clearance.* Nat Med. 2011;17(2):200-5.

179. **Wu Q, Kazantzis M, Doege H, Ortegon AM, Tsang B, Falcon A, Stahl A.** *Fatty acid transport protein 1 is required for nonshivering thermogenesis in brown adipose tissue.* Diabetes. 2006;55(12):3229-37.

180. **Greco-Perotto R, Zaninetti D, Assimacopoulos-Jeannet F, Bobbioni E, Jeanrenaud B.** *Stimulatory effect of cold adaptation on glucose utilization by brown adipose tissue. Relationship with changes in the glucose transporter system.* J Biol Chem. 1987;262(16):7732-6.

181. **Shibata H, Pérusse F, Vallerand A, Bukowiecki LJ.** *Cold exposure reverses inhibitory effects of fasting on peripheral glucose uptake in rats.* Am J Physiol. 1989;257(1 Pt 2):R96-101.

182. **Vallerand AL, Pérusse F, Bukowiecki LJ.** *Stimulatory effects of cold exposure and cold acclimation on glucose uptake in rat peripheral tissues.* Am J Physiol. 1990;259(5 Pt 2):R1043-9.

183. **Santalucía T, Camps M, Castelló A, Muñoz P, Nuel A, Testar X, Palacin M, Zorzano A.** *Developmental regulation of GLUT-1 (erythroid/Hep G2) and GLUT-4 (muscle/fat) glucose transporter expression in rat heart, skeletal muscle, and brown adipose tissue.* Endocrinology. 1992;130(2):837-46.

184. **Postic C, Leturque A, Printz RL, Maulard P, Loizeau M, Granner DK, Girard J.** *Development and regulation of glucose transporter and hexokinase expression in rat.* Am J Physiol. 1994;266(4 Pt 1):E548-59.

185. **Cooney GJ, Caterson ID, Newsholme EA.** *The effect of insulin and noradrenaline on the uptake of 2-[1-14C]deoxyglucose in vivo by brown adipose tissue and other glucose-utilising tissues of the mouse.* FEBS Lett. 1985;188(2):257-61.

186. **Shimizu Y, Kielar D, Minokoshi Y, Shimazu T.** *Noradrenaline increases glucose transport into brown adipocytes in culture by a mechanism different from that of insulin.* Biochem J. 1996;314 (Pt 2):485-90.

187. **Shimizu Y, Satoh S, Yano H, Minokoshi Y, Cushman SW, Shimazu T.** *Effects of noradrenaline on the cell-surface glucose transporters in cultured brown adipocytes: novel mechanism for selective activation of GLUT1 glucose transporters.* Biochem J. 1998;330 (Pt 1):397-403.

188. **Dallner OS, Chernogubova E, Brolinson KA, Bengtsson T.** *Beta3-adrenergic receptors stimulate glucose uptake in brown adipocytes by two mechanisms independently of glucose transporter 4 translocation.* Endocrinology. 2006;147(12):5730-9.

189. **Ma SW, Foster DO.** *Uptake of glucose and release of fatty acids and glycerol by rat brown adipose tissue in vivo.* Can J Physiol Pharmacol. 1986;64(5):609-14.

190. **Isler D, Hill HP, Meier MK.** *Glucose metabolism in isolated brown adipocytes under beta-adrenergic stimulation. Quantitative contribution of glucose to total thermogenesis.* Biochem J. 1987;245(3):789-93.

191. **Wilson S, Thurlby PL, Arch JR.** *Substrate supply for thermogenesis induced by the beta-adrenoceptor agonist BRL 26830A.* Can J Physiol Pharmacol. 1987;65(2):113-9.

192. **Cannon B, Nedergaard J.** *The physiological role of pyruvate carboxylation in hamster brown adipose tissue.* Eur J Biochem. 1979;94(2):419-26.

193. **Enerbäck S, Jacobsson A, Simpson EM, Guerra C, Yamashita H, Harper ME, Kozak LP.** *Mice lacking mitochondrial uncoupling protein are cold-sensitive but not obese.* Nature. 1997;387(6628):90-4.

194. **Matthias A, Ohlson KB, Fredriksson JM, Jacobsson A, Nedergaard J, Cannon B.** *Thermogenic responses in brown fat cells are fully UCP1-dependent. UCP2 or UCP3 do not substitute for UCP1 in adrenergically or fatty scid-induced thermogenesis.* J Biol Chem. 2000;275(33):25073-81.

195. **Erlanson-Albertsson C.** *Uncoupling proteins--a new family of proteins with unknown function.* Nutr Neurosci. 2002;5(1):1-11.

196. **Pirola L, Johnston AM, Van Obberghen E.** *Modulation of insulin action.* Diabetologia. 2004;47(2):170-84.

197. **White MF.** *IRS proteins and the common path to diabetes.* Am J Physiol Endocrinol Metab. 2002;283(3):E413-22.

198. **Ebner S, Burnol AF, Ferre P, de Saintaurin MA, Girard J.** *Effects of insulin and norepinephrine on glucose transport and metabolism in rat brown adipocytes. Potentiation by insulin of norepinephrine-induced glucose oxidation.* Eur J Biochem. 1987;170(1-2):469-74.

199. **Klein J, Fasshauer M, Klein HH, Benito M, Kahn CR.** *Novel adipocyte lines from brown fat: a model system for the study of differentiation, energy metabolism, and insulin action.* Bioessays. 2002;24(4):382-8.

200. **Inokuma K, Ogura-Okamatsu Y, Toda C, Kimura K, Yamashita H, Saito M.** *Uncoupling protein 1 is necessary for norepinephrine-induced glucose utilization in brown adipose tissue.* Diabetes. 2005;54(5):1385-91.

201. **Omatsu-Kanbe M, Zarnowski MJ, Cushman SW.** *Hormonal regulation of glucose transport in a brown adipose cell preparation isolated from rats that shows a large response to insulin.* Biochem J. 1996;315 (Pt 1):25-31.

202. **Fasshauer M, Klein J, Ueki K, Kriauciunas KM, Benito M, White MF, Kahn CR.** *Essential role of insulin receptor substrate-2 in insulin stimulation of Glut4 translocation and glucose uptake in brown adipocytes.* J Biol Chem. 2000;275(33):25494-501.

203. **Teruel T, Valverde AM, Benito M, Lorenzo M.** *Insulin-like growth factor I and insulin induce adipogenic-related gene expression in fetal brown adipocyte primary cultures.* Biochem J. 1996;319 (Pt 2):627-32.

204. **Zanquetta MM, Nascimento ME, Mori RC, D'Agord Schaan B, Young ME, Machado UF.** *Participation of beta-adrenergic activity in modulation of GLUT4 expression during fasting and refeeding in rats.* Metabolism. 2006;55(11):1538-45.

205. **Konrad D, Bilan PJ, Nawaz Z, Sweeney G, Niu W, Liu Z, Antonescu CN, Rudich A, Klip A.** *Need for GLUT4 activation to reach maximum effect of insulin-mediated glucose uptake in brown adipocytes isolated from GLUT4myc-expressing mice.* Diabetes. 2002;51(9):2719-26.

206. **Nilsson NO, Strålfors P, Fredrikson G, Belfrage P.** *Regulation of adipose tissue lipolysis: effects of noradrenaline and insulin on phosphorylation of hormone-sensitive lipase and on lipolysis in intact rat adipocytes.* FEBS Lett. 1980;111(1):125-30.

207. **Carneheim CM, Alexson SE.** *Refeeding and insulin increase lipoprotein lipase activity in rat brown adipose tissue.* Am J Physiol. 1989;256(5 Pt 1):E645-50.

208. **Sugihara H, Miyabara S, Yonemitsu N, Ohta K.** *Hormonal sensitivity of brown fat cells of fetal rats in monolayer culture.* Exp Clin Endocrinol. 1983;82(3):309-19.

209. **Kawashita NH, Moura MA, Brito MN, Brito SM, Garofalo MA, Kettelhut IC, Migliorini RH.** *Relative importance of sympathetic outflow and insulin in the reactivation of brown adipose tissue lipogenesis in rats adapted to a high-protein diet.* Metabolism. 2002;51(3):343-9.

210. **Kozak UC, Held W, Kreutter D, Kozak LP.** *Adrenergic regulation of the mitochondrial uncoupling protein gene in brown fat tumor cells.* Mol Endocrinol. 1992;6(5):763-72.

211. **Rothwell NJ, Stock MJ.** *A role for insulin in the diet-induced thermogenesis of cafeteria-fed rats.* Metabolism. 1981;30(7):673-8.

212. **Shibata H, Pérusse F, Bukowiecki LJ.** *The role of insulin in nonshivering thermogenesis.* Can J Physiol Pharmacol. 1987;65(2):152-8.

213. **Boucher J, Mori MA, Lee KY, Smyth G, Liew CW, Macotela Y, Rourk M, Bluher M, Russell SJ, Kahn CR.** *Impaired thermogenesis and adipose tissue development in mice with fat-specific disruption of insulin and IGF-1 signalling.* Nat Commun. 2012;3:902.

214. **Marette A, Bukowiecki LJ.** *Stimulation of glucose transport by insulin and norepinephrine in isolated rat brown adipocytes.* Am J Physiol. 1989;257(4 Pt 1):C714-21.

215. **Sanchez-Alavez M, Tabarean IV, Osborn O, Mitsukawa K, Schaefer J, Dubins J, Holmberg KH, Klein I, Klaus J, Gomez LF, Kolb H, Secrest J, Jochems J, Myashiro K, Buckley P, Hadcock JR, Eberwine J, Conti B, Bartfai T.** *Insulin causes hyperthermia by direct inhibition of warm-sensitive neurons.* Diabetes. 2010;59(1):43-50.

216. **Vallerand AL, Pérusse F, Bukowiecki LJ.** *Cold exposure potentiates the effect of insulin on in vivo glucose uptake.* Am J Physiol. 1987;253(2 Pt 1):E179-86.

217. **Cederberg A, Grønning LM, Ahrén B, Taskén K, Carlsson P, Enerbäck S.** *FOXC2 is a winged helix gene that counteracts obesity, hypertriglyceridemia, and diet-induced insulin resistance.* Cell. 2001;106(5):563-73.

218. **Seale P, Conroe HM, Estall J, Kajimura S, Frontini A, Ishibashi J, Cohen P, Cinti S, Spiegelman BM.** *Prdm16 determines the thermogenic program of subcutaneous white adipose tissue in mice.* J Clin Invest. 2011;121(1):96-105.

219. **Stanford KI, Middelbeek RJ, Townsend KL, An D, Nygaard EB, Hitchcox KM, Markan KR, Nakano K, Hirshman MF, Tseng YH, Goodyear LJ.** *Brown adipose tissue regulates glucose homeostasis and insulin sensitivity.* J Clin Invest. 2013;123(1):215-23.

220. **Gunawardana SC, Piston DW.** *Reversal of type 1 diabetes in mice by brown adipose tissue transplant.* Diabetes. 2012;61(3):674-82.

221. **Ma SW, Foster DO, Nadeau BE, Triandafillou J.** *Absence of increased oxygen consumption in brown adipose tissue of rats exhibiting "cafeteria" diet-induced thermogenesis.* Can J Physiol Pharmacol. 1988;66(11):1347-54.

222. **Leibel RL, Rosenbaum M, Hirsch J.** *Changes in energy expenditure resulting from altered body weight.* N Engl J Med. 1995;332(10):621-8.

223. **Bouchard C, Tremblay A, Després JP, Nadeau A, Lupien PJ, Thériault G, Dussault J, Moorjani S, Pinault S, Fournier G.** *The response to long-term overfeeding in identical twins.* N Engl J Med. 1990;322(21):1477-82.

224. **van Baak MA.** *Meal-induced activation of the sympathetic nervous system and its cardiovascular and thermogenic effects in man.* Physiol Behav. 2008;94(2):178-86.

225. **Rothwell NJ, Stock MJ.** *A role for brown adipose tissue in diet-induced thermogenesis.* Nature. 1979;281(5726):31-5.

226. **Glick Z, Bray GA, Teague RJ.** *Effect of prandial glucose on brown fat thermogenesis in rats: possible implications for dietary obesity.* J Nutr. 1984;114(2):286-91.

227. **Tovar S, Paeger L, Hess S, Morgan DA, Hausen AC, Brönneke HS, Hampel B, Ackermann PJ, Evers N, Büning H, Wunderlich FT, Rahmouni K, Kloppenburg P, Brüning JC.** *KATP-Channel-Dependent Regulation of Catecholaminergic Neurons Controls BAT Sympathetic Nerve Activity and Energy Homeostasis.* Cell Metab. 2013;18(3):445-55.

228. **Kozak LP.** *Brown fat and the myth of diet-induced thermogenesis.* Cell Metab. 2010;11(4):263-7.

229. **LeBlanc J, Labrie A.** *A possible role for palatability of the food in diet-induced thermogenesis.* Int J Obes Relat Metab Disord. 1997;21(12):1100-3.

230. **Rothwell NJ, Stock MJ.** *Influence of noradrenaline on blood flow to brown adipose tissue in rats exhibiting diet-induced thermogenesis.* Pflugers Arch. 1981;389(3):237-42.

231. **Surwit RS, Wang S, Petro AE, Sanchis D, Raimbault S, Ricquier D, Collins S.** *Diet-induced changes in uncoupling proteins in obesity-prone and obesity-resistant strains of mice.* Proc Natl Acad Sci U S A. 1998;95(7):4061-5.

232. **Glick Z, Wickler SJ, Stern JS, Horwitz BA.** *Regional blood flow in rats after a single low-protein, high-carbohydrate test meal.* Am J Physiol. 1984;247(1 Pt 2):R160-6.

233. **Nedergaard J, Becker W, Cannon B.** *Effects of dietary essential fatty acids on active thermogenin content in rat brown adipose tissue.* J Nutr. 1983;113(9):1717-24.

234. **Lowell BB, S-Susulic V, Hamann A, Lawitts JA, Himms-Hagen J, Boyer BB, Kozak LP, Flier JS.** *Development of obesity in transgenic mice after genetic ablation of brown adipose tissue.* Nature. 1993;366(6457):740-2.

235. **Ma SW, Foster DO.** *Brown adipose tissue, liver, and diet-induced thermogenesis in cafeteria diet-fed rats.* Can J Physiol Pharmacol. 1989;67(4):376-81.

236. **Anunciado-Koza R, Ukropec J, Koza RA, Kozak LP.** *Inactivation of UCP1 and the glycerol phosphate cycle synergistically increases energy expenditure to resist diet-induced obesity.* J Biol Chem. 2008;283(41):27688-97.

237. **Feldmann HM, Golozoubova V, Cannon B, Nedergaard J.** *UCP1 ablation induces obesity and abolishes diet-induced thermogenesis in mice exempt from thermal stress by living at thermoneutrality.* Cell Metab. 2009;9(2):203-9.

238. **Kuroshima A, Yahata T.** *Effect of food restriction on cold adaptability of rats.* Can J Physiol Pharmacol. 1985;63(1):68-71.

239. **Wang Q, Bing C, Al-Barazanji K, Mossakowaska DE, Wang XM, McBay DL, Neville WA, Taddayon M, Pickavance L, Dryden S, Thomas ME, McHale MT, Gloyer IS, Wilson S, Buckingham R, Arch JR, Trayhurn P, Williams G.** *Interactions between leptin and hypothalamic neuropeptide Y neurons in the control of food intake and energy homeostasis in the rat.* Diabetes. 1997;46(3):335-41.

240. **Maffei M, Halaas J, Ravussin E, Pratley RE, Lee GH, Zhang Y, Fei H, Kim S, Lallone R, Ranganathan S, Kern PA, Friedman JM.** *Leptin levels in human and rodent: measurement of plasma leptin and ob RNA in obese and weight-reduced subjects.* Nat Med. 1995;1(11):1155-61.

241. **Rouru J, Cusin I, Zakrzewska KE, Jeanrenaud B, Rohner-Jeanrenaud F.** *Effects of intravenously infused leptin on insulin sensitivity and on the expression of uncoupling proteins in brown adipose tissue.* Endocrinology. 1999;140(8):3688-92.

242. **Kakuma T, Wang ZW, Pan W, Unger RH, Zhou YT.** *Role of leptin in peroxisome proliferator-activated receptor gamma coactivator-1 expression.* Endocrinology. 2000;141(12):4576-82.

243. **Commins SP, Marsh DJ, Thomas SA, Watson PM, Padgett MA, Palmiter R, Gettys TW.** *Norepinephrine is required for leptin effects on gene expression in brown and white adipose tissue.* Endocrinology. 1999;140(10):4772-8.

244. **Enriori PJ, Sinnayah P, Simonds SE, Garcia Rudaz C, Cowley MA.** *Leptin action in the dorsomedial hypothalamus increases sympathetic tone to brown adipose tissue in spite of systemic leptin resistance.* J Neurosci. 2011;31(34):12189-97.

245. **Goodbody AE, Trayhurn P.** *Studies on the activity of brown adipose tissue in suckling, pre-obese, ob/ob mice.* Biochim Biophys Acta. 1982;680(2):119-26.

246. **Halaas JL, Gajiwala KS, Maffei M, Cohen SL, Chait BT, Rabinowitz D, Lallone RL, Burley SK, Friedman JM.** *Weight-reducing effects of the plasma protein encoded by the obese gene.* Science. 1995;269(5223):543-6.

247. **Chiamolera MI, Wondisford FE.** *Minireview: Thyrotropin-releasing hormone and the thyroid hormone feedback mechanism.* Endocrinology. 2009;150(3):1091-6.

248. **Endo T, Ohta K, Haraguchi K, Onaya T.** *Cloning and functional expression of a thyrotropin receptor cDNA from rat fat cells.* J Biol Chem. 1995;270(18):10833-7.

249. **Crisp MS, Lane C, Halliwell M, Wynford-Thomas D, Ludgate M.** *Thyrotropin receptor transcripts in human adipose tissue.* J Clin Endocrinol Metab. 1997;82(6):2003-5.

250. **Zhang L, Baker G, Janus D, Paddon CA, Fuhrer D, Ludgate M.** *Biological effects of thyrotropin receptor activation on human orbital preadipocytes.* Invest Ophthalmol Vis Sci. 2006;47(12):5197-203.

251. **Endo T, Kobayashi T.** *Thyroid-stimulating hormone receptor in brown adipose tissue is involved in the regulation of thermogenesis.* Am J Physiol Endocrinol Metab. 2008;295(2):E514-8.

252. **Silva JE.** *Thermogenic mechanisms and their hormonal regulation.* Physiol Rev. 2006;86(2):435-64.

253. **Bianco AC, Kim BW.** *Deiodinases: implications of the local control of thyroid hormone action.* J Clin Invest. 2006;116(10):2571-9.

254. **Hall JA, Ribich S, Christoffolete MA, Simovic G, Correa-Medina M, Patti ME, Bianco AC.** *Absence of thyroid hormone activation during development underlies a permanent defect in adaptive thermogenesis.* Endocrinology. 2010;151(9):4573-82.

255. **de Jesus LA, Carvalho SD, Ribeiro MO, Schneider M, Kim SW, Harney JW, Larsen PR, Bianco AC.** *The type 2 iodothyronine deiodinase is essential for adaptive thermogenesis in brown adipose tissue.* J Clin Invest. 2001;108(9):1379-85.

256. **Marsili A, Aguayo-Mazzucato C, Chen T, Kumar A, Chung M, Lunsford EP, Harney JW, Van-Tran T, Gianetti E, Ramadan W, Chou C, Bonner-Weir S, Larsen PR, Silva JE, Zavacki AM.** *Mice with a targeted deletion of the type 2 deiodinase are insulin resistant and susceptible to diet induced obesity.* PLoS One. 2011;6(6):e20832.

257. **Silva JE, Larsen PR.** *Adrenergic activation of triiodothyronine production in brown adipose tissue.* Nature. 1983;305(5936):712-3.

258. **Cheng SY, Leonard JL, Davis PJ.** *Molecular aspects of thyroid hormone actions.* Endocr Rev. 2010;31(2):139-70.

259. **Ribeiro MO, Bianco SD, Kaneshige M, Schultz JJ, Cheng SY, Bianco AC, Brent GA.** *Expression of uncoupling protein 1 in mouse brown adipose tissue is thyroid hormone receptor-beta isoform specific and required for adaptive thermogenesis.* Endocrinology. 2010;151(1):432-40.

260. **Ribeiro MO, Carvalho SD, Schultz JJ, Chiellini G, Scanlan TS, Bianco AC, Brent GA.** *Thyroid hormone--sympathetic interaction and adaptive thermogenesis are thyroid hormone receptor isoform--specific.* J Clin Invest. 2001;108(1):97-105.

261. **Silva JE, Larsen PR.** *Potential of brown adipose tissue type II thyroxine 5'-deiodinase as a local and systemic source of triiodothyronine in rats.* J Clin Invest. 1985;76(6):2296-305.

262. **López M, Varela L, Vázquez MJ, Rodríguez-Cuenca S, González CR, Velagapudi VR, Morgan DA,**

Schoenmakers E, Agassandian K, Lage R, Martínez de Morentin PB, Tovar S, Nogueiras R, Carling D, Lelliott C, Gallego R, Oresic M, Chatterjee K, Saha AK, Rahmouni K, Diéguez C, Vidal-Puig A. *Hypothalamic AMPK and fatty acid metabolism mediate thyroid regulation of energy balance.* Nat Med. 2010;16(9):1001-8.

263. **Watanabe M, Houten SM, Mataki C, Christoffolete MA, Kim BW, Sato H, Messaddeq N, Harney JW, Ezaki O, Kodama T, Schoonjans K, Bianco AC, Auwerx J.** *Bile acids induce energy expenditure by promoting intracellular thyroid hormone activation.* Nature. 2006;439(7075):484-9.

264. **Klieverik LP, Coomans CP, Endert E, Sauerwein HP, Havekes LM, Voshol PJ, Rensen PC, Romijn JA, Kalsbeek A, Fliers E.** *Thyroid hormone effects on whole-body energy homeostasis and tissue-specific fatty acid uptake in vivo.* Endocrinology. 2009;150(12):5639-48.

265. **Mory G, Ricquier D, Pesquiés P, Hémon P.** *Effects of hypothyroidism on the brown adipose tissue of adult rats: comparison with the effects of adaptation to cold.* J Endocrinol. 1981;91(3):515-24.

266. **Woodward JA, Saggerson ED.** *Effects of hypothyroidism and hyperthyroidism on GDP binding to brown-adipocyte mitochondria from rats.* Biochem J. 1989;263(2):341-5.

267. **Carvalho SD, Bianco AC, Silva JE.** *Effects of hypothyroidism on brown adipose tissue adenylyl cyclase activity.* Endocrinology. 1996;137(12):5519-29.

268. **Andersen S, Kleinschmidt K, Hvingel B, Laurberg P.** *Thyroid hyperactivity with high thyroglobulin in serum despite sufficient iodine intake in chronic cold adaptation in an Arctic Inuit hunter population.* Eur J Endocrinol. 2012;166(3):433-40.

269. **Lahesmaa M, Orava J, Schalin-Jäntti C, Soinio M, Hannukainen JC, Noponen T, Kirjavainen A, Iida H, Kudomi N, Enerbäck S, Virtanen KA, Nuutila P.** *Hyperthyroidism increases brown fat metabolism in humans.* J Clin Endocrinol Metab. 2014;99(1):E28-35.

270. **Skarulis MC, Celi FS, Mueller E, Zemskova M, Malek R, Hugendubler L, Cochran C, Solomon J, Chen C, Gorden P.** *Thyroid hormone induced brown adipose tissue and amelioration of diabetes in a patient with extreme insulin resistance.* J Clin Endocrinol Metab. 2010;95(1):256-62.

271. **Lee JY, Takahashi N, Yasubuchi M, Kim YI, Hashizaki H, Kim MJ, Sakamoto T, Goto T, Kawada T.** *Triiodothyronine induces UCP-1 expression and mitochondrial biogenesis in human adipocytes.* Am J Physiol Cell Physiol. 2012;302(2):C463-72.

272. **Azhdarinia A, Daquinag AC, Tseng C, Ghosh SC, Ghosh P, Amaya-Manzanares F, Sevick-Muraca E, Kolonin MG.** *A peptide probe for targeted brown adipose tissue imaging.* Nat Commun. 2013;4:2472.

273. **Bullard RW, Funkhouser GE.** *Estimated regional blood flow by rubidium 86 distribution during arousal from hibernation.* Am J Physiol. 1962;203:266-70.

274. **Evonuk E, Hannon JP.** *Pulmonary function during norepinephrine-induced calorigenesis in cold-acclimatized rats.* J Appl Physiol. 1963;18:1213-6.

275. **Heim T, Hull D.** *The blood flow and oxygen consumption of brown adipose tissue in the new-born rabbit.* J Physiol. 1966;186(1):42-55.

276. **Heim T, Hull D.** *The effect of propranalol on the calorigenic response in brown adipose tissue of new-born rabbits to catecholamines, glucagon, corticotrophin and cold exposure.* J Physiol. 1966;187(2):271-83.

277. **Rudolph AM, Heymann MA.** *The circulation of the fetus in utero. Methods for studying distribution of blood flow, cardiac output and organ blood flow.* Circ Res. 1967;21(2):163-84.

278. **Foster DO, Frydman ML.** *Nonshivering thermogenesis in the rat. II. Measurements of blood flow with microspheres point to brown adipose tissue as the dominant site of the calorigenesis induced by noradrenaline.* Can J Physiol Pharmacol. 1978;56(1):110-22.

279. **Foster DO, Frydman ML.** *Tissue distribution of cold-induced thermogenesis in conscious warm- or cold-acclimated rats reevaluated from changes in tissue blood flow: the dominant role of brown adipose tissue in the replacement of shivering by nonshivering thermogenesis.* Can J Physiol Pharmacol. 1979;57(3):257-70.

280. **Mortola JP, Merazzi D, Naso L.** *Blood flow to the brown adipose tissue of conscious young rabbits during hypoxia in cold and warm conditions.* Pflugers Arch. 1999;437(2):255-60.

281. **Cypess AM, Doyle AN, Sass CA, Huang TL, Mowschenson PM, Rosen HN, Tseng YH, Palmer EL 3rd, Kolodny GM.** *Quantification of human and rodent brown adipose tissue function using 99mTc-methoxyisobutylisonitrile SPECT/CT and 18F-FDG PET/CT.* J Nucl Med. 2013;54(11):1896-901.

282. **Nisoli E, Tonello C, Briscini L, Carruba MO.** *Inducible nitric oxide synthase in rat brown adipocytes: implications for blood flow to brown adipose tissue.* Endocrinology. 1997;138(2):676-82.

283. **Kikuchi-Utsumi K, Gao B, Ohinata H, Hashimoto M, Yamamoto N, Kuroshima A.** *Enhanced gene expression of endothelial nitric oxide synthase in brown adipose tissue during cold exposure.* Am J Physiol Regul Integr Comp Physiol. 2002;282(2):R623-6.

284. **Giordano A, Tonello C, Bulbarelli A, Cozzi V, Cinti S, Carruba MO, Nisoli E.** *Evidence for a functional nitric oxide synthase system in brown adipocyte nucleus.* FEBS Lett. 2002;514(2-3):135-40.

285. **Nagashima T, Ohinata H, Kuroshima A.** *Involvement of nitric oxide in noradrenaline-induced increase in blood flow through brown adipose tissue.* Life Sci. 1994;54(1):17-25.

286. **Segal SS.** *Regulation of blood flow in the microcirculation.* Microcirculation. 2005;12(1):33-45.

287. **Foster DO, Depocas F.** *Evidence against noradrenergic regulation of vasodilation in rat brown adipose tissue.* Can J Physiol Pharmacol. 1980;58(12):1418-25.

288. **Ma SW, Foster DO.** *Redox state of brown adipose tissue as a possible determinant of its blood flow.* Can J Physiol Pharmacol. 1984;62(8):949-56.

289. **Granneman JG, Burnazi M, Zhu Z, Schwamb LA.** *White adipose tissue contributes to UCP1-independent thermogenesis.* Am J Physiol Endocrinol Metab. 2003;285(6):E1230-6.

290. **Wiesinger H, Klaus S, Heldmaier G, Champigny O, Ricquier D.** *Increased nonshivering thermogenesis, brown fat cytochrome-c oxidase activity, GDP binding, and uncoupling protein mRNA levels after short daily cold exposure of Phodopus sungorus.* Can J Physiol Pharmacol. 1990;68(2):195-200.

291. **Brooks SL, Neville AM, Rothwell NJ, Stock MJ, Wilson S.** *Sympathetic activation of brown-adipose-tissue thermogenesis in cachexia.* Biosci Rep. 1981;1(6):509-17.

292. **Tsoli M, Moore M, Burg D, Painter A, Taylor R, Lockie SH, Turner N, Warren A, Cooney G, Oldfield B, Clarke S, Robertson G.** *Activation of thermogenesis in brown adipose tissue and dysregulated lipid metabolism associated with cancer cachexia in mice.* Cancer Res. 2012;72(17):4372-82.

293. **Shellock FG, Riedinger MS, Fishbein MC.** *Brown adipose tissue in cancer patients: possible cause of cancer-induced cachexia.* J Cancer Res Clin Oncol. 1986;111(1):82-5.

294. **Döbert N, Menzel C, Hamscho N, Wördehoff W, Kranert WT, Grünwald F.** *Atypical thoracic and supraclavicular FDG-uptake in patients with Hodgkin's and non-Hodgkin's lymphoma.* Q J Nucl Med Mol Imaging. 2004;48(1):33-8.

295. **Emorine LJ, Marullo S, Briend-Sutren MM, Patey G, Tate K, Delavier-Klutchko C, Strosberg AD.** *Molecular characterization of the human beta 3-adrenergic receptor.* Science. 1989;245(4922):1118-21.

296. **Nahmias C, Blin N, Elalouf JM, Mattei MG, Strosberg AD, Emorine LJ.** *Molecular characterization of the mouse beta 3-adrenergic receptor: relationship with the atypical receptor of adipocytes.* EMBO J. 1991;10(12):3721-7.

297. **Granneman JG, Lahners KN, Chaudhry A.** *Molecular cloning and expression of the rat beta 3-adrenergic receptor.* Mol Pharmacol. 1991;40(6):895-9.

298. **Krief S, Lönnqvist F, Raimbault S, Baude B, Van Spronsen A, Arner P, Strosberg AD, Ricquier D, Emorine LJ.** *Tissue distribution of beta 3-adrenergic receptor mRNA in man.* J Clin Invest. 1993;91(1):344-9.

299. **Lönnqvist F, Krief S, Strosberg AD, Nyberg S, Emorine LJ, Arner P.** *Evidence for a functional beta 3-adrenoceptor in man.* Br J Pharmacol. 1993;110(3):929-36.

300. **De Matteis R, Arch JR, Petroni ML, Ferrari D, Cinti S, Stock MJ.** *Immunohistochemical identification of the beta(3)-adrenoceptor in intact human adipocytes and ventricular myocardium: effect of obesity and treatment with ephedrine and caffeine.* Int J Obes Relat Metab Disord. 2002;26(11):1442-50.

301. **Muzzin P, Revelli JP, Kuhne F, Gocayne JD, McCombie WR, Venter JC, Giacobino JP, Fraser CM.** *An adipose tissue-specific beta-adrenergic receptor. Molecular cloning and down-regulation in obesity.* J Biol Chem. 1991;266(35):24053-8.

302. **Collins S, Daniel KW, Rohlfs EM, Ramkumar V, Taylor IL, Gettys TW.** *Impaired expression and functional activity of the beta 3- and beta 1-adrenergic receptors in adipose tissue of congenitally obese (C57BL/6J ob/ob) mice.* Mol Endocrinol. 1994;8(4):518-27.

303. **Milner RE, Wilson S, Arch JR, Trayhurn P.** *Acute effects of a beta-adrenoceptor agonist (BRL 26830A) on rat brown-adipose-tissue mitochondria. Increased GDP binding and GDP-sensitive proton conductance without changes in the concentration of uncoupling protein.* Biochem J. 1988;249(3):759-63.

304. **Holloway BR, Howe R, Rao BS, Stribling D, Mayers RM, Briscoe MG, Jackson JM.** *ICI D7114 a novel selective beta-adrenoceptor agonist selectively stimulates brown fat and increases whole-body oxygen consumption.* Br J Pharmacol. 1991;104(1):97-104.

305. **Santti E, Rouvari T, Rouru J, Huupponen R, Koulu M.** *Effect of chronic treatment with ICI D7114, a selective beta 3-adrenoceptor agonist, on macronutrient selection and brown adipose tissue thermogenesis in Sprague-Dawley rats.* Pharmacol Toxicol. 1994;75(3-4):166-9.

306. **Arch JR, Ainsworth AT, Ellis RD, Piercy V, Thody VE, Thurlby PL, Wilson C, Wilson S, Young P.** *Treatment of obesity with thermogenic beta-adrenoceptor agonists: studies on BRL 26830A in rodents.* Int J Obes. 1984;8 Suppl 1:1-11.

307. **Yoshida T, Yoshioka K, Kamanaru K, Hiraoka N, Kondo M.** *Mitigation of obesity by BRL 26830A, a new beta-adrenoceptor agonist, in MSG obese mice.* J Nutr Sci Vitaminol (Tokyo). 1990;36(1):75-80.

308. **Santti E, Huupponen R, Rouru J, Hänninen V, Pesonen U, Jhanwar-Uniyal M, Koulu M.** *Potentiation of the anti-obesity effect of the selective beta 3-adrenoceptor agonist BRL 35135 in obese Zucker rats by exercise.* Br J Pharmacol. 1994;113(4):1231-6.

309. **Berraondo B, Bonafonte A, Fernandez-Otero MP, Martinez JA.** *Effects on energy utilization of a beta3-adrenergic agonist in rats fed on a cafeteria diet.* Eat Weight Disord. 1997;2(3):130-7.

310. **Nikami H, Shimizu Y, Sumida M, Minokoshi Y, Yoshida T, Saito M, Shimazu T.** *Expression of beta3-adrenoceptor and stimulation of glucose transport by beta3-agonists in brown adipocyte primary culture.* J Biochem. 1996;119(1):120-5.

311. **Cawthorne MA, Carroll MJ, Levy AL, Lister CA, Sennitt MV, Smith SA, Young P.** *Effects of novel beta-adrenoceptor agonists on carbohydrate metabolism: relevance for the treatment of non-insulin-dependent diabetes.* Int J Obes. 1984;8 Suppl 1:93-102.

312. **Young P, Cawthorne MA, Levy AL, Wilson K.** *Reduced maximum capacity of glycolysis in brown adipose tissue of genetically obese, diabetic (db/db) mice and its restoration following treatment with a thermogenic beta-adrenoceptor agonist.* FEBS Lett. 1984;176(1):16-20.

313. **Rochet N, Tanti JF, Grémeaux T, Van Obberghen E, Le Marchand-Brustel Y.** *Effect of a thermogenic agent, BRL 26830A, on insulin receptors in obese mice.* Am J Physiol. 1988;255(2 Pt 1):E101-9.

314. **de Souza CJ, Hirshman MF, Horton ES.** *CL-316,243, a beta3-specific adrenoceptor agonist, enhances insulin-stimulated glucose disposal in nonobese rats.* Diabetes. 1997;46(8):1257-63.

315. **Young P, King L, Cawthorne MA.** *Increased insulin binding and glucose transport in white adipocytes isolated from C57B1/6 ob/ob mice treated with the thermogenic beta-adrenoceptor agonist BRL 26830.* Biochem Biophys Res Commun. 1985;133(2):457-61.

316. **Mittra E, Quon A.** *Positron emission tomography/computed tomography: the current technology and applications.* Radiol Clin North Am. 2009;47(1):147-60.

317. **Ter-Pogossian MM.** *The origins of positron emission tomography.* Semin Nucl Med. 1992;22(3):140-9.

318. **Basu S, Kwee TC, Surti S, Akin EA, Yoo D, Alavi A.** *Fundamentals of PET and PET/CT imaging.* Ann N Y Acad Sci. 2011;1228:1-18.

319. **Accorsi R.** *Brain single-photon emission CT physics principles.* AJNR Am J Neuroradiol. 2008;29(7):1247-56.

320. **El Fakhri G, Surti S, Trott CM, Scheuermann J, Karp JS.** *Improvement in lesion detection with whole-body oncologic time-of-flight PET.* J Nucl Med. 2011;52(3):347-53.

321. **Tarantola G, Zito F, Gerundini P.** *PET instrumentation and reconstruction algorithms in whole-body applications.* J Nucl Med. 2003;44(5):756-69.

322. **Okuyama C, Sakane N, Yoshida T, Shima K, Kurosawa H, Kumamoto K, Ushijima Y, Nishimura T.** *(123)I- or (125)I-metaiodobenzylguanidine visualization of brown adipose tissue.* J Nucl Med. 2002;43(9):1234-40.

323. **Tatsumi M, Engles JM, Ishimori T, Nicely O, Cohade C, Wahl RL.** *Intense (18)F-FDG uptake in brown fat can be reduced pharmacologically.* J Nucl Med. 2004;45(7):1189-93.

324. **Wang X, Minze LJ, Shi ZZ.** *Functional imaging of brown fat in mice with 18F-FDG micro-PET/CT.* J Vis Exp. 2012;(69).

325. **Fueger BJ, Czernin J, Hildebrandt I, Tran C, Halpern BS, Stout D, Phelps ME, Weber WA.** *Impact of animal handling on the results of 18F-FDG PET studies in mice.* J Nucl Med. 2006;47(6):999-1006.

326. **Wu C, Cheng W, Xing H, Dang Y, Li F, Zhu Z.** *Brown adipose tissue can be activated or inhibited within an hour before 18F-FDG injection: a preliminary study with microPET.* J Biomed Biotechnol. 2011;2011:159834.

327. **Mirbolooki MR, Constantinescu CC, Pan ML, Mukherjee J.** *Quantitative assessment of brown adipose tissue metabolic activity and volume using 18F-FDG PET/CT and β3-adrenergic receptor activation.* EJNMMI Res. 2011;1(1):30.

328. **Mirbolooki MR, Upadhyay SK, Constantinescu CC, Pan ML, Mukherjee J.** *Adrenergic pathway activation enhances brown adipose tissue metabolism: a [^{18}F]FDG PET/CT study in mice.* Nucl Med Biol. 2014;41(1):10-6.

329. **Mirbolooki MR, Constantinescu CC, Pan ML, Mukherjee J.** *Targeting presynaptic norepinephrine transporter in brown adipose tissue: a novel imaging approach and potential treatment for diabetes and obesity.* Synapse. 2013;67(2):79-93.

330. **Quarta C, Lodi F, Mazza R, Giannone F, Boschi L, Nanni C, Nisoli E, Boschi S, Pasquali R, Fanti S, Iozzo P, Pagotto U.** *(11)C-meta-hydroxyephedrine PET/CT imaging allows in vivo study of adaptive thermogenesis and white-to-brown fat conversion.* Mol Metab. 2013;2(3):153-60.

331. **Lin SF, Fan X, Yeckel CW, Weinzimmer D, Mulnix T, Gallezot JD, Carson RE, Sherwin RS, Ding YS.** *Ex vivo and in vivo evaluation of the norepinephrine transporter ligand [11C]MRB for brown adipose tissue imaging.* Nucl Med Biol. 2012;39(7):1081-6.

332. **Pérez-Medina C, Patel N, Robson M, Badar A, Lythgoe MF, Årstad E.** *Evaluation of a 125I-labelled benzazepinone derived voltage-gated sodium channel blocker for imaging with SPECT.* Org Biomol Chem. 2012;10(47):9474-80.

333. **Norris AW, Wang C, Yao J, Walsh SA, Sawatzke AB, Hu S, Sunderland JJ, Segar JL, Ponto LL.** *Effect of insulin and dexamethasone on fetal assimilation of maternal glucose.* Endocrinology. 2011;152(1):255-62.

334. **Baba S, Tatsumi M, Ishimori T, Lilien DL, Engles JM, Wahl RL.** *Effect of nicotine and ephedrine on the accumulation of 18F-FDG in brown adipose tissue.* J Nucl Med. 2007;48(6):981-6.

335. **Carter EA, Bonab AA, Hamrahi V, Pitman J, Winter D, Macintosh LJ, Cyr EM, Paul K, Yerxa J, Jung W, Tompkins RG, Fischman AJ.** *Effects of burn injury, cold stress and cutaneous wound injury on the morphology and energy metabolism of murine brown adipose tissue (BAT) in vivo.* Life Sci. 2011;89(3-4):78-85.

336. **Carter EA, Bonab AA, Paul K, Yerxa J, Tompkins RG, Fischman AJ.** *Association of heat production with 18F-FDG accumulation in murine brown adipose tissue after stress.* J Nucl Med. 2011;52(10):1616-20.

337. **van der Veen DR, Shao J, Chapman S, Leevy WM, Duffield GE.** *A diurnal rhythm in glucose uptake in brown adipose tissue revealed by in vivo PET-FDG imaging.* Obesity (Silver Spring). 2012;20(7):1527-9.

338. **Mathew D, Zhou P, Pywell CM, van der Veen DR, Shao J, Xi Y, Bonar NA, Hummel AD, Chapman S, Leevy WM, Duffield GE.** *Ablation of the id2 gene results in altered circadian feeding behavior, and sex-specific enhancement of insulin sensitivity and elevated glucose uptake in skeletal muscle and brown adipose tissue.* PLoS One. 2013;8(9):e73064.

339. **Hankir M, Bueter M, Gsell W, Seyfried F, Khalil M, Smith KL, Bloom SR, Bell JD, le Roux CW.** *Increased energy expenditure in gastric bypass rats is not caused by activated brown adipose tissue.* Obes Facts. 2012;5(3):349-58.

340. **Shaw HB.** *A Contribution to the Study of the Morphology of Adipose Tissue.* J Anat Physiol. 1901;36(Pt 1):1-13.

341. **Bonnot E.** *The Interscapular Gland.* J Anat Physiol. 1908;43(Pt 1):43-58.

342. **Heaton JM.** *The distribution of brown adipose tissue in the human.* J Anat. 1972;112(Pt 1):35-9.

343. **Tanuma Y, Ohata M, Ito T, Yokochi C.** *Possible function of human brown adipose tissue as suggested by observation on perirenal brown fats from necropsy cases of variable age groups.* Arch Histol Jpn. 1976;39(2):117-45.

344. **Lean ME, James WP.** *Uncoupling protein in human brown adipose tissue mitochondria. Isolation and detection by specific antiserum.* FEBS Lett. 1983;163(2):235-40.

345. **Lean ME, James WP, Jennings G, Trayhurn P.** *Brown adipose tissue uncoupling protein content in human infants, children and adults.* Clin Sci (Lond). 1986;71(3):291-7.

346. **Kortelainen ML, Pelletier G, Ricquier D, Bukowiecki LJ.** *Immunohistochemical detection of human brown adipose tissue uncoupling protein in an autopsy series.* J Histochem Cytochem. 1993;41(5):759-64.

347. **Houstěk J, Vízek K, Pavelka S, Kopecký J, Krejcová E, Hermanská J, Cermáková M.** *Type II iodothyronine 5'-deiodinase and uncoupling protein in brown adipose tissue of human newborns.* J Clin Endocrinol Metab. 1993;77(2):382-7.

348. **Nnodim JO.** *The occurrence of brown adipose in man inhabiting the tropics.* Z Mikrosk Anat Forsch. 1990;104(5):721-8.

349. **Kortelainen ML.** *Association between cardiac pathology and fat tissue distribution in an autopsy series of men without premortem evidence of cardiovascular disease.* Int J Obes Relat Metab Disord. 1996;20(3):245-52.

350. **Barrington SF, Maisey MN.** *Skeletal muscle uptake of fluorine-18-FDG: effect of oral diazepam.* J Nucl Med. 1996;37(7):1127-9.

351. **Bonnin F, Lumbroso J, Tenenbaum F, Hartmann O, Parmentier C.** *Refining interpretation of MIBG scans in children.* J Nucl Med. 1994;35(5):803-10.

352. **Schöder H, Yeung HW, Gonen M, Kraus D, Larson SM.** *Head and neck cancer: clinical usefulness and accuracy of PET/CT image fusion.* Radiology. 2004;231(1):65-72.

353. **Cohade C, Osman M, Pannu HK, Wahl RL.** *Uptake in supraclavicular area fat ("USA-Fat"): description on 18F-FDG PET/CT.* J Nucl Med. 2003;44(2):170-6.

354. **Cohade C, Mourtzikos KA, Wahl RL.** *"USA-Fat": prevalence is related to ambient outdoor temperature-evaluation with 18F-FDG PET/CT.* J Nucl Med. 2003;44(8):1267-70.

355. **Okuyama C, Ushijima Y, Kubota T, Yoshida T, Nakai T, Kobayashi K, Nishimura T.** *123I-Metaiodobenzylguanidine uptake in the nape of the neck of children: likely visualization of brown adipose tissue.* J Nucl Med. 2003;44(9):1421-5.

356. **Fukuchi K, Ono Y, Nakahata Y, Okada Y, Hayashida K, Ishida Y.** *Visualization of interscapular brown adipose tissue using (99m)Tc-tetrofosmin in pediatric patients.* J Nucl Med. 2003;44(10):1582-5.

357. **Minotti AJ, Shah L, Keller K.** *Positron emission tomography/computed tomography fusion imaging in brown adipose tissue.* Clin Nucl Med. 2004;29(1):5-11.

358. **Bar-Shalom R, Gaitini D, Keidar Z, Israel O.** *Non-malignant FDG uptake in infradiaphragmatic adipose tissue: a new site of physiological tracer biodistribution characterised by PET/CT.* Eur J Nucl Med Mol Imaging. 2004;31(8):1105-13.

359. **Higuchi T, Kinuya S, Taki J, Nakajima K, Ikeda M, Namura M, Tonami N.** *Brown adipose tissue: evaluation with 201Tl and 99mTc-sestamibi dual-tracer SPECT.* Ann Nucl Med. 2004;18(6):547-9.

360. **Truong MT, Erasmus JJ, Munden RF, Marom EM, Sabloff BS, Gladish GW, Podoloff DA, Macapinlac HA.** *Focal FDG uptake in mediastinal brown fat mimicking malignancy: a potential pitfall resolved on PET/CT.* AJR Am J Roentgenol. 2004;183(4):1127-32.

361. **Garcia CA, Van Nostrand D, Majd M, Atkins F, Acio E, Sheikh A, Butler C.** *Benzodiazepine-resistant "brown fat" pattern in positron emission tomography: two case reports of resolution with temperature control.* Mol Imaging Biol. 2004;6(6):368-72.

362. **Reddy MP, Ramaswamy MR.** *FDG uptake in brown adipose tissue mimicking an adrenal metastasis: source of false-positive interpretation.* Clin Nucl Med. 2005;30(4):257-8.

363. **Gelfand MJ, O'hara SM, Curtwright LA, Maclean JR.** *Pre-medication to block [(18)F]FDG uptake in the brown adipose tissue of pediatric and adolescent patients.* Pediatr Radiol. 2005;35(10):984-90.

364. **Castellucci P, Nanni C, Farsad M, Alinari L, Zinzani P, Stefoni V, Battista G, Valentini D, Pettinato C, Marengo M, Boschi S, Canini R, Baccarani M, Monetti N, Franchi R, Rampin L, Fanti S, Rubello D.** *Potential pitfalls of 18F-FDG PET in a large series of patients treated for malignant lymphoma: prevalence and scan interpretation.* Nucl Med Commun. 2005;26(8):689-94.

365. **Jacobsson H, Bruzelius M, Larsson SA.** *Reduction of FDG uptake in brown adipose tissue by propranolol.* Eur J Nucl Med Mol Imaging. 2005;32(9):1130.

366. **Heiba SI, Bernik S, Raphael B, Sandella N, Cholewinski W, Klein P.** *The distinctive role of positron emission tomography/computed tomography in breast carcinoma with brown adipose tissue 2-fluoro-2-deoxy-d-glucose uptake.* Breast J. 2005;11(6):457-61.

367. **Garcia CA, Van Nostrand D, Atkins F, Acio E, Butler C, Esposito G, Kulkarni K, Majd M.** *Reduction of brown fat 2-deoxy-2-[F-18]fluoro-D-glucose uptake by controlling environmental temperature prior to positron emission tomography scan.* Mol Imaging Biol. 2006;8(1):24-9.

368. **Christensen CR, Clark PB, Morton KA.** *Reversal of hypermetabolic brown adipose tissue in F-18 FDG PET imaging.* Clin Nucl Med. 2006;31(4):193-6.

369. **Rousseau C, Bourbouloux E, Campion L, Fleury N, Bridji B, Chatal JF, Resche I, Campone M.** *Brown fat in breast cancer patients: analysis of serial (18)F-FDG PET/CT scans.* Eur J Nucl Med Mol Imaging. 2006;33(7):785-91.

370. **Belhocine T, Shastry A, Driedger A, Urbain JL.** *Detection of 99mTc-sestamibi uptake in brown adipose tissue with SPECT-CT.* Eur J Nucl Med Mol Imaging. 2007;34(1):149.

371. **Söderlund V, Larsson SA, Jacobsson H.** *Reduction of FDG uptake in brown adipose tissue in clinical patients by a single dose of propranolol.* Eur J Nucl Med Mol Imaging. 2007;34(7):1018-22.

372. **Parysow O, Mollerach AM, Jager V, Racioppi S, San Roman J, Gerbaudo VH.** *Low-dose oral propranolol could reduce brown adipose tissue F-18 FDG uptake in patients undergoing PET scans.* Clin Nucl Med. 2007;32(5):351-7.

373. **Wehrli NE, Bural G, Houseni M, Alkhawaldeh K, Alavi A, Torigian DA.** *Determination of age-related changes in structure and function of skin, adipose tissue, and skeletal muscle with computed tomography, magnetic resonance imaging, and positron emission tomography.* Semin Nucl Med. 2007;37(3):195-205.

374. **Kim S, Krynyckyi BR, Machac J, Kim CK.** *Temporal relation between temperature change and FDG uptake in brown adipose tissue.* Eur J Nucl Med Mol Imaging. 2008;35(5):984-9.

375. **Goetze S, Lavely WC, Ziessman HA, Wahl RL.** *Visualization of brown adipose tissue with 99mTc-methoxyisobutylisonitrile on SPECT/CT.* J Nucl Med. 2008;49(5):752-6.

376. **Wong KK, Brown RK, Avram AM.** *Potential false positive Tc-99m sestamibi parathyroid study due to uptake in brown adipose tissue.* Clin Nucl Med. 2008;33(5):346-8.

377. **Williams G, Kolodny GM.** *Method for decreasing uptake of 18F-FDG by hypermetabolic brown adipose tissue on PET.* AJR Am J Roentgenol. 2008;190(5):1406-9.

378. **Alkhawaldeh K, Alavi A.** *Quantitative assessment of FDG uptake in brown fat using standardized uptake value and dual-time-point scanning.* Clin Nucl Med. 2008;33(10):663-7.

379. **Hyun IY, Kim SG.** *FDG uptake in parahepatic brown fat mimics peritoneal carcinomatosis in a malignant ovarian germ cell tumor: resolution with temperature control.* Clin Nucl Med. 2008;33(11):799-801.

380. **Zukotynski KA, Fahey FH, Laffin S, Davis R, Treves ST, Grant FD, Drubach LA.** *Constant ambient temperature of 24 degrees C significantly reduces FDG uptake by brown adipose tissue in children scanned during the winter.* Eur J Nucl Med Mol Imaging. 2009;36(4):602-6.

381. **Agrawal A, Nair N, Baghel NS.** *A novel approach for reduction of brown fat uptake on FDG PET.* Br J Radiol. 2009;82(980):626-31.

382. **Sturkenboom MG, Hoekstra OS, Postema EJ, Zijlstra JM, Berkhof J, Franssen EJ.** *A randomised controlled trial assessing the effect of oral diazepam on 18F-FDG uptake in the neck and upper chest region.* Mol Imaging Biol. 2009;11(5):364-8.

383. **Cheng WY, Zhu ZH, Ouyang M.** *Patterns and characteristics of brown adipose tissue uptake of 18F-FDG positron emission tomograph/computed tomography imaging.* Zhongguo Yi Xue Ke Xue Yuan Xue Bao. 2009;31(3):370-3.

384. **Au-Yong IT, Thorn N, Ganatra R, Perkins AC, Symonds ME.** *Brown adipose tissue and seasonal variation in humans.* Diabetes. 2009;58(11):2583-7.

385. **Huang YC, Wang PW, Tang SW, Hung PL, Hsu CC.** *Identifying Ga-67 uptake in brown adipose tissue with SPECT/CT.* Clin Nucl Med. 2009;34(12):964-6.

386. **Baba S, Jacene HA, Engles JM, Honda H, Wahl RL.** *CT Hounsfield units of brown adipose tissue increase with activation: preclinical and clinical studies.* J Nucl Med. 2010;51(2):246-50.

387. **Hairil Rashmizal AR, Noraini AR, Rossetti C, Abdul Jalil N.** *Brown fat uptake of 18F-FDG on dual time point PET/CT imaging.* Singapore Med J. 2010;51(2):e37-9.

388. **Aukema TS, Vogel WV, Hoefnagel CA, Valdés Olmos RA.** *Prevention of brown adipose tissue activation in 18F-FDG PET/CT of breast cancer patients receiving neoadjuvant systemic therapy.* J Nucl Med Technol. 2010;38(1):24-7.

389. **Pfannenberg C, Werner MK, Ripkens S, Stef I, Deckert A, Schmadl M, Reimold M, Häring HU, Claussen CD, Stefan N.** *Impact of age on the relationships of brown adipose tissue with sex and adiposity in humans.* Diabetes. 2010;59(7):1789-93.

390. **Zukotynski KA, Fahey FH, Laffin S, Davis R, Treves ST, Grant FD, Drubach LA.** *Seasonal variation in the effect of constant ambient temperature of 24 degrees C in reducing FDG uptake by brown adipose tissue in children.* Eur J Nucl Med Mol Imaging. 2010;37(10):1854-60.

391. **Lee P, Greenfield JR, Ho KK, Fulham MJ.** *A critical appraisal of the prevalence and metabolic significance of brown adipose tissue in adult humans.* Am J Physiol Endocrinol Metab. 2010;299(4):E601-6.

392. **Esen Akkas B, Gökaslan D, Güner L, Ilgin Karabacak N.** *FDG uptake in brown adipose tissue-a brief report on brown fat with FDG uptake mechanisms and quantitative analysis using dual-time-point FDG PET/CT.* Rev Esp Med Nucl. 2011;30(1):14-8.

393. **Ouellet V, Routhier-Labadie A, Bellemare W, Lakhal-Chaieb L, Turcotte E, Carpentier AC, Richard D.** *Outdoor temperature, age, sex, body mass index, and diabetic status determine the prevalence, mass, and glucose-uptake activity of 18F-FDG-detected BAT in humans.* J Clin Endocrinol Metab. 2011;96(1):192-9.

394. **Lebron L, Chou AJ, Carrasquillo JA.** *Interesting image. Unilateral F-18 FDG uptake in the neck, in patients with sympathetic denervation.* Clin Nucl Med. 2010;35(11):899-901.

395. **Garcia C, Bandaru V, Van Nostrand D, Chennupati S, Atkins F, Acio E, Kulkarni K, Majd M.** *Effective reduction of brown fat FDG uptake by controlling environmental temperature prior to PET scan: an expanded case series.* Mol Imaging Biol. 2010;12(6):652-6.

396. **Gilsanz V, Chung SA, Jackson H, Dorey FJ, Hu HH.** *Functional brown adipose tissue is related to muscle volume in children and adolescents.* J Pediatr. 2011;158(5):722-6.

397. **Hu HH, Chung SA, Nayak KS, Jackson HA, Gilsanz V.** *Differential computed tomographic attenuation of metabolically active and inactive adipose tissues: preliminary findings.* J Comput Assist Tomogr. 2011;35(1):65-71.

398. **Lee P, Zhao JT, Swarbrick MM, Gracie G, Bova R, Greenfield JR, Freund J, Ho KK.** *High prevalence of brown adipose tissue in adult humans.* J Clin Endocrinol Metab. 2011;96(8):2450-5.

399. **Yilmaz Y, Ones T, Purnak T, Ozguven S, Kurt R, Atug O, Turoglu HT, Imeryuz N.** *Association between the presence of brown adipose tissue and non-alcoholic fatty liver disease in adult humans.* Aliment Pharmacol Ther. 2011;34(3):318-23.

400. **Drubach LA, Palmer EL 3rd, Connolly LP, Baker A, Zurakowski D, Cypess AM.** *Pediatric brown adipose tissue: detection, epidemiology, and differences from adults.* J Pediatr. 2011;159(6):939-44.

401. **Ichimiya H, Arakawa S, Sato T, Shimada T, Chiba M, Soma Y, Mizoguchi M, Tomonari K, Iwasaka H, Hatano Y, Okamoto O, Fujiwara S.** *Involvement of brown adipose tissue in subcutaneous fat necrosis of the newborn.* Dermatology. 2011;223(3):207-10.

402. **Pace L, Nicolai E, D'Amico D, Ibello F, Della Morte AM, Salvatore B, Pizzuti LM, Salvatore M, Soricelli A.** *Determinants of physiologic 18F-FDG uptake in brown adipose tissue in sequential PET/CT examinations.* Mol Imaging Biol. 2011;13(5):1029-35.

403. **Gilsanz V, Smith ML, Goodarzian F, Kim M, Wren TA, Hu HH.** *Changes in brown adipose tissue in boys and girls during childhood and puberty.* J Pediatr. 2012;160(4):604-609.e1.

404. **Jacene HA, Cohade CC, Zhang Z, Wahl RL.** *The relationship between patients' serum glucose levels and metabolically active brown adipose tissue detected by PET/CT.* Mol Imaging Biol. 2011;13(6):1278-83.

405. **Huang YC, Chen TB, Hsu CC, Li SH, Wang PW, Lee BF, Kuo CY, Chiu NT.** *The relationship between brown adipose tissue activity and neoplastic status: an (18)F-FDG PET/CT study in the tropics.* Lipids Health Dis. 2011;10:238.

406. **Chalfant JS, Smith ML, Hu HH, Dorey FJ, Goodarzian F, Fu CH, Gilsanz V.** *Inverse association between brown adipose tissue activation and white adipose tissue accumulation in successfully treated pediatric malignancy.* Am J Clin Nutr. 2012;95(5):1144-9.

407. **Gilsanz V, Hu HH, Smith ML, Goodarzian F, Carcich SL, Warburton NM, Malogolowkin M.** *The depiction of brown adipose tissue is related to disease status in pediatric patients with lymphoma.* AJR Am J Roentgenol. 2012;198(4):909-13.

408. **Huang YC, Hsu CC, Wang PW, Chang YH, Chen TB, Lee BF, Chiu NT.** *Review analysis of the association between the prevalence of activated brown adipose tissue and outdoor temperature.* ScientificWorldJournal. 2012;2012:793039.

409. **Skillen A, Currie GM, Wheat JM.** *Thermal control of brown adipose tissue in 18F-FDG PET.* J Nucl Med Technol. 2012;40(2):99-103.

410. **Vogel WV, Valdés Olmos RA, Tijs TJ, Gillies MF, van Elswijk G, Vogt J.** *Intervention to lower anxiety of 18F-FDG PET/CT patients by use of audiovisual imagery during the uptake phase before imaging.* J Nucl Med Technol. 2012;40(2):92-8.

411. **Ponrartana S, Aggabao PC, Hu HH, Aldrovandi GM, Wren TA, Gilsanz V.** *Brown adipose tissue and its relationship to bone structure in pediatric patients.* J Clin Endocrinol Metab. 2012;97(8):2693-8.

412. **Cronin CG, Prakash P, Daniels GH, Boland GW, Kalra MK, Halpern EF, Palmer EL, Blake MA.** *Brown fat at PET/CT: correlation with patient characteristics.* Radiology. 2012;263(3):836-42.

413. **Perkins AC, Mshelia DS, Symonds ME, Sathekge M.** *Prevalence and pattern of brown adipose tissue distribution of 18F-FDG in patients undergoing PET-CT in a subtropical climatic zone.* Nucl Med Commun. 2013;34(2):168-74.

414. **Persichetti A, Sciuto R, Rea S, Basciani S, Lubrano C, Mariani S, Ulisse S, Nofroni I, Maini CL, Gnessi L.** *Prevalence, mass, and glucose-uptake activity of ^{18}F-FDG-detected brown adipose tissue in humans living in a temperate zone of Italy.* PLoS One. 2013;8(5):e63391.

415. **Harris SM, Davis JC, Snyder SE, Butch ER, Vavere AL, Kocak M, Shulkin BL.** *Evaluation of the biodistribution of 11C-methionine in children and young adults.* J Nucl Med. 2013;54(11):1902-8.

416. **Ahmadi N, Hajsadeghi F, Conneely M, Mingos M, Arora R, Budoff M, Ebrahimi R.** *Accurate Detection of Metabolically Active "Brown" and "White" Adipose Tissues with Computed Tomography.* Acad Radiol. 2013;20(11):1443-1447.

417. **Lee P, Swarbrick MM, Zhao JT, Ho KK.** *Inducible brown adipogenesis of supraclavicular fat in adult humans.* Endocrinology. 2011;152(10):3597-602.

418. **Huang SC.** *Anatomy of SUV. Standardized uptake value.* Nucl Med Biol. 2000;27(7):643-6.

419. **Merkel H.** *Über ein Pseudolipon der Mamma.* Beitr Path anat. 1906;39:152-7.

420. **Minni A, Barbaro M, Vitolo D, Filipo R.** *Hibernoma of the para-glottic space: an unusual tumour of the larynx.* Acta Otorhinolaryngol Ital. 2008;28(3):141-3.

421. **Mavrogenis AF, Coll-Mesa L, Drago G, Gambarotti M, Ruggieri P.** *Hibernomas: clinicopathological features, diagnosis, and treatment of 17 cases.* Orthopedics. 2011;34(11):e755-9.

422. **Furlong MA, Fanburg-Smith JC, Miettinen M.** *The morphologic spectrum of hibernoma: a clinicopathologic study of 170 cases.* Am J Surg Pathol. 2001;25(6):809-14.

423. **Carinci F, Carls FP, Pelucchi S, Grandi E, Hassanipour A, Pastore A.** *Hibernoma of the neck.* J Craniofac Surg. 2001;12(3):284-6.

424. **Giblin E, Lynn D, Mortman K.** *Cervical hibernoma demonstrating uptake on Tc-99m lymphoscintigraphy.* Clin Nucl Med. 2006;31(11):694-6.

425. **Smith CS, Teruya-Feldstein J, Caravelli JF, Yeung HW.** *False-positive findings on 18F-FDG PET/CT: differentiation of hibernoma and malignant fatty tumor on the basis of fluctuating standardized uptake values.* AJR Am J Roentgenol. 2008;190(4):1091-6.

426. **Cantisani V, Mortele KJ, Glickman JN, Ricci P, Passariello R, Ros PR, Silverman SG.** *Large retroperitoneal hibernoma in an adult male: CT imaging findings with pathologic correlation.* Abdom Imaging. 2003;28(5):721-4.

427. **Ritchie DA, Aniq H, Davies AM, Mangham DC, Helliwell TR.** *Hibernoma--correlation of histopathology and magnetic-resonance-imaging features in 10 cases.* Skeletal Radiol. 2006;35(8):579-89.

428. **Colville J, Feigin K, Tang L, Keating D, Cohen MA.** *Mammary hibernoma.* Breast J. 2006;12(6):563-5.

429. **Vijgen GH, Bouvy ND, Smidt M, Kooreman L, Schaart G, van Marken Lichtenbelt W.** *Hibernoma with metabolic impact?* BMJ Case Rep. 2012;2012.

430. **Essadel A, Bensaid Alaoui S, Mssrouri R, Mohammadine E, Benamr S, Taghy A, Lahlou MK, Chad B, Belmahi A.** *[Hibernoma: a rare case of massive weight loss].* Ann Chir. 2002;127(3):215-7.

431. **Gadea E, Thivat E, Paulon R, Mishellany F, Gimbergues P, Capel F, Mosoni L, Merlin C, Lombès M, Morio B, Durando X.** *Hibernoma: a clinical model for exploring the role of brown adipose tissue in the regulation of body weight?* J Clin Endocrinol Metab. 2014;99(1):1-6.

432. **Liu W, Bui MM, Cheong D, Caracciolo JT.** *Hibernoma: comparing imaging appearance with more commonly encountered benign or low-grade lipomatous neoplasms.* Skeletal Radiol. 2013;42(8):1073-8.

433. **Bancroft LW, Kransdorf MJ, Peterson JJ, O'Connor MI.** *Benign fatty tumors: classification, clinical course, imaging appearance, and treatment.* Skeletal Radiol. 2006;35(10):719-33.

434. **Shah U, Giubellino A, Pacak K.** *Pheochromocytoma: implications in tumorigenesis and the actual management.* Minerva Endocrinol. 2012;37(2):141-56.

435. **Petri BJ, van Eijck CH, de Herder WW, Wagner A, de Krijger RR.** *Phaeochromocytomas and sympathetic paragangliomas.* Br J Surg. 2009;96(12):1381-92.

436. **English JT, Patel SK, Flanagan MJ.** *Association of pheochromocytomas with brown fat tumors.* Radiology. 1973;107(2):279-81.

437. **Ricquier D, Nechad M, Mory G.** *Ultrastructural and biochemical characterization of human brown adipose tissue in pheochromocytoma.* J Clin Endocrinol Metab. 1982;54(4):803-7.

438. **Lean ME, James WP, Jennings G, Trayhurn P.** *Brown adipose tissue in patients with phaeochromocytoma.* Int J Obes. 1986;10(3):219-27.

439. **Fukuchi K, Tatsumi M, Ishida Y, Oku N, Hatazawa J, Wahl RL.** *Radionuclide imaging metabolic activity of brown adipose tissue in a patient with pheochromocytoma.* Exp Clin Endocrinol Diabetes. 2004;112(10):601-3.

440. **Ramacciotti C, Schneegans O, Lang H, Lindner V, Claria M, Moreau F, Chenard MP, Pinget M, Kessler L.** *Diffuse uptake of brown fat on computed-tomography coupled positron emission tomoscintigraphy (PET-CT) for the exploration of extra-adrenal pheochromocytoma.* Ann Endocrinol (Paris). 2006;67(1):14-9.

441. **Dundamadappa SK, Shankar S, Danrad R, Singh A, Vijayaraghavan G, Kim Y, Perugini R.** *Imaging of brown fat associated with adrenal pheochromocytoma.* Acta Radiol. 2007;48(4):468-72.

442. **Yamaga LY, Thom AF, Wagner J, Baroni RH, Hidal JT, Funari MG.** *The effect of catecholamines on the glucose uptake in brown adipose tissue demonstrated by (18)F-FDG PET/CT in a patient with adrenal pheochromocytoma.* Eur J Nucl Med Mol Imaging. 2008;35(2):446-7.

443. **Kuji I, Imabayashi E, Minagawa A, Matsuda H, Miyauchi T.** *Brown adipose tissue demonstrating intense FDG uptake in a patient with mediastinal pheochromocytoma.* Ann Nucl Med. 2008;22(3):231-5.

444. **Sekizawa N, Yoshimoto T, Izumiyama H, Hirata Y.** *Distinct uptake of 18F-fluorodeoxyglucose by brown adipose tissue with a catecholamine-secreting tumor.* Intern Med. 2010;49(21):2363.

445. **Ochoa-Figueroa MA, Muñoz-Iglesias J, Allende-Riera A, Cabello-García D, Martínez-Gimeno E, Desequera-Rahola M.** *Incidental uptake of 123I MIBG in brown fat.* Rev Esp Med Nucl Imagen Mol. 2012;31(5):290-1.

446. **Banzo J, Ubieto MA, Berisa MF, Andrés A, Mateo ML, Tardín L, Parra A, Razola P, Prats E.** *Extensive hypermetabolic pattern of brown adipose tissue activation on 18F-FDG PET/CT in a patient diagnosed of catecholamine-secreting para-vesical paraganglioma.* Rev Esp Med Nucl Imagen Mol. 2013;32(6):397-9.

447. **Hadi M, Chen CC, Whatley M, Pacak K, Carrasquillo JA.** *Brown fat imaging with (18)F-6-fluorodopamine PET/CT, (18)F-FDG PET/CT, and (123)I-MIBG SPECT: a study of patients being evaluated for pheochromocytoma.* J Nucl Med. 2007;48(7):1077-83.

448. **Wang Q, Zhang M, Ning G, Gu W, Su T, Xu M, Li B, Wang W.** *Brown adipose tissue in humans is activated by elevated plasma catecholamines levels and is inversely related to central obesity.* PLoS One. 2011;6(6):e21006.

449. **Iyer RB, Guo CC, Perrier N.** *Adrenal pheochromocytoma with surrounding brown fat stimulation.* AJR Am J Roentgenol. 2009;192(1):300-1.

450. **Joshi PV, Lele VR.** *Unexpected visitor on FDG PET/CT--brown adipose tissue (BAT) in mesentery in a case of retroperitoneal extra-adrenal pheochromocytoma: is the BAT activation secondary to catecholamine-secreting pheochromocytoma?* Clin Nucl Med. 2012;37(5):e119-20.

451. **Dong A, Wang Y, Lu J, Zuo C.** *Hypermetabolic Mesenteric Brown Adipose Tissue on Dual-Time Point FDG PET/CT in a Patient With Benign Retroperitoneal Pheochromocytoma.* Clin Nucl Med. 2014;39(3):e229-32.

452. **Grinspoon S, Carr A.** *Cardiovascular risk and body-fat abnormalities in HIV-infected adults.* N Engl J Med. 2005;352(1):48-62.

453. **Guallar JP, Gallego-Escuredo JM, Domingo JC, Alegre M, Fontdevila J, Martínez E, Hammond EL, Domingo P, Giralt M, Villarroya F.** *Differential gene expression indicates that 'buffalo hump' is a distinct adipose tissue disturbance in HIV-1-associated lipodystrophy.* AIDS. 2008;22(5):575-84.

454. **Bérériat V, Cervera P, Le Dour C, Verpont MC, Dumont S, Vantyghem MC, Capeau J, Vigouroux C (Lipodystrophy Study Group).** *LMNA mutations induce a non-inflammatory fibrosis and a brown fat-like dystrophy of enlarged cervical adipose tissue.* Am J Pathol. 2011;179(5):2443-53.

455. **Torriani M, Fitch K, Stavrou E, Bredella MA, Lim R, Sass CA, Cypess AM, Grinspoon S.** *Deiodinase 2 expression is increased in dorsocervical fat of patients with HIV-associated lipohypertrophy syndrome.* J Clin Endocrinol Metab. 2012;97(4):E602-7.

456. **Sevastianova K, Sutinen J, Greco D, Sievers M, Salmenkivi K, Perttilä J, Olkkonen VM, Wågsäter D, Lidell ME, Enerbäck S, Eriksson P, Walker UA, Auvinen P, Ristola M, Yki-Järvinen H.** *Comparison of dorsocervical with abdominal subcutaneous adipose tissue in patients with and without antiretroviral therapy-associated lipodystrophy.* Diabetes. 2011;60(7):1894-900.

457. **Kosmiski LA, Sage-El A, Kealey EH, Bessesen DH.** *Brown fat activity is not apparent in subjects with HIV lipodystrophy and increased resting energy expenditure.* Obesity (Silver Spring). 2011;19(10):2096-8.

458. **Salisbury E, Hipp J, Olmsted-Davis EA, Davis AR, Heggeness MH, Gannon FH.** *Histologic identification of brown adipose and peripheral nerve involvement in human atherosclerotic vessels.* Hum Pathol. 2012;43(12):2213-22.

459. **Holopainen J, Helama S, Partonen T.** *Does diurnal temperature range influence seasonal suicide mortality? Assessment of daily data of the Helsinki metropolitan area from 1973 to 2010.* Int J Biometeorol. 2013 Jun 18. [Epub ahead of print].

460. **Holopainen J, Helama S, Björkenstam C, Partonen T.** *Variation and seasonal patterns of suicide mortality in Finland and Sweden since the 1750s.* Environ Health Prev Med. 2013;18(6):494-501.

461. **Pasanisi F, Pace L, Fonti R, Marra M, Sgambati D, De Caprio C, De Filippo E, Vaccaro A, Salvatore M, Contaldo F.** *Evidence of brown fat activity in constitutional leanness.* J Clin Endocrinol Metab. 2013;98(3):1214-8.

462. **Brooke OG, Harris M, Salvosa CB.** *The response of malnourished babies to cold.* J Physiol. 1973;233(1):75-91.

463. **Padidela R, Bennett K, Nessa A, Wells J, Aufieri R, James C, Smith VV, Brain C, Eaton S, Hussain K.** *Severe resistance to weight gain, lack of stored triglycerides in adipose tissue, hypoglycaemia, and increased energy expenditure: a novel disorder of energy homeostasis.* Horm Res Paediatr. 2012;77(4):261-8.

464. **Stephenson TJ, Variend S.** *Visceral brown fat necrosis in postperinatal mortality.* J Clin Pathol. 1987;40(8):896-900.

465. **Miller SF.** *Resolution of calcific brown fat necrosis associated with prostaglandin therapy for cyanotic congenital heart disease in neonates: report of two cases.* Pediatr Radiol. 2004;34(11):919-23.

466. **Oppert JM, Vohl MC, Chagnon M, Dionne FT, Cassard-Doulcier AM, Ricquier D, Pérusse L, Bouchard C.** *DNA polymorphism in the uncoupling protein (UCP) gene and human body fat.* Int J Obes Relat Metab Disord. 1994;18(8):526-31.

467. **Fumeron F, Durack-Bown I, Betoulle D, Cassard-Doulcier AM, Tuzet S, Bouillaud F, Melchior JC, Ricquier D, Apfelbaum M.** *Polymorphisms of uncoupling protein (UCP) and beta 3 adrenoreceptor genes in obese people submitted to a low calorie diet.* Int J Obes Relat Metab Disord. 1996;20(12):1051-4.

468. **Clément K, Ruiz J, Cassard-Doulcier AM, Bouillaud F, Ricquier D, Basdevant A, Guy-Grand B, Froguel P.** *Additive effect of A-->G (-3826) variant of the uncoupling protein gene and the Trp64Arg mutation of the beta 3-adrenergic receptor gene on weight gain in morbid obesity.* Int J Obes Relat Metab Disord. 1996;20(12):1062-6.

469. **Heilbronn LK, Kind KL, Pancewicz E, Morris AM, Noakes M, Clifton PM.** *Association of -3826 G variant in uncoupling protein-1 with increased BMI in overweight Australian women.* Diabetologia. 2000;43(2):242-4.

470. **Ukkola O, Tremblay A, Sun G, Chagnon YC, Bouchard C.** *Genetic variation at the uncoupling protein 1, 2 and 3 loci and the response to long-term overfeeding.* Eur J Clin Nutr. 2001;55(11):1008-15.

471. **Herrmann SM, Wang JG, Staessen JA, Kertmen E, Schmidt-Petersen K, Zidek W, Paul M, Brand E.** *Uncoupling protein 1 and 3 polymorphisms are associated with waist-to-hip ratio.* J Mol Med (Berl). 2003;81(5):327-32.

472. **Kim KS, Cho DY, Kim YJ, Choi SM, Kim JY, Shin SU, Yoon YS.** *The finding of new genetic polymorphism of UCP-1 A-1766G and its effects on body fat accumulation.* Biochim Biophys Acta. 2005;1741(1-2):149-55.

473. **Alonso A, Martí A, Corbalán MS, Martínez-González MA, Forga L, Martínez JA.** *Association of UCP3 gene -55C>T polymorphism and obesity in a Spanish population.* Ann Nutr Metab. 2005;49(3):183-8.

474. **Shin HD, Kim KS, Cha MH, Yoon Y.** *The effects of UCP-1 polymorphisms on obesity phenotypes among Korean female subjects.* Biochem Biophys Res Commun. 2005;335(2):624-30.

475. **Nakano T, Shinka T, Sei M, Sato Y, Umeno M, Sakamoto K, Nomura I, Nakahori Y.** *A/G heterozygote of the A-3826G polymorphism in the UCP-1 gene has higher BMI than A/A and G/G homozygote in young Japanese males.* J Med Invest. 2006;53(3-4):218-22.

476. **Schäffler A, Palitzsch KD, Watzlawek E, Drobnik W, Schwer H, Schölmerich J, Schmitz G.** *Frequency and significance of the A-->G (-3826) polymorphism in the promoter of the gene for uncoupling protein-1 with regard to metabolic parameters and adipocyte transcription factor binding in a large population-based Caucasian cohort.* Eur J Clin Invest. 1999;29(9):770-9.

477. **Evans D, Minouchehr S, Hagemann G, Mann WA, Wendt D, Wolf A, Beisiegel U.** *Frequency of and interaction between polymorphisms in the beta3-adrenergic receptor and in uncoupling proteins 1 and 2 and obesity in Germans.* Int J Obes Relat Metab Disord. 2000;24(10):1239-45.

478. **Nagai N, Sakane N, Tsuzaki K, Moritani T.** *UCP1 genetic polymorphism (-3826 A/G) diminishes resting energy expenditure and thermoregulatory sympathetic nervous system activity in young females.* Int J Obes (Lond). 2011;35(8):1050-5.

479. **Nagai N, Sakane N, Kotani K, Hamada T, Tsuzaki K, Moritani T.** *Uncoupling protein 1 gene -3826 A/G polymorphism is associated with weight loss on a short-term, controlled-energy diet in young women.* Nutr Res. 2011;31(4):255-61.

480. **de Souza BM, Brondani LA, Bouças AP, Sortica DA, Kramer CK, Canani LH, Leitão CB, Crispim D.** *Associations between UCP1 -3826A/G, UCP2 -866G/A, Ala55Val and Ins/Del, and UCP3 -55C/T polymorphisms and susceptibility to type 2 diabetes mellitus: case-control study and meta-analysis.* PLoS One. 2013;8(1):e54259.

481. **Clément K, Vaisse C, Manning BS, Basdevant A, Guy-Grand B, Ruiz J, Silver KD, Shuldiner AR, Froguel P, Strosberg AD.** *Genetic variation in the beta 3-adrenergic receptor and an increased capacity to gain weight in patients with morbid obesity.* N Engl J Med. 1995;333(6):352-4.

482. **Sakane N, Yoshida T, Umekawa T, Kondo M, Sakai Y, Takahashi T.** *Beta 3-adrenergic-receptor polymorphism: a genetic marker for visceral fat obesity and the insulin resistance syndrome.* Diabetologia. 1997;40(2):200-4.

483. **Clement K, Manning BS, Basdevant A, Strosberg AD, Guy-Grand B, Froguel P.** *Gender effect of the Trp64Arg mutation in the beta 3 adrenergic receptor gene on weight gain in morbid obesity.* Diabetes Metab. 1997;23(5):424-7.

484. **Shima Y, Tsukada T, Nakanishi K, Ohta H.** *Association of the Trp64Arg mutation of the beta3-adrenergic receptor with fatty liver and mild glucose intolerance in Japanese subjects.* Clin Chim Acta. 1998;274(2):167-76.

485. **Kawamura T, Egusa G, Okubo M, Imazu M, Yamakido M.** *Association of beta3-adrenergic receptor gene polymorphism with insulin resistance in Japanese-American men.* Metabolism. 1999;48(11):1367-70.

486. **Oizumi T, Daimon M, Saitoh T, Kameda W, Yamaguchi H, Ohnuma H, Igarashi M, Eguchi H, Manaka H, Tominaga M, Kato T.** *Genotype Arg/Arg, but not Trp/Arg, of the Trp64Arg polymorphism of the beta(3)-adrenergic receptor is associated with type 2 diabetes and obesity in a large Japanese sample.* Diabetes Care. 2001;24(9):1579-83.

487. **de Luis DA, Aller R, Izaola O, Conde R, Eiros Bouza JM.** *Genetic Variation in the Beta 3-Adrenoreceptor Gene (Trp64Arg Polymorphism) and Its Influence on Anthropometric Parameters and Insulin Resistance Under a High Monounsaturated versus a High Polyunsaturated Fat Hypocaloric Diet.* Ann Nutr Metab. 2013;62(4):303-9.

488. **Evans D, Wolf AM, Nellessen U, Ahle S, Kortner B, Kuhlmann HW, Beisiegel U.** *Association between polymorphisms in candidate genes and morbid obesity.* Int J Obes Relat Metab Disord. 2001;25 Suppl 1:S19-21.

489. **Morita E, Taniguchi H, Sakaue M.** *Trp64Arg polymorphism in beta3-adrenergic receptor gene is associated with decreased fat oxidation both in resting and aerobic exercise in the Japanese male.* Exp Diabetes Res. 2009;2009:605139.

490. **Kahara T, Takamura T, Hayakawa T, Nagai Y, Yamaguchi H, Katsuki T, Katsuki K, Katsuki M, Kobayashi K.** *Prediction of exercise-mediated changes in metabolic markers by gene polymorphism.* Diabetes Res Clin Pract. 2002;57(2):105-10.

491. **Tafel J, Branscheid I, Skwarna B, Schlimme M, Morcos M, Algenstaedt P, Hinney A, Hebebrand J, Nawroth P, Hamann A.** *Variants in the human beta 1-, beta 2-, and beta 3-adrenergic receptor genes are not associated with morbid obesity in children and adolescents.* Diabetes Obes Metab. 2004;6(6):452-5.

492. **Zingaretti MC, Crosta F, Vitali A, Guerrieri M, Frontini A, Cannon B, Nedergaard J, Cinti S.** *The presence of UCP1 demonstrates that metabolically active adipose tissue in the neck of adult humans truly represents brown adipose tissue.* FASEB J. 2009;23(9):3113-20.

493. **Yang X, Enerbäck S, Smith U.** *Reduced expression of FOXC2 and brown adipogenic genes in human subjects with insulin resistance.* Obes Res. 2003;11(10):1182-91.

494. **Yoneshiro T, Ogawa T, Okamoto N, Matsushita M, Aita S, Kameya T, Kawai Y, Iwanaga T, Saito M.** *Impact of UCP1 and β3AR gene polymorphisms on age-related changes in brown adipose tissue and adiposity in humans.* Int J Obes (Lond). 2013;37(7):993-8.

495. **Sokoloff L, Reivich M, Kennedy C, Des Rosiers MH, Patlak CS, Pettigrew KD, Sakurada O, Shinohara M.** *The [14C]deoxyglucose method for the measurement of local cerebral glucose utilization: theory, procedure, and normal values in the conscious and anesthetized albino rat.* J Neurochem. 1977;28(5):897-916.

496. **Gjedde A.** *Calculation of cerebral glucose phosphorylation from brain uptake of glucose analogs in vivo: a re-examination.* Brain Res. 1982;257(2):237-74.

497. **Patlak CS, Blasberg RG, Fenstermacher JD.** *Graphical evaluation of blood-to-brain transfer constants from multiple-time uptake data.* J Cereb Blood Flow Metab. 1983;3(1):1-7.

498. **Ishizu K, Nishizawa S, Yonekura Y, Sadato N, Magata Y, Tamaki N, Tsuchida T, Okazawa H, Miyatake S, Ishikawa M, Kikuchi H, Konishi J.** *Effects of hyperglycemia on FDG uptake in human brain and glioma.* J Nucl Med. 1994;35(7):1104-9.

499. **Thie JA.** *Clarification of a fractional uptake concept.* J Nucl Med. 1995;36(4):711-2.

500. **Vijgen GH, Bouvy ND, Teule GJ, Brans B, Schrauwen P, van Marken Lichtenbelt WD.** *Brown adipose tissue in morbidly obese subjects.* PLoS One. 2011;6(2):e17247.

501. **Yoneshiro T, Aita S, Matsushita M, Okamatsu-Ogura Y, Kameya T, Kawai Y, Miyagawa M, Tsujisaki M, Saito M.** *Age-related decrease in cold-activated brown adipose tissue and accumulation of body fat in healthy humans.* Obesity (Silver Spring). 2011;19(9):1755-60.

502. **Matsushita M, Yoneshiro T, Aita S, Kameya T, Sugie H, Saito M.** *Impact of brown adipose tissue on body fatness and glucose metabolism in healthy humans.* Int J Obes (Lond). 2013 Nov 11. [Epub ahead of print].

503. **Zhang Q, Ye H, Miao Q, Zhang Z, Wang Y, Zhu X, Zhang S, Zuo C, Zhang Z, Huang Z, Xue R, Zeng M, Huang H, Jin W, Tang Q, Guan Y, Li Y.** *Differences in the metabolic status of healthy adults with and without active brown adipose tissue.* Wien Klin Wochenschr. 2013;125(21-22):687-95.

504. **Vijgen GH, Bouvy ND, Teule GJ, Brans B, Hoeks J, Schrauwen P, van Marken Lichtenbelt WD.** *Increase in brown adipose tissue activity after weight loss in morbidly obese subjects.* J Clin Endocrinol Metab. 2012;97(7):E1229-33.

505. **Vrieze A, Schopman JE, Admiraal WM, Soeters MR, Nieuwdorp M, Verberne HJ, Holleman F.** *Fasting and postprandial activity of brown adipose tissue in healthy men.* J Nucl Med. 2012;53(9):1407-10.

506. **Schlögl M, Piaggi P, Thiyyagura P, Reiman EM, Chen K, Lutrin C, Krakoff J, Thearle MS.** *Overfeeding over 24 hours does not activate brown adipose tissue in humans.* J Clin Endocrinol Metab. 2013;98(12):E1956-60.

507. **Vosselman MJ, Brans B, van der Lans AA, Wierts R, van Baak MA, Mottaghy FM, Schrauwen P, van Marken Lichtenbelt WD.** *Brown adipose tissue activity after a high-calorie meal in humans.* Am J Clin Nutr. 2013;98(1):57-64.

508. **Bredella MA, Fazeli PK, Freedman LM, Calder G, Lee H, Rosen CJ, Klibanski A.** *Young women with cold-activated brown adipose tissue have higher bone mineral density and lower Pref-1 than women without brown adipose tissue: a study in women with anorexia nervosa, women recovered from anorexia nervosa, and normal-weight women.* J Clin Endocrinol Metab. 2012;97(4):E584-90.

509. **Bredella MA, Fazeli PK, Lecka-Czernik B, Rosen CJ, Klibanski A.** *IGFBP-2 is a negative predictor of cold-induced brown fat and bone mineral density in young non-obese women.* Bone. 2013;53(2):336-9.

510. **Lee P, Brychta RJ, Collins MT, Linderman J, Smith S, Herscovitch P, Millo C, Chen KY, Celi FS.** *Cold-activated brown adipose tissue is an independent predictor of higher bone mineral density in women.* Osteoporos Int. 2013;24(4):1513-8.

511. **Admiraal WM, Holleman F, Bahler L, Soeters MR, Hoekstra JB, Verberne HJ.** *Combining 123I-metaiodobenzylguanidine SPECT/CT and 18F-FDG PET/CT for the assessment of brown adipose tissue activity in humans during cold exposure.* J Nucl Med. 2013;54(2):208-12.

512. **Admiraal WM, Verberne HJ, Karamat FA, Soeters MR, Hoekstra JB, Holleman F.** *Cold-induced activity of brown adipose tissue in young lean men of South-Asian and European origin.* Diabetologia. 2013;56(10):2231-7.

513. **Astrup A, Bülow J, Christensen NJ, Madsen J.** *Ephedrine-induced thermogenesis in man: no role for interscapular brown adipose tissue.* Clin Sci (Lond). 1984;66(2):179-86.

514. **Astrup A, Bülow J, Madsen J, Christensen NJ.** *Contribution of BAT and skeletal muscle to thermogenesis induced by ephedrine in man.* Am J Physiol. 1985;248(5 Pt 1):E507-15.

515. **Kety SS, Schmidt CF.** *The determination of cerebral blood flow in man by the use of nitrous oxide in low concentrations.* Am J Physiol. 1945;143:53-66.

516. **Celi FS, Brychta RJ, Linderman JD, Butler PW, Alberobello AT, Smith S, Courville AB, Lai EW, Costello R, Skarulis MC, Csako G, Remaley A, Pacak**

K, Chen KY. *Minimal changes in environmental temperature result in a significant increase in energy expenditure and changes in the hormonal homeostasis in healthy adults.* Eur J Endocrinol. 2010;163(6):863-72.

517. **Yoneshiro T, Aita S, Matsushita M, Kameya T, Nakada K, Kawai Y, Saito M.** *Brown adipose tissue, whole-body energy expenditure, and thermogenesis in healthy adult men.* Obesity (Silver Spring). 2011;19(1):13-6.

518. **Vijgen GH, Sparks LM, Bouvy ND, Schaart G, Hoeks J, van Marken Lichtenbelt WD, Schrauwen P.** *Increased oxygen consumption in human adipose tissue from the "brown adipose tissue" region.* J Clin Endocrinol Metab. 2013;98(7):E1230-4.

519. **Mintun MA, Raichle ME, Martin WR, Herscovitch P.** *Brain oxygen utilization measured with O-15 radiotracers and positron emission tomography.* J Nucl Med. 1984;25(2):177-87.

520. **Muzik O, Mangner TJ, Granneman JG.** *Assessment of oxidative metabolism in brown fat using PET imaging.* Front Endocrinol (Lausanne). 2012;3:15.

521. **Muzik O, Mangner TJ, Leonard WR, Kumar A, Janisse J, Granneman JG.** *15O PET measurement of blood flow and oxygen consumption in cold-activated human brown fat.* J Nucl Med. 2013;54(4):523-31.

522. **Weyer C, Tataranni PA, Snitker S, Danforth E Jr, Ravussin E.** *Increase in insulin action and fat oxidation after treatment with CL 316,243, a highly selective beta3-adrenoceptor agonist in humans.* Diabetes. 1998;47(10):1555-61.

523. **Cawthorne MA, Sennitt MV, Arch JR, Smith SA.** *BRL 35135, a potent and selective atypical beta-adrenoceptor agonist.* Am J Clin Nutr. 1992;55(1 Suppl):252S-257S.

524. **Champigny O, Ricquier D.** *Evidence from in vitro differentiating cells that adrenoceptor agonists can increase uncoupling protein mRNA level in adipocytes of adult humans: an RT-PCR study.* J Lipid Res. 1996;37(9):1907-14.

525. **Jockers R, Issad T, Zilberfarb V, de Coppet P, Marullo S, Strosberg AD.** *Desensitization of the beta-adrenergic response in human brown adipocytes.* Endocrinology. 1998;139(6):2676-84.

526. **Fisher MH, Amend AM, Bach TJ, Barker JM, Brady EJ, Candelore MR, Carroll D, Cascieri MA, Chiu SH, Deng L, Forrest MJ, Hegarty-Friscino B, Guan XM, Hom GJ, Hutchins JE, Kelly LJ, Mathvink RJ, Metzger JM, Miller RR, Ok HO, Parmee ER, Saperstein R, et al.** *A selective human beta3 adrenergic receptor agonist increases metabolic rate in rhesus monkeys.* J Clin Invest. 1998;101(11):2387-93.

527. **Carey AL, Formosa MF, Van Every B, Bertovic D, Eikelis N, Lambert GW, Kalff V, Duffy SJ, Cherk MH, Kingwell BA.** *Ephedrine activates brown adipose tissue in lean but not obese humans.* Diabetologia. 2013;56(1):147-55.

528. **Vosselman MJ, van der Lans AA, Brans B, Wierts R, van Baak MA, Schrauwen P, van Marken Lichtenbelt WD.** *Systemic β-adrenergic stimulation of thermogenesis is not accompanied by brown adipose tissue activity in humans.* Diabetes. 2012;61(12):3106-13.

529. **Yoneshiro T, Aita S, Kawai Y, Iwanaga T, Saito M.** *Nonpungent capsaicin analogs (capsinoids) increase energy expenditure through the activation of brown adipose tissue in humans.* Am J Clin Nutr. 2012;95(4):845-50.

530. **Sugita J, Yoneshiro T, Hatano T, Aita S, Ikemoto T, Uchiwa H, Iwanaga T, Kameya T, Kawai Y, Saito M.** *Grains of paradise (Aframomum melegueta) extract activates brown adipose tissue and increases whole-body energy expenditure in men.* Br J Nutr. 2013;110(4):733-8.

531. **Symonds ME, Henderson K, Elvidge L, Bosman C, Sharkey D, Perkins AC, Budge H.** *Thermal imaging to assess age-related changes of skin temperature within the supraclavicular region co-locating with brown adipose tissue in healthy children.* J Pediatr. 2012;161(5):892-8.

532. **Robinson L, Ojha S, Symonds ME, Budge H.** *Body mass index as a determinant of brown adipose tissue function in healthy children.* J Pediatr. 2014;164(2):318-322.e1.

533. **Hu HH, Perkins TG, Chia JM, Gilsanz V.** *Characterization of human brown adipose tissue by chemical-shift water-fat MRI.* AJR Am J Roentgenol. 2013;200(1):177-83.

534. **Chen YC, Cypess AM, Chen YC, Palmer M, Kolodny G, Kahn CR, Kwong KK.** *Measurement of human brown adipose tissue volume and activity using anatomic MR imaging and functional MR imaging.* J Nucl Med. 2013;54(9):1584-7.

535. **Osculati F, Leclercq F, Sbarbati A, Zancanaro C, Cinti S, Antonakis K.** *Morphological identification of brown adipose tissue by magnetic resonance imaging in the rat.* Eur J Radiol. 1989;9(2):112-4.

536. **Sbarbati A, Guerrini U, Marzola P, Asperio R, Osculati F.** *Chemical shift imaging at 4.7 tesla of brown adipose tissue.* J Lipid Res. 1997;38(2):343-7.

537. **Hamilton G, Smith DL Jr, Bydder M, Nayak KS, Hu HH.** *MR properties of brown and white adipose tissues.* J Magn Reson Imaging. 2011;34(2):468-73.

538. **Chen YI, Cypess AM, Sass CA, Brownell AL, Jokivarsi KT, Kahn CR, Kwong KK.** *Anatomical and functional assessment of brown adipose tissue by magnetic resonance imaging.* Obesity (Silver Spring). 2012;20(7):1519-26.

539. **Holstila M, Virtanen KA, Grönroos TJ, Laine J, Lepomäki V, Saunavaara J, Lisinen I, Komu M,**

Hannukainen JC, Nuutila P, Parkkola R, Borra RJ. *Measurement of brown adipose tissue mass using a novel dual-echo magnetic resonance imaging approach: A validation study.* Metabolism. 2013;62(8):1189-98.

540. **Hu HH, Tovar JP, Pavlova Z, Smith ML, Gilsanz V.** *Unequivocal identification of brown adipose tissue in a human infant.* J Magn Reson Imaging. 2012;35(4):938-42.

541. **Smith DL Jr, Yang Y, Hu HH, Zhai G, Nagy TR.** *Measurement of interscapular brown adipose tissue of mice in differentially housed temperatures by chemical-shift-encoded water-fat MRI.* J Magn Reson Imaging. 2013;38(6):1425-33.

542. **Hu HH, Yin L, Aggabao PC, Perkins TG, Chia JM, Gilsanz V.** *Comparison of brown and white adipose tissues in infants and children with chemical-shift-encoded water-fat MRI.* J Magn Reson Imaging. 2013;38(4):885-96.

543. **Branca RT, Zhang L, Warren WS, Auerbach E, Khanna A, Degan S, Ugurbil K, Maronpot R.** *In Vivo Noninvasive Detection of Brown Adipose Tissue through Intermolecular Zero-Quantum MRI.* PLoS One. 2013;8(9):e74206.

544. **van Rooijen BD, van der Lans AA, Brans B, Wildberger JE, Mottaghy FM, Schrauwen P, Backes WH, van Marken Lichtenbelt WD.** *Imaging Cold-Activated Brown Adipose Tissue Using Dynamic T2*-Weighted Magnetic Resonance Imaging and 2-Deoxy-2-[18F]fluoro-D-glucose Positron Emission Tomography.* Invest Radiol. 2013;48(10):708-14.

545. **World Medical Association Declaration of Helsinki.** *Ethical Principles for Medical Research Involving Human Subjects.* 55th WMA General Assembly, Tokyo 2004.

546. **Working group appointed by the Finnish Medical Society Duodecim and the Finnish Association for the Study of Obesity.** *Current Care guideline on obesity.* Accessed in 2009: http://www.kaypahoito.fi/web/kh/suositukset/naytaartikkeli/tunnus/hoi24010.

547. **Abe T, Bemben MG, Kondo M, Kawakami Y, Fukunaga T.** *Comparison of skeletal muscle mass to fat-free mass ratios among different ethnic groups.* J Nutr Health Aging. 2012;16(6):534-8.

548. **DeFronzo RA, Tobin JD, Andres R.** *Glucose clamp technique: a method for quantifying insulin secretion and resistance.* Am J Physiol. 1979;237(3):E214-23.

549. **Saito M, Okamatsu-Ogura Y, Tsujisaki M, Kaji T, Nakada K.** *Human brown adipose tissue evaluated by FDG-PET: activation by cold exposure.* Int J Obes. 2007;31:S32(T3:OS4.4) [Abstract].

550. **Sipilä HT, Clark JC, Peltola O, Teräs M.** *An automatic [15O]H2O production system for heart and brain studies.* J Labelled Compd Radiopharm. 2001;44 Suppl 1:S1066-8.

551. **Hamacher K, Coenen HH, Stöcklin G.** *Efficient stereospecific synthesis of no-carrier-added 2-[18F]-fluoro-2-deoxy-D-glucose using aminopolyether supported nucleophilic substitution.* J Nucl Med. 1986;27(2):235-8.

552. **Maldjian JA, Laurienti PJ, Kraft RA, Burdette JH.** *An automated method for neuroanatomic and cytoarchitectonic atlas-based interrogation of fMRI data sets.* Neuroimage. 2003;19(3):1233-9.

553. **Hoekstra CJ, Hoekstra OS, Lammertsma AA.** *On the use of image-derived input functions in oncological fluorine-18 fluorodeoxyglucose positron emission tomography studies.* Eur J Nucl Med. 1999;26(11):1489-92.

554. **Phelps ME, Huang SC, Hoffman EJ, Selin C, Sokoloff L, Kuhl DE.** *Tomographic measurement of local cerebral glucose metabolic rate in humans with (F-18)2-fluoro-2-deoxy-D-glucose: validation of method.* Ann Neurol. 1979;6(5):371-88.

555. **de Langen AJ, Lubberink M, Boellaard R, Spreeuwenberg MD, Smit EF, Hoekstra OS, Lammertsma AA.** *Reproducibility of tumor perfusion measurements using 15O-labeled water and PET.* J Nucl Med. 2008;49(11):1763-8.

556. **Patlak CS, Blasberg RG.** *Graphical evaluation of blood-to-brain transfer constants from multiple-time uptake data. Generalizations.* J Cereb Blood Flow Metab. 1985;5(4):584-90.

557. **Virtanen KA, Peltoniemi P, Marjamäki P, Asola M, Strindberg L, Parkkola R, Huupponen R, Knuuti J, Lönnroth P, Nuutila P.** *Human adipose tissue glucose uptake determined using [(18)F]-fluoro-deoxy-glucose ([(18)F]FDG) and PET in combination with microdialysis.* Diabetologia. 2001;44(12):2171-9.

558. **Peltoniemi P, Lönnroth P, Laine H, Oikonen V, Tolvanen T, Grönroos T, Strindberg L, Knuuti J, Nuutila P.** *Lumped constant for [(18)F]fluorodeoxyglucose in skeletal muscles of obese and nonobese humans.* Am J Physiol Endocrinol Metab. 2000;279(5):E1122-30.

559. **Reivich M, Alavi A, Wolf A, Fowler J, Russell J, Arnett C, MacGregor RR, Shiue CY, Atkins H, Anand A, Dann R, Greenberg JH.** *Glucose metabolic rate kinetic model parameter determination in humans: the lumped constants and rate constants for [18F]fluorodeoxyglucose and [11C]deoxyglucose.* J Cereb Blood Flow Metab. 1985;5(2):179-92.

560. **Scheinin M, Karhuvaara S, Ojala-Karlsson P, Kallio A, Koulu M.** *Plasma 3,4-dihydroxyphenylglycol (DHPG) and 3-methoxy-4-hydroxyphenylglycol (MHPG) are insensitive indicators of alpha 2-adrenoceptor mediated regulation of norepinephrine release in healthy human volunteers.* Life Sci. 1991;49(1):75-84.

561. **Matsuda M, DeFronzo RA.** *Insulin sensitivity indices obtained from oral glucose tolerance testing: comparison with the euglycemic insulin clamp.* Diabetes Care. 1999;22(9):1462-70.

562. **Friedewald WT, Levy RI, Fredrickson DS.** *Estimation of the concentration of low-density lipoprotein cholesterol in plasma, without use of the preparative ultracentrifuge.* Clin Chem. 1972;18(6):499-502.

563. **IBM Corp.** 2011. IBM SPSS Statistics for Windows, Version 20.0. Armonk, NY: IBM Corp.

564. **StataCorp.** 2009. Stata Statistical Software: Release 11. College Station, TX: StataCorp LP.

565. **Nookaew I, Svensson PA, Jacobson P, Jernås M, Taube M, Larsson I, Andersson-Assarsson JC, Sjöström L, Froguel P, Walley A, Nielsen J, Carlsson LM.** *Adipose tissue resting energy expenditure and expression of genes involved in mitochondrial function are higher in women than in men.* J Clin Endocrinol Metab. 2013;98(2):E370-8.

566. **Lever JD, Jung RT, Nnodim JO, Leslie PJ, Symons D.** *Demonstration of a catecholaminergic innervation in human perirenal brown adipose tissue at various ages in the adult.* Anat Rec. 1986;215(3):251-5, 227-9.

567. **Marette A, Bukowiecki LJ.** *Mechanism of norepinephrine stimulation of glucose transport in isolated rat brown adipocytes.* Int J Obes. 1990;14(10):857-67.

568. **Kern W, Peters A, Born J, Fehm HL, Schultes B.** *Changes in blood pressure and plasma catecholamine levels during prolonged hyperinsulinemia.* Metabolism. 2005;54(3):391-6.

569. **Bisquolo VA, Cardoso CG Jr, Ortega KC, Gusmão JL, Tinucci T, Negrão CE, Wajchenberg BL, Mion D Jr, Forjaz CL.** *Previous exercise attenuates muscle sympathetic activity and increases blood flow during acute euglycemic hyperinsulinemia.* J Appl Physiol. 2005;98(3):866-71.

570. **Arruda AP, Milanski M, Coope A, Torsoni AS, Ropelle E, Carvalho DP, Carvalheira JB, Velloso LA.** *Low-grade hypothalamic inflammation leads to defective thermogenesis, insulin resistance, and impaired insulin secretion.* Endocrinology. 2011;152(4):1314-26.

571. **Sokoloff L.** *The metabolism of the central nervous system in vivo. In: Handbook of physiology (Field L, Magoun H, Hall VE, eds).* Washington, D.C. : American Physiological Society, 1960;1843-64.

572. **Gallagher D, Belmonte D, Deurenberg P, Wang Z, Krasnow N, Pi-Sunyer FX, Heymsfield SB.** *Organ-tissue mass measurement allows modeling of REE and metabolically active tissue mass.* Am J Physiol. 1998;275(2 Pt 1):E249-58.

573. **Heiss WD, Herholz K, Pawlik G, Wagner R, Wienhard K.** *Positron emission tomography in neuropsychology.* Neuropsychologia. 1986;24(1):141-9.

574. **Critchley HD, Mathias CJ, Josephs O, O'Doherty J, Zanini S, Dewar BK, Cipolotti L, Shallice T, Dolan RJ.** *Human cingulate cortex and autonomic control: converging neuroimaging and clinical evidence.* Brain. 2003;126(Pt 10):2139-52.

575. **Gao JH, Parsons LM, Bower JM, Xiong J, Li J, Fox PT.** *Cerebellum implicated in sensory acquisition and discrimination rather than motor control.* Science. 1996;272(5261):545-7.

576. **Lutherer LO, Lutherer BC, Dormer KJ, Janssen HF, Barnes CD.** *Bilateral lesions of the fastigial nucleus prevent the recovery of blood pressure following hypotension induced by hemorrhage or administration of endotoxin.* Brain Res. 1983;269(2):251-7.

577. **Nunneley SA, Martin CC, Slauson JW, Hearon CM, Nickerson LD, Mason PA.** *Changes in regional cerebral metabolism during systemic hyperthermia in humans.* J Appl Physiol. 2002;92(2):846-51.

578. **Brix G, Zaers J, Adam LE, Bellemann ME, Ostertag H, Trojan H, Haberkorn U, Doll J, Oberdorfer F, Lorenz WJ.** *Performance evaluation of a whole-body PET scanner using the NEMA protocol. National Electrical Manufacturers Association.* J Nucl Med. 1997;38(10):1614-23.

579. **Teräs M, Tolvanen T, Johansson JJ, Williams JJ, Knuuti J.** *Performance of the new generation of whole-body PET/CT scanners: Discovery STE and Discovery VCT.* Eur J Nucl Med Mol Imaging. 2007;34(10):1683-92.